ÉCOLE DE
PHYSIQUE DES HOUCHES

February 9-14, 2025
Les Houches

Large eddy simulation of particle transport by environmental flows

Ivana Vinkovic – LMFA UMR 5509, ECL, INSA, UCBL, CNRS

Serge Simoëns – LMFA, CNRS
Catherine Le Ribault – LMFA, CNRS

Cristian Escauriaza – Universidad Catolica de Chile
Maria Magdalena Barros – Universidad Catolica de Chile

CO_2 captation, dust and sediments

Desert dust blown to the sea surface spurring phytoplankton blooms. Image from MODIS, NASA Terra satellite, April 8, 2011

Phytoplankton produce oxygen and sequester CO_2

Dust deposition over the ocean supports 4.5% of the yearly global export production

20-40% in some regions

Phytoplankton blooms can also be triggered by river flows into the sea

River sediment transport

Dams on the Yangtze River. NASA Landsat/USGS

To estimate the incoming sediment flux from rivers, we need to improve the prediction of river sediment transport models

Highly influenced by human activity

Varying in space and time

Global sediment transport models

Global sediment transport models considering both bedload transport and suspended sediments in rivers mostly based on : river discharge, Rouse number, sediment concentration, **shear velocity and critical shear stress** (Hatono and Yoshimura 2020)

Fail to predict reliable values

Need to improve global estimates reflecting changes in sediment flow over time

Need for constantly improving and updating global sediment transport models

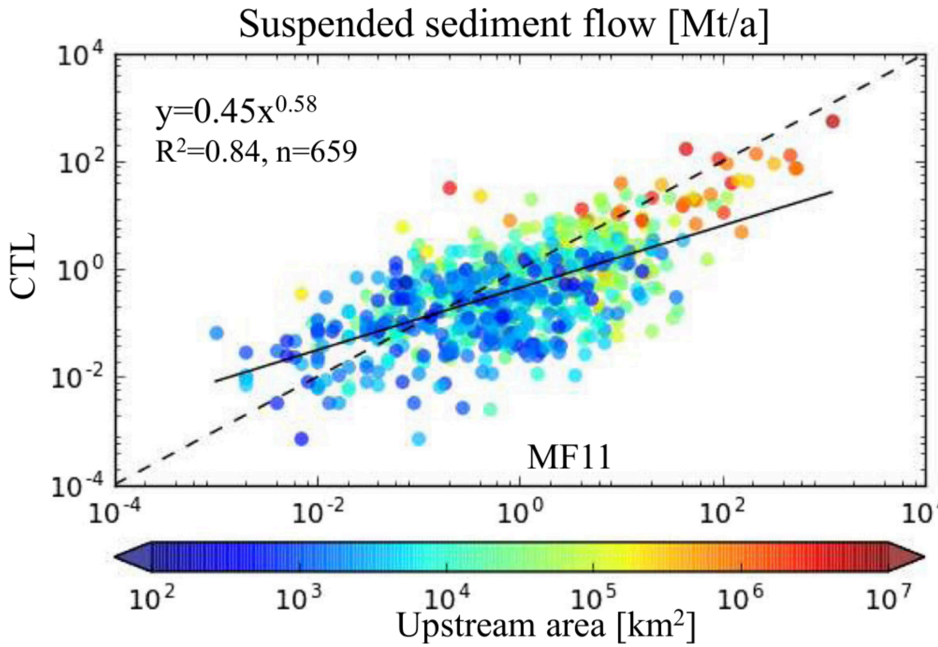

Scatter plot of annual suspended sediment flow $[Mt/a]$ between two global models. Figure from Hatono and Yoshimura 2020)

Multiscale problem

Downscaling problem

Upscaling modelling

Study at small scales

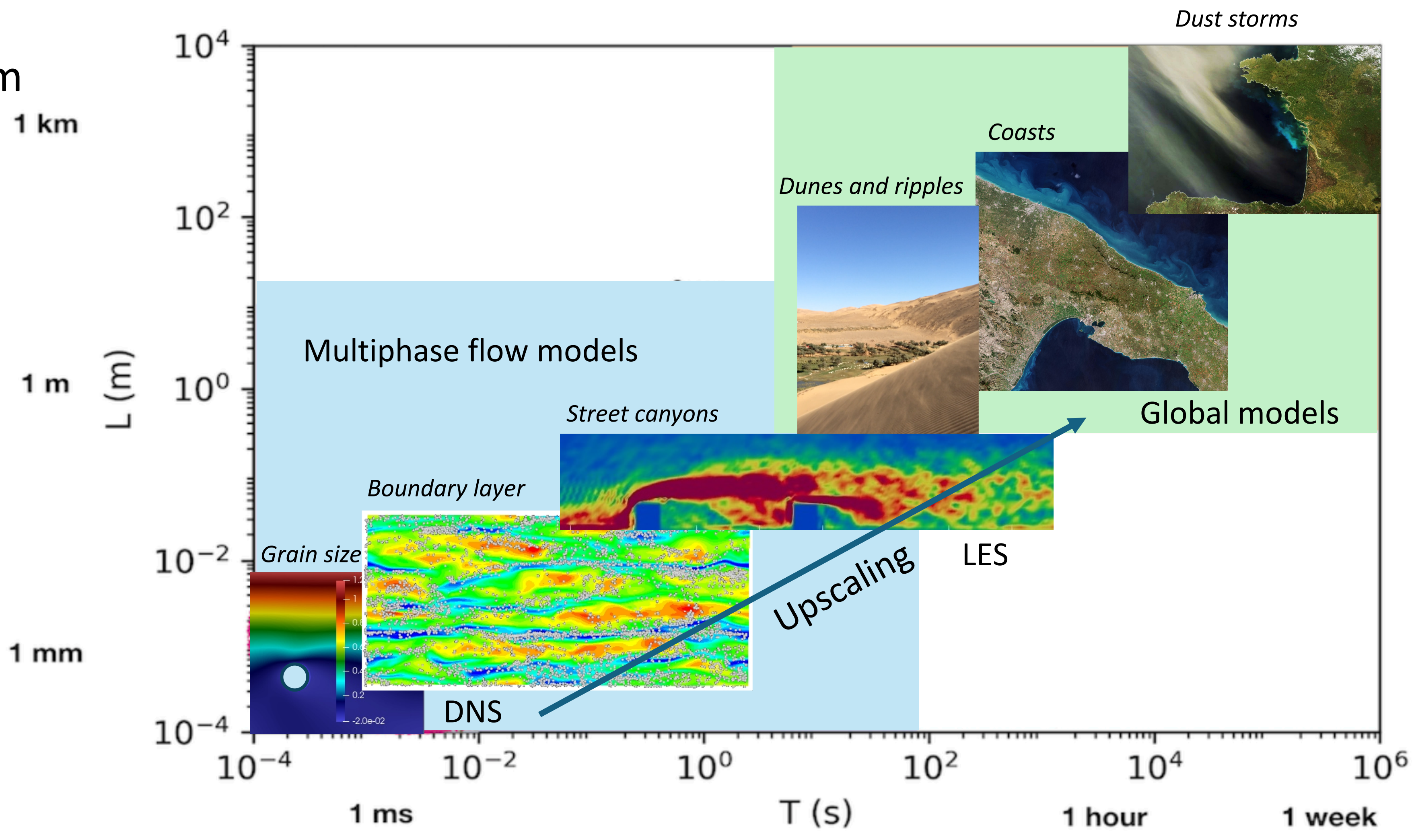

Outline

1. General introduction
2. Introduction on Large eddy simulation
3. Introduction on modelling particle – laden turbulent flows
4. Example study : Bedload transport around boulders in river flows
   - Analysis of the flow
   - Particle transport and fluxes
5. Other examples of studied issues
   - Particle transport in street canyons
   - Particle transport above dunes
6. Conclusions and perspectives

Numerical simulation and turbulence modelling

DNS	LES	RANS
All space and time scales are resolved $L/\eta \sim Re^{3/4}$ and $\mathrm{T} \sim Re^{3/4}$ $\Rightarrow$ Required resolution Re^3 $\Rightarrow$ Environmental flows $Re \sim 10^8$ $\Rightarrow$ Grids $Re \sim 10^{24}$ $\Rightarrow$ Highest DNS $Re \sim 45\ 000$ in open channel flow	Scale separation decomposition $u(x,t) = \tilde{u}(x,t) + u''(x,t)$ Subgrid scales Subgrid scale model	Reynolds averaged decomposition : $u(x,t) = \bar{u}(x,t) + u'(x,t)$ Turbulence model
Detailed description (up to the smallest scales) of initial and boundary conditions Forcing strategy	Scale separation with a cut-off length $\Rightarrow$ Performance of subgrid scale models $\Rightarrow$ Initial and boundary conditions	Lacks a fine description Cannot isolate rare events The performance of turbulence models depends on the studied configurations
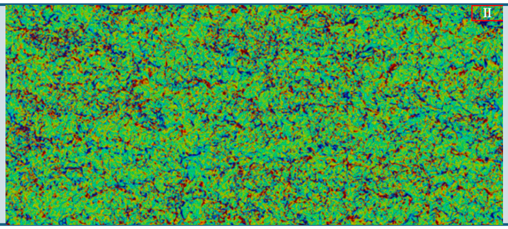	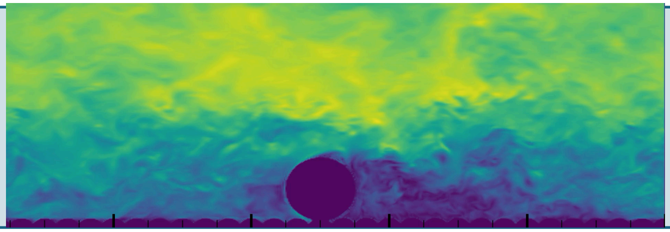	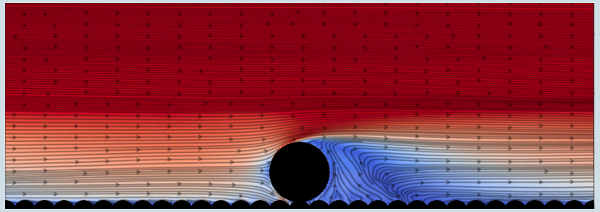

Instantaneous wall normal vorticity (Yao et al. 2022 JFM)

Large eddy simulation

Sagaut (2001) "LES of incompressible flows"

Length scale high pass filtering $\tilde{u}_i(\boldsymbol{x},t) = \iint_{-\infty}^{+\infty} u_i(\boldsymbol{\xi},t)\, G(\boldsymbol{x}-\boldsymbol{\xi}, t-t')dt'd^3\boldsymbol{\xi}$

Top hat filtering $G(\boldsymbol{x}-\boldsymbol{\xi}) = \begin{cases} \frac{1}{\Delta} \text{ if } |\boldsymbol{x}-\boldsymbol{\xi}| < \frac{\Delta}{2} \\ 0 \text{ otherwise} \end{cases}$

Numerous physical and spectral filters

Procedure based on the scale separation assumption

- The complexity of the solution is reduced by retaining only the resolved (filtered) scales
- Subgrid scales are unresolved => The information is lost but the their influence is grouped and modelled through the subgrid scale tensor

Filtered Navier Stokes equations

$$\frac{\partial \tilde{u}_i}{\partial x_i} = 0$$

$$\frac{\partial \tilde{u}_i}{\partial t} + \tilde{u}_j \frac{\partial \tilde{u}_i}{\partial x_j} = -\frac{1}{\rho}\frac{\partial \tilde{p}}{\partial x_i} + \frac{1}{Re}\frac{\partial^2 \tilde{u}_i}{\partial x_j \partial x_j} - \frac{\partial \tau_{ij}}{\partial x_j} + \frac{f_i}{\rho}$$

Link the existence of subgrid scales to the resolved flow ?

Large eddy simulation – subgrid model

Sagaut (2001) "LES of incompressible flows"

LES subgrid-scale model
Dynamic Smagorinsky

$$\tau_{ij} - \frac{1}{3}\delta_{ij}\tau_{kk} = -2\nu_t\widetilde{S_{ij}}$$

$$\boxed{\nu_t = C_s\Delta^2|\tilde{S}|}$$

Universal form of the small scales

Energy transfer analogue to diffusion

Dynamic adjustment of Cs

C_s fixes the ratio of the kinetic energy that will be dissipated ($C_s = 0.2$ for HIT, Deradorff uses $C_s = 0.1$ for a turbulent channel flow => idea of Germano and Lilly with the dynamic adjustment of Cs based on the a second filtering over larger scales in order to determine the energy transfer ratio.

Automatic adjustment of the constant C_s in time and space :
1. Application of a test filter
2. Scale invariance between both filtering levels
3. Applying a least square method for calculating the given constant

Unbounded of negative values => statistical averages in homogeneity directions

Outline

1. General introduction
2. Introduction on Large eddy simulation
3. Introduction on modelling particle – laden turbulent flows
4. Example study : Bedload transport around boulders in river flows
   - Analysis of the flow
   - Particle transport and fluxes
5. Other examples of studied issues
   - Particle transport in street canyons
   - Particle transport above dunes
6. Conclusions and perspectives

What about particles ?

Particle response time $\tau_p = \frac{\rho_p d_p^2}{18\mu}$

Non dimensional groups

Stokes number $St = \frac{\tau_p}{\tau}$

Settling parameter $Sv = \frac{\tau_p g}{u_\eta}$

Size and density ratio $\frac{d_p}{L}$ $\frac{\rho_p}{\rho}$

Lagrangian / Eulerian approach

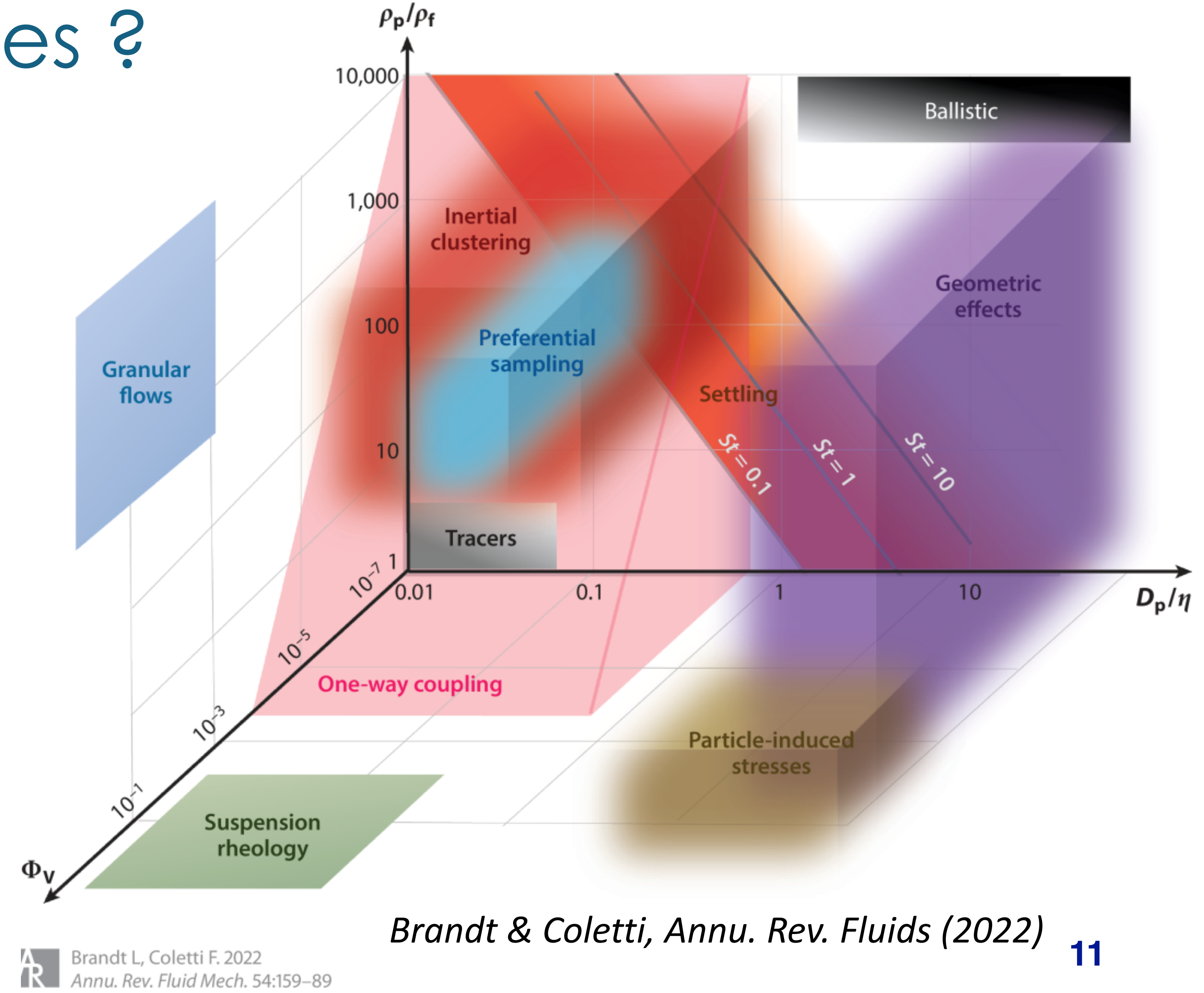

Brandt & Coletti, Annu. Rev. Fluids (2022)

Turbulence – particles interaction regimes

Finn & Li, Int. J. Multiphase Flow (2017)

Gravitational velocity

$$u_g = \sqrt{\left(\frac{\rho_p}{\rho} - 1\right) g d_p}$$

Shields number

$$\theta = \frac{u_\tau^2}{u_g^2}$$

Galileo number

$$Ga = \frac{u_g d_p}{\nu}$$

Interaction regimes | **Method of choice**

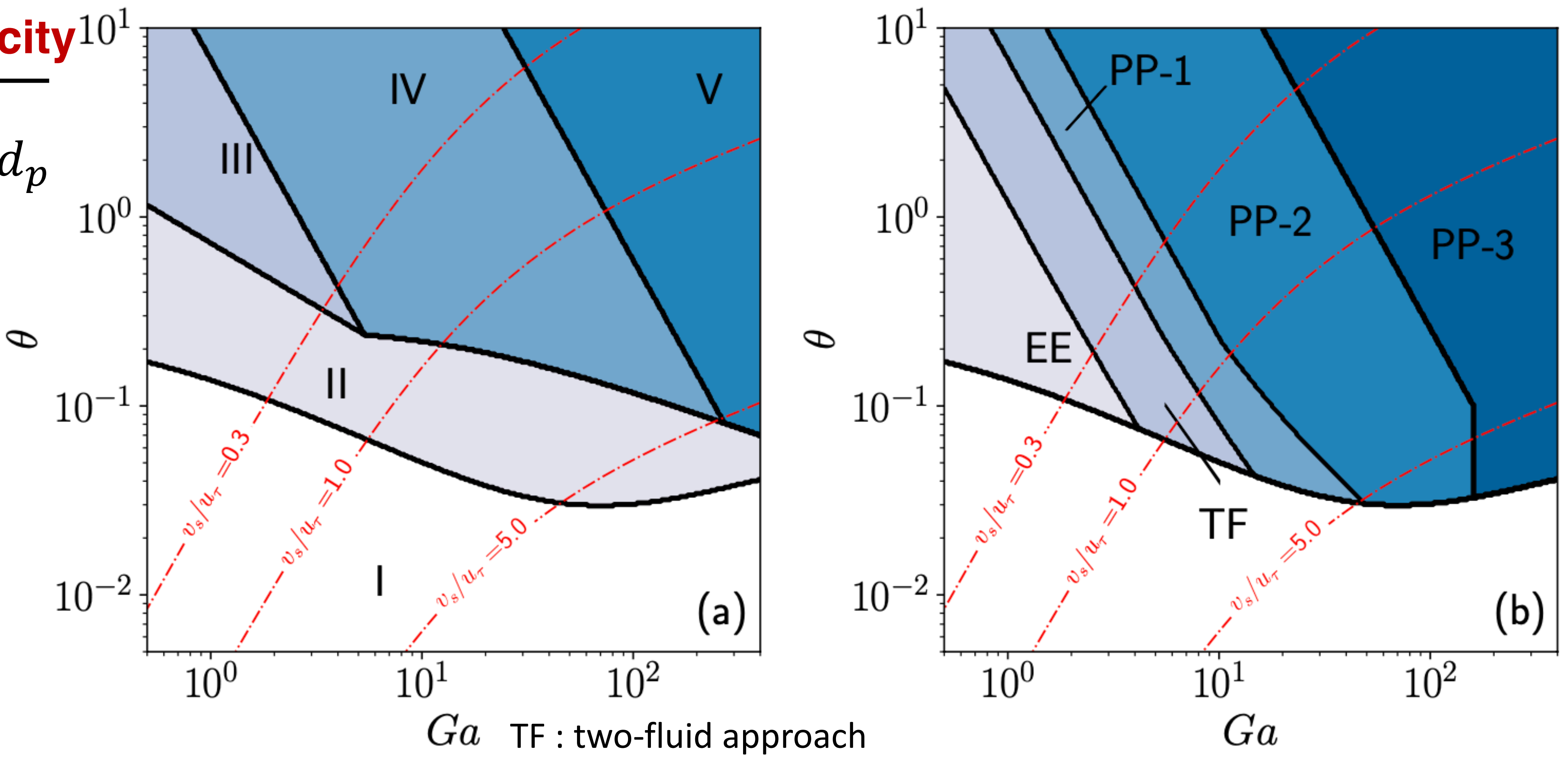

I : no motion
II : gravitational settling
III : turbulent suspension
IV and V : particles influenced by inertial scales

TF : two-fluid approach
EE : equilibrium Eulerian approach
PP : point particle Lagrangian methodology

Eulerian approach

Two fluid approach

- Dispersed phase considered as a second fluid with an Eulerian field representation
- Equations of conservation of mass, momentum and energy obtained by appropriate averaging
- Different averaging techniques (time, space, ensemble …)
- Closure problem
- Suitable when a vary large number of particles is considered

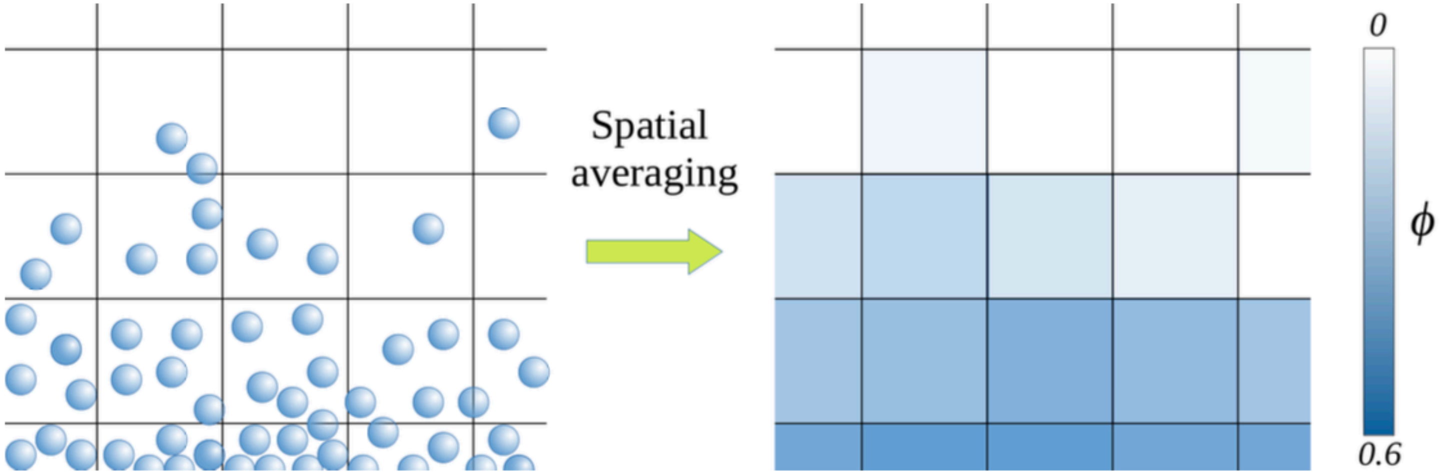

Zhang & Prosperetti, JFM (1994), Kaufmann et al., JCP (2008), Chauchat et al., Geosci. Model Dev. (2017)

Eulerian approach

Shotorban & Balanchandar, Phys. Rev. Lett. E (2009)

Equilibrium approach

For $St \ll 1$ particle Eulerian velocity approximated by the surrounding fluid phase velocity and its temporal and spatial derivates through a series expansion

$$\frac{dx_{pi}}{dt} = v_i \text{ and } \frac{dv_i}{dt} = \frac{1}{\tau_p}(u_i - v_i)$$

other forces can be included

For $St \ll 1$ **equilibrium Eulerian velocity**

$$v_i = u_i - \tau_p \frac{Du_i}{Dt}$$

acceleration of the fluid phase

$$v_i = u_i - \tau_p \frac{Du_i}{Dt} + \tau_P^2 \left(\frac{D^2 u_i}{Dt^2} + \frac{Du_j}{Dt} \frac{\partial u_i}{\partial x_j} \right)$$

2nd order expansion

Transport equation for **particle volume fraction** or concentration

$$\frac{\partial \phi}{\partial t} + \frac{\partial \phi v_i}{\partial x_i} = 0$$

Eulerian approach

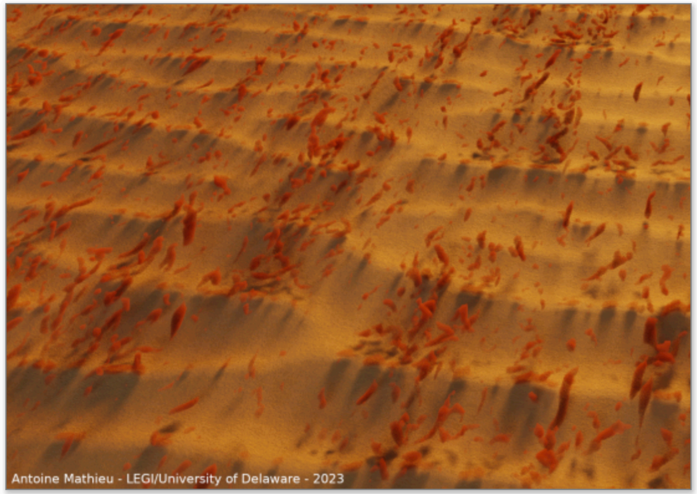

Equilibrium approach

- Tested in HIT for small Stokes numbers and one way coupling
- No differential equation for the dispersed phase
- Extended to LES, two-way coupling and finite size particles
- Applied to gravity currents, sheet flows and environmental engineering

Illustration by Antoine Mathieu (2020)
Prix CNRS – particle concentration obtained by sedfoam

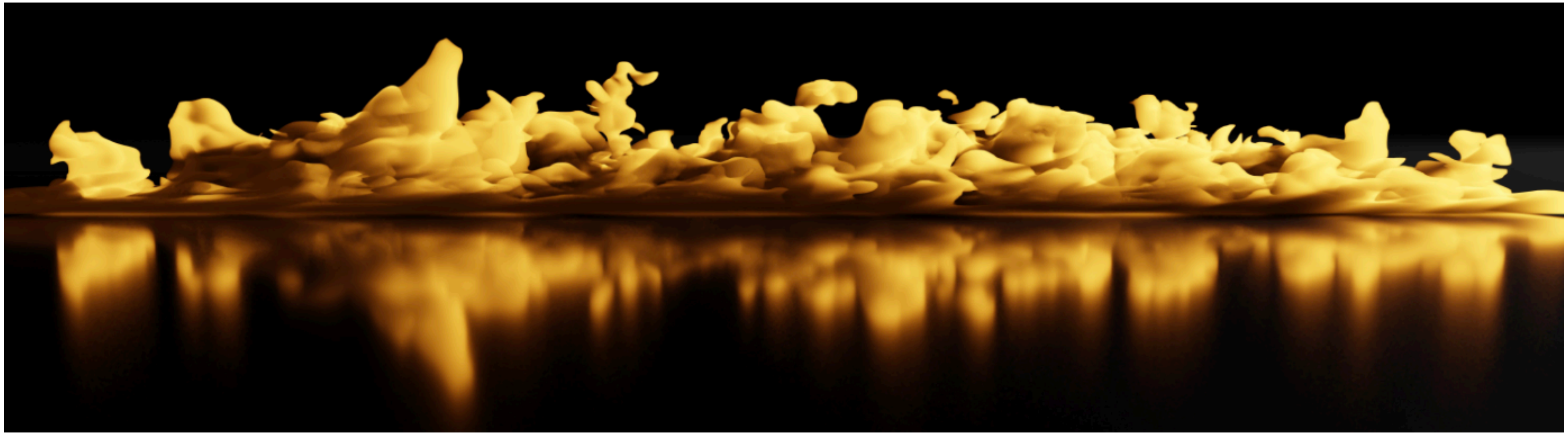

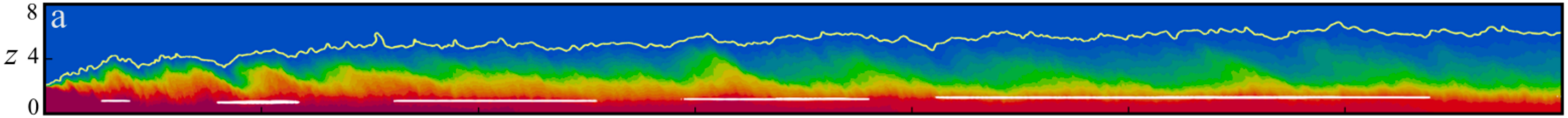

Salinas et al., Nature Comm. (2021) Gravity current in subcritical submarine flow

Lagrangian approach

Brandt and Coletti (2022) Annu. Rev. Fluid Mech.

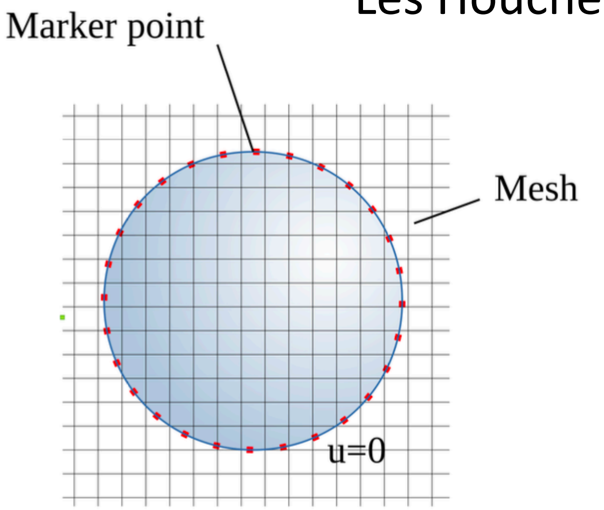

Particle resolved DNS

- interface resolved methods such as overset grids or immersed boundary methods accounting for the flow around each particle
- ideal for dilute systems and highly inertial particles (large Re_p)
- need for an accurate modelling of lubrication and contact forces, short – range interaction forces and granular friction

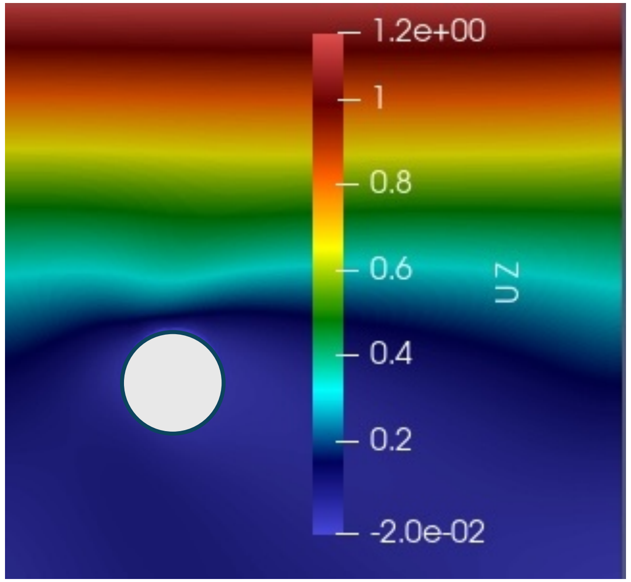

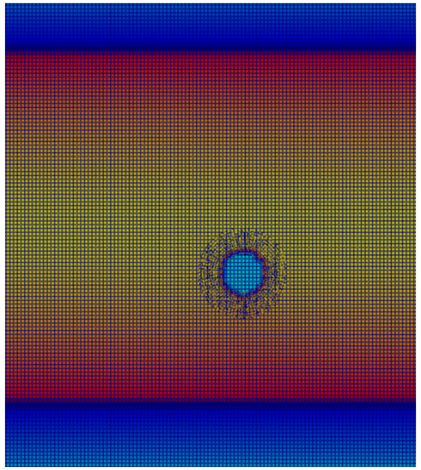

Overset method for Segré Silberberg migration in channel flow

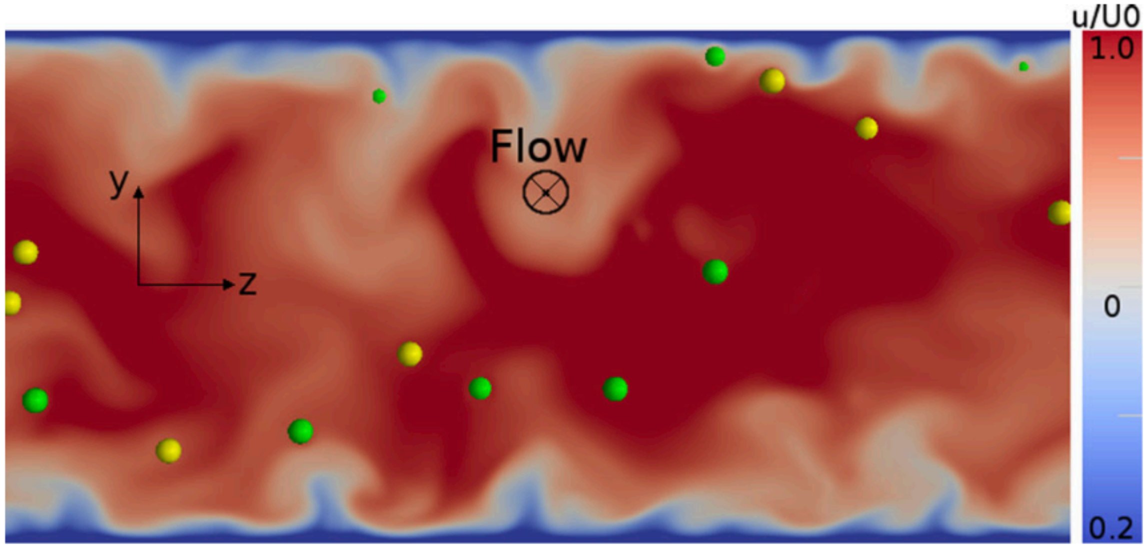

Turbulent channel flow DNS coupled with IBM for low density ratio particles (Yu et al. 2015)

Lagrangian approach

Brandt and Coletti (2022) Annu. Rev. Fluid Mech.

Point particle approach

- Maxey – Riley – Gatignol equation for point particle movement => forces acting on a small particle in arbitrary motion in an unsteady inhomogeneous flow

$$\frac{dx_{pi}}{dt} = v_i \text{ and } \frac{dv_i}{dt} = \frac{1}{\tau_p}(u_i - v_i)$$

other forces can be included

- vanishing Re_p and dilute conditions
- need for improvements in two-way coupling modelling : is turbulence attenuated or augmented ? Regularization procedures when particles are not much smaller than the grid
- hydrodynamic forcing leads to interscale energy transfers not easily discernible from intephase coupling
- modelling of wall – particle interactions and particle – particle interactions

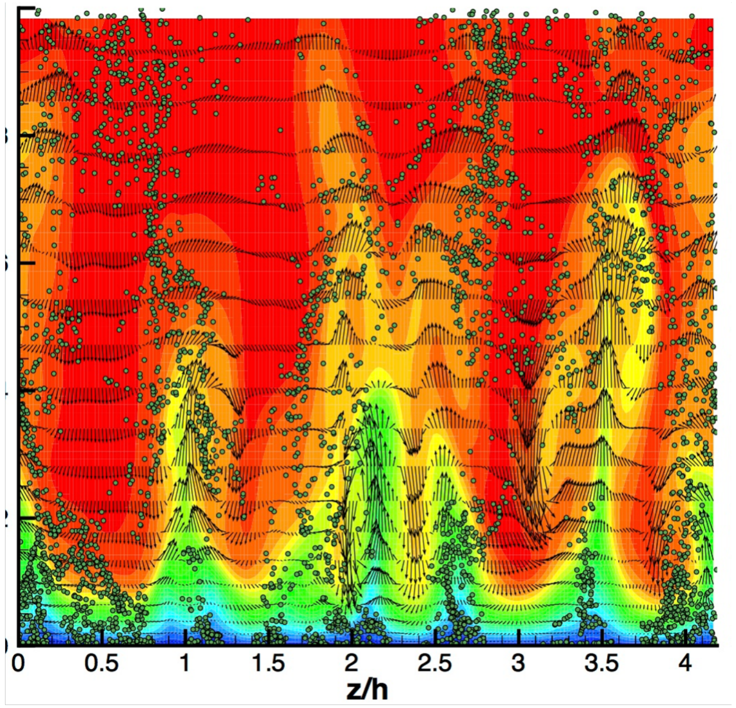

Sweep – ejection cycle and preferential concentration

Vinkovic et al. (2011)

Lagrangian approach

Brandt and Coletti (2022) Annu. Rev. Fluid Mech.

Point particle or resolved particle approach

- Particles affect the ejection – sweep cycle, the dynamics of streamwise vortices and the formation of hairpin eddies
- This modifies Reynolds stresses altering in return particle segregation
- Most studies have been done in zero gravity conditions –> conclusions should not be extrapolated
- Wall turbulence is significantly altered by particle migration
- Most studies = small heavy particles vs large weakly buoyant particle => need to bridge this gap
- Need of a more accurate representation of forces acting on non isolated particles in turbulence

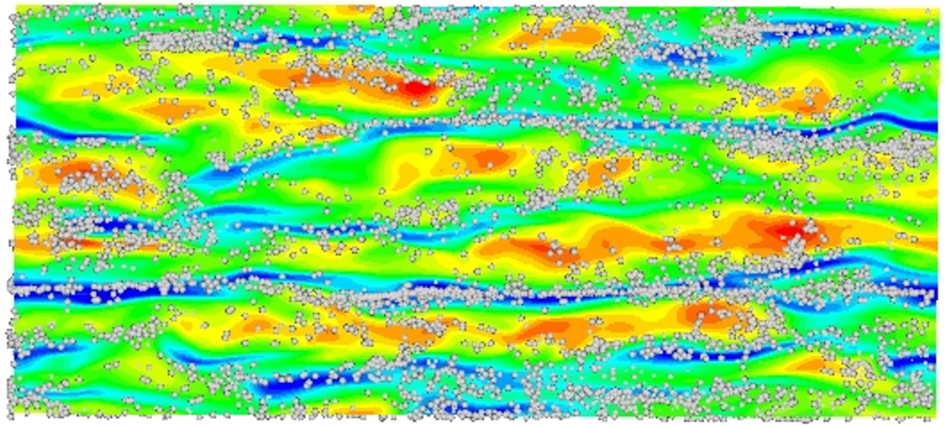

Preferential concentration
Turbophoresis

Outline

1. General introduction
2. Introduction on Large eddy simulation
3. Introduction on modelling particle – laden turbulent flows
4. Example study : Bedload transport around boulders in river flows
   - Analysis of the flow
   - Particle transport and fluxes
5. Other examples of studied issues
   - Particle transport in street canyons
   - Particle transport above dunes
6. Conclusions and perspectives

ÉCOLE DE
PHYSIQUE DES HOUCHES

February 9-14, 2025
Les Houches

Bedload transport over a rough bed with an array of boulders

PhD of Maria Magdalena Barros – Universidad Catolica de Chile

Ivana Vinkovic – LMFA UMR 5509, ECL, INSA, UCBL, CNRS

Cristian Escauriaza – Universidad Catolica de Chile

Bedload transport through an array of boulders

- The array of boulders **increase flow resistance** and produce **spatial flow variability**, **separation**, **recirculation** and **coherent structures**.
- Local flow variability produces **local bedload transport variability**.
- Such **spatial flow variations** are ignored with the commonly used **reach-averaged shear stress** in bedload transport estimations (Yager et al., 2018).
- Few studies have tried to include **flow spatial variability** on **bedload transport estimations.**
- It is not clear what is the local flow variable more **correlated** with local bedload fluxes.

$$q_s = a(\tau_{bed} - \tau_{cr})^b$$

Futaleifú River, Chile

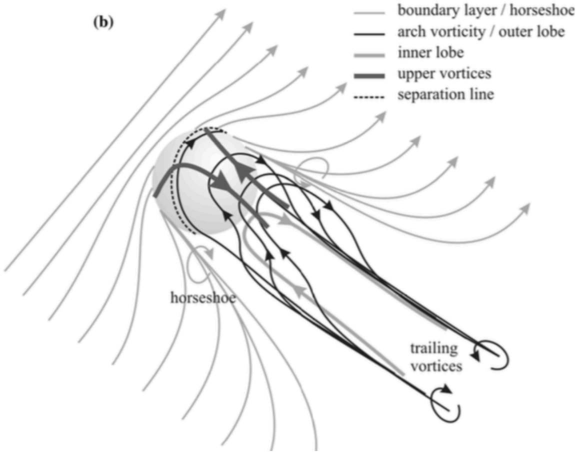

Hajimirzaie et al. (2014)

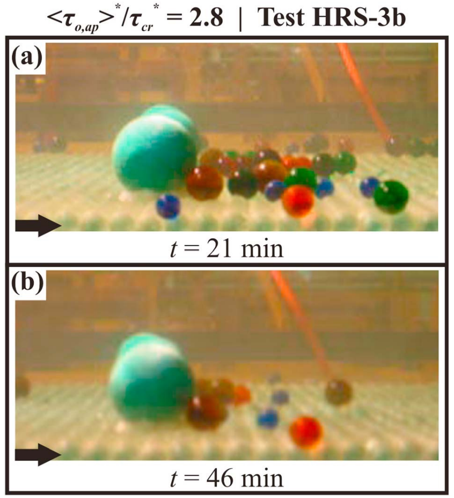

Papanicolaou et al. (2018)

Bedload transport

- Bedload transport is affected by a wide range of **temporal** and **spatial scales** in fluvial systems.

- Highly fluctuating fluxes results from the competition of instantaneous local **stresses** with **resistive forces** and particle **collisions**.

- Sediment particles mobilized in contact with the bed are influenced by **coherent structures** and **turbulent events**.

Macroroughness elements

- A complex 3-D flow is generated around them.
- They induce changes on **shear stress distribution** and **bedload transport** conditions.
- They generate significant **drag** increasing **flow resistance**.

Problem

- How the **3-D flow** features generated around the macroroughness elements contribute to the terms in the **double-averaged momentum** and **kinetic energy** balances?

- What is the **effective shear stress** that mobilize sediments in this context?

- How the **spatial** and **temporal** flow **variations** induced by macroroughness elements influence **bedload transport**? How can we improve it estimation?

Methodology : large eddy simulation

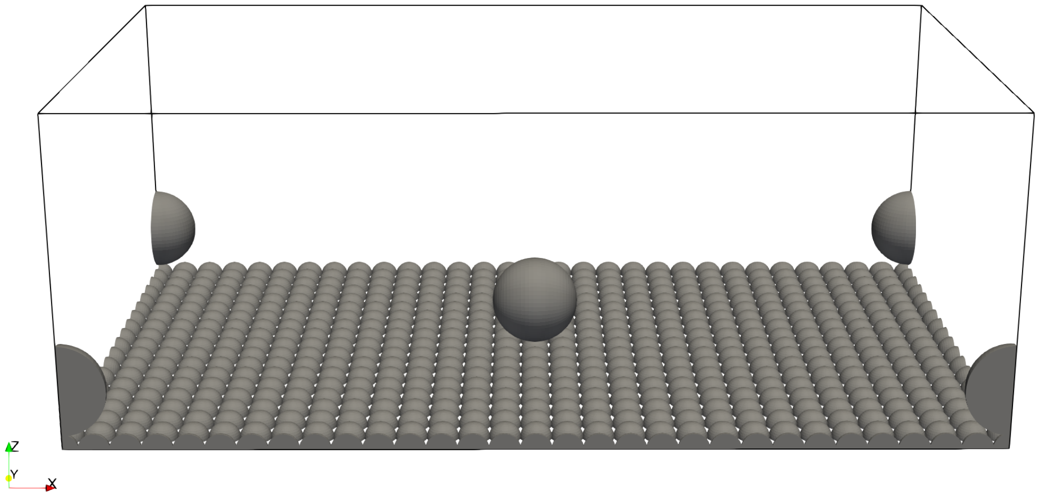

Periodic boundary conditions in the streamwise (x) and spanwise (y) directions.

Cartesian grid : 501×301×221
Grid resolution : $\Delta x^{+} = \Delta y^{+} = \Delta z^{+} = 45$

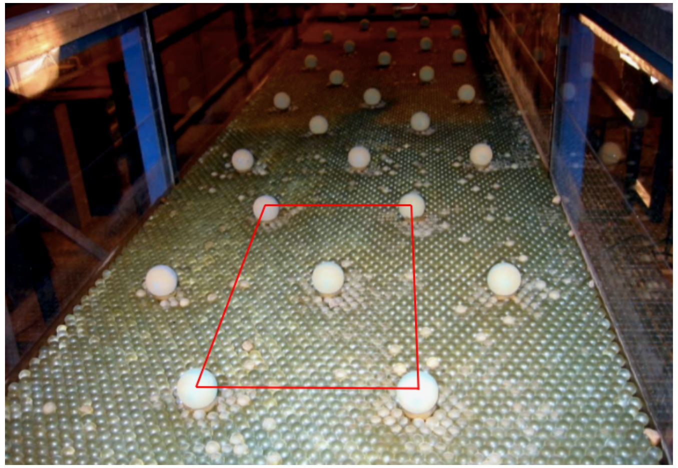

Papanicolaou et al. (2012)

$$Re = 1.505 \times 10^5 \quad Fr = 0.56$$

$$d_1 = 55 \text{ mm} \qquad h = 0.19 \text{ m}$$

$$d_2 = 18 \text{ mm} \qquad B = 0.91 \text{ m}$$

Methodology : numerical methods

- **Large-Eddy Simulation (LES):**

$$\frac{\partial \overline{u}_i}{\partial x_i} = 0 \qquad \frac{\partial \overline{u}_i}{\partial t} + u_j \frac{\partial \overline{u}_i}{\partial x_j} = -\frac{\partial \overline{P}}{\partial x_i} + \frac{1}{Re}\frac{\partial^2 \overline{u}_i}{\partial x_j \partial x_j} - \frac{\partial \tau_{ij}}{\partial x_j} + F_i$$

- **Immersed Boundary Method (IBM):** Boulders and the rough bed

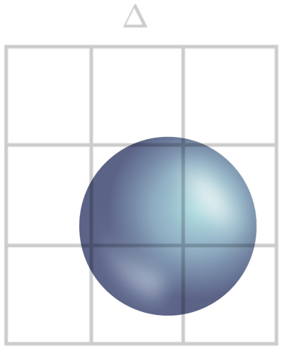

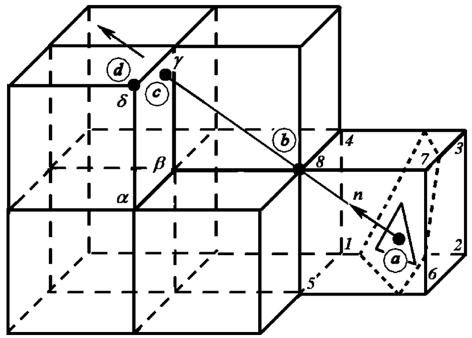

Gilmanov et al., 2003

- **Discrete Element Method (DEM):** Mobile smaller sediments

$$\frac{dx_i}{dt} = v_i \qquad m\frac{dv_i}{dt} = f_i \qquad I\frac{d\omega_i}{dt} = m_i \qquad \text{drag, gravity, added mass, Hertz-Mindlin contact model}$$

Large eddy simulation for the flow

$$\frac{\partial u_i}{\partial x_i} = 0$$

Continuity

$$\frac{\partial u_i}{\partial t} + u_j \frac{\partial u_i}{\partial x_j} = -\frac{1}{\rho_f}\frac{\partial P_i}{\partial x_i} + \frac{1}{Re}\frac{\partial^2 u_i}{\partial x_j \partial x_j} - \frac{\partial \tau_{ij}}{\partial x_j} + \frac{f_i}{\rho_f}$$

Momentum

$$\tau_{ij} - \frac{1}{3}\delta_{ij}\tau_{kk} = -2\nu_t \overline{S_{ij}}$$

$$\boxed{\nu_t = C_s \Delta^2 |\bar{S}|}$$

LES subgrid-scale model
Dynamic Smagorinsky

Dynamic subgrid scale model for LES

- ✓ Modification of the Smagorinsky model (1963) by Germano (1991) and Lilly (1962).
- ✓ The method calculates ν_t based on the smallest resolved scales and adjusts the value of the constant C_S dynamically in time and space

Strain rate Tensor

$$S_{ij} = \frac{1}{2}\left(\frac{\partial u_i}{\partial x_j} + \frac{\partial u_j}{\partial x_i}\right) \quad |S| = \sqrt{2S_{ij}S_{ij}}$$

Filters

$$\widehat{\triangle} = 2\triangle \qquad \triangle = \sqrt[3]{\triangle x \triangle y \triangle z}$$

Test filter — Grid filter

Tensors

$$L_{ij} = \widehat{u_i u_j} - \widehat{u_i}\widehat{u_j}$$

Leonard Tensor

$$M_{ij} = \widehat{\triangle}^2 \widehat{S_{ij}}\widehat{|S|} - \triangle^2 \widehat{S_{ij}|S|}$$

Dynamic Constant

$$C_s = -\frac{1}{2}\left\langle \frac{L_{ij}M_{ij}}{M_{kl}M_{kl}} \right\rangle$$

$$\boxed{\nu_t = C_s \triangle^2 |S|}$$

Turbulent viscosity

Two LES codes for the turbulent flow

In-house code (Chile)

- **Fortran 90**
- Parallelized with **MPI**
- **Non-staggered grids** with artificial dissipation (Sotiropoulus and Abdallah, 1992)
- **Structured Mesh**
- **Finite-volume** numerical method
- For the viscous fluxes, pressure gradient, and source terms, central differences (2^{st} order) are employed. For the convective term an upwind QUICK scheme is used (2^{st} order) .
- Implicit three-point-backward Euler scheme for the time derivative (2^{st} order).
- **Artificial compressibility** method (AC) (Constantinescu and Sotiropoulos, 1997)
- Outputs: **Tecplot** visualization.

OpenFOAM

- **C++**
- Parallelized with **MPI**
- **Staggered grids**
- **Structured/unstructured mesh**
- **Finite-volume** numerical method
- Different schemes can be used of 1^{st} and 2^{st} order depending on the term. Eg: Gauss upwind, Gauss linear (div schemes); upwind, linear, linear upwind, TVD schemes, limited linear (convective terms), etc
- Euler (implicit/explicit, 1^{st} order), Backward Euler (implicit, 2^{st} order), Cranck Nickelson (implicit, 2^{st} order) for time derivative
- **Poisson Equation (SIMPLE, PISO, PIMPLE)**
- Outputs: **VTK** format and **Paraview** visualization.

Immersed boundary method

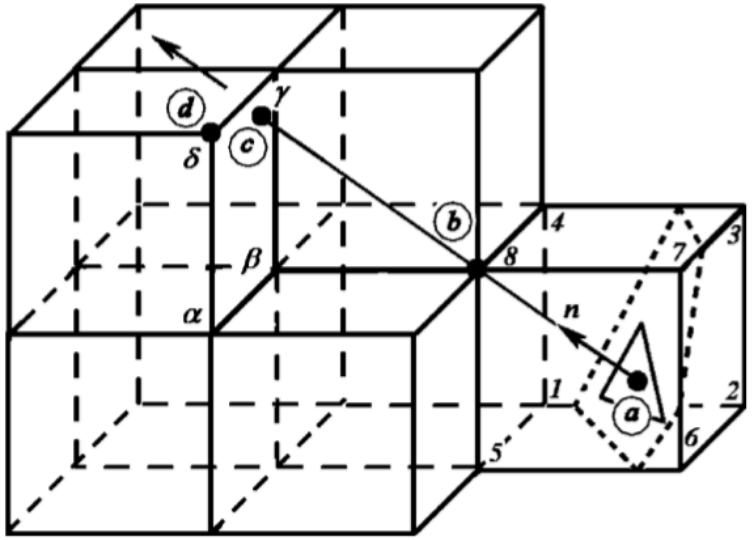

Gilmanov et al. (2003)

- **a: Sphere surface,**

$$u = v = w = \frac{dP}{dn} = 0$$

- **b: IBM-node**

  u, v, w, P to be determined

- **c: Projected point**

  u, v, w, P interpolated using the values of the face

STEPS:

- Interpolate $\boldsymbol{u}, \boldsymbol{v}, \boldsymbol{w}, \boldsymbol{P}$ at ***point c*** using the values of the face
- Calculate $\boldsymbol{dP/dx}, \boldsymbol{dP/dy}$ and $\boldsymbol{dP/dz}$ in each node of the face
- Interpolate $\boldsymbol{dP/dx}, \boldsymbol{dP/dy}$ and $\boldsymbol{dP/dz}$ at ***point c*** using the values of the face
- Compute $\boldsymbol{dP/dn}$ at ***point c*** multiplying by normal direction
- Having the values of $\boldsymbol{u}, \boldsymbol{v}, \boldsymbol{w}$ at ***point c*** and ***point a,*** interpolate values at ***point b***
- Interpolate $\boldsymbol{dP/dn}$ at **midpoint of b-c** using the values of points **a** and **c**
- Having the values of $\boldsymbol{dP/dn}$ at **point c** and **midpoint of b-c,** interpolate values at ***point b***

Immersed boundary method – wall model

$$\frac{1}{\rho}\frac{\partial}{\partial l}\left((\mu+\mu_t)\frac{\partial u_s}{\partial l}\right)=\frac{1}{\rho}\frac{\partial p}{\partial s}+\frac{\partial u_s}{\partial t}+\frac{(\partial u_l u_s)}{\partial s}$$

Boundary Layer Equation

Neglecting the righ-hand side terms the equilibrium stress model is obtained:

$$\frac{1}{\rho}\frac{\partial}{\partial l}\left((\mu+\mu_t)\frac{\partial u_{si}}{\partial l}\right)=0.$$

$$\tau_w=\mu\left.\frac{\partial u_s}{\partial l}\right|_{l=0}=\frac{1}{\int_0^{\delta_c}\frac{1}{\mu+\mu_t}dl}(u_s(\delta_c)-u_s(0)),$$

$$\rho u_\tau^2=\tau_w,$$

u_s: velocity at tagential direction

Mixing length model with the near-wall damping

$$\mu_t=\mu\kappa l^+(1-e^{-l^+/19})^2$$

$$l^+=\rho u_\tau l/\mu$$

Immersed boundary methods – wall model

$$s_i = \frac{u_i^C - \left(u_j^C l_j\right) l_i}{\left|u_i^C - \left(u_j^C l_j\right) l_i\right|},$$

Tangential direction

Once u_τ is computed, the **tangential velocity** component at the first off wall node (point b, IBM-node) is obtained by:

$$u_s(\delta_b) = \frac{\int_0^{\delta_b} \frac{1}{\mu+\mu_t} dl}{\int_0^{\delta_c} \frac{1}{\mu+\mu_t} dl} \left(u_s(\delta_c) - u_s(0)\right) + u_s(0)$$

The **normal velocity** component at the IB nodes is obtained by the wall normal linear interpolation method.

IBM vs body-fitted meshes

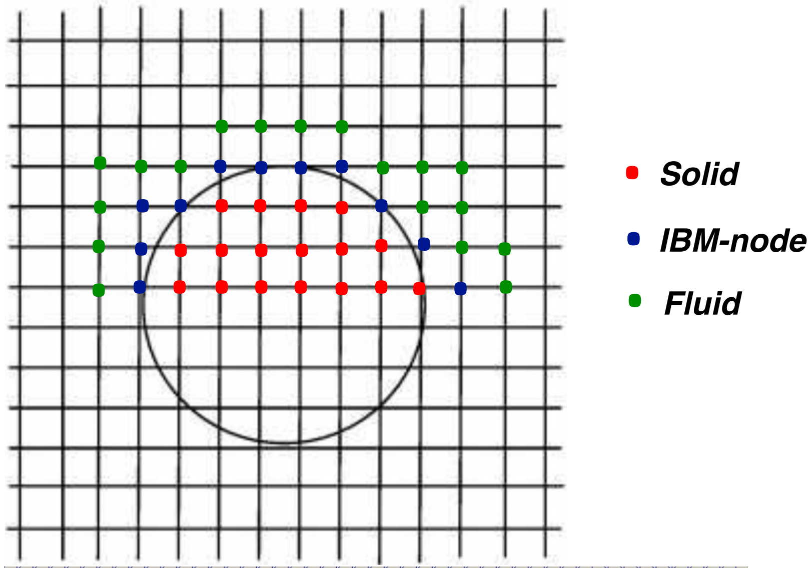

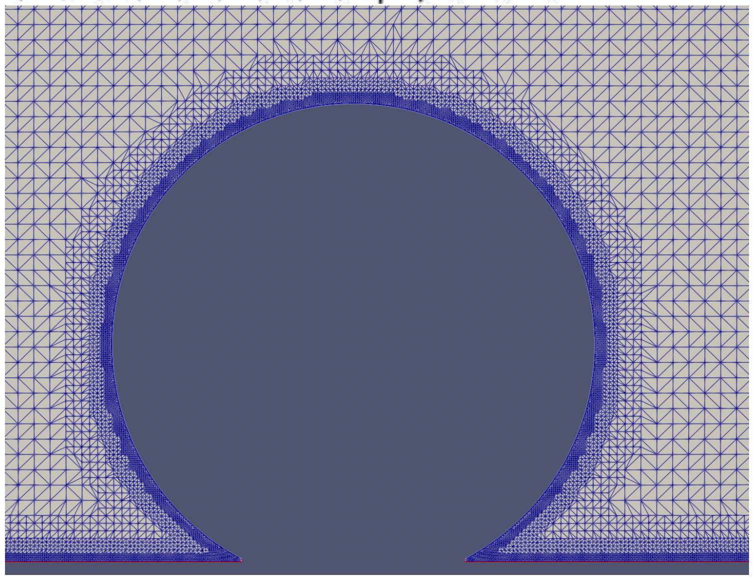

IBM

- A method needs to be implemented but no complex mesh is required
- Allows to have a uniform grid which is needed for particles. Results depend on the method.

Body-fitted mesh

- No method needs to be implemented but a complex mesh is required.
- The results strongly depend on the mesh (***structured vs unstructured).***

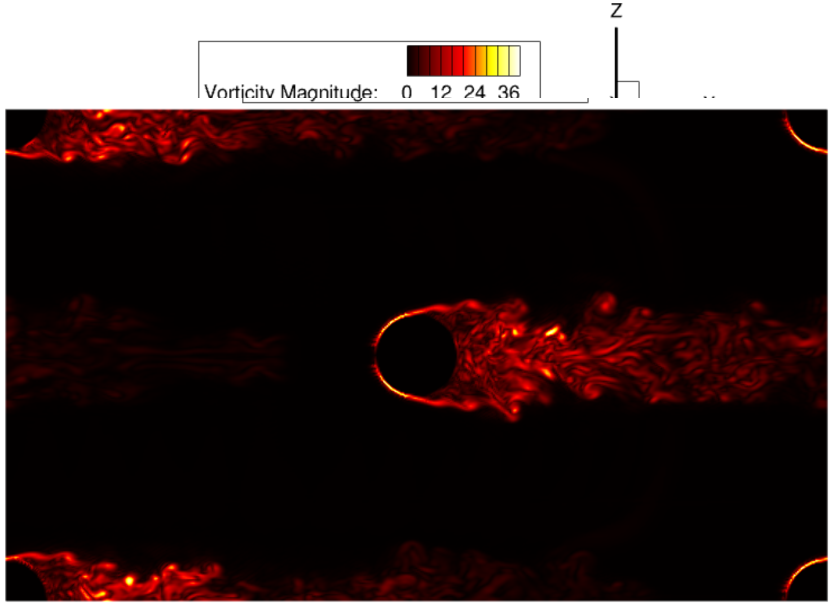

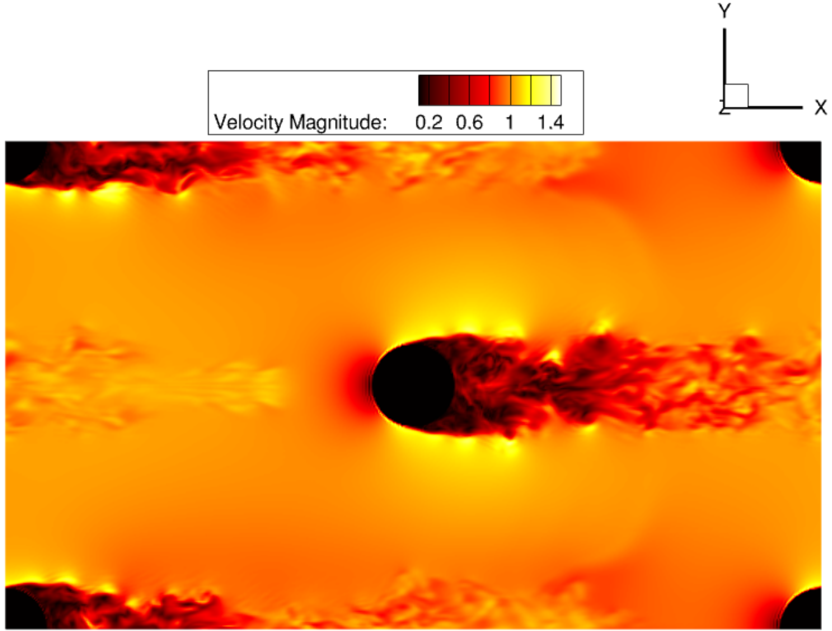

IBM vs body-fitted meshes

In-house code + LIGGGHTS

- **33.3 million** grid points
- **IBM** based on Gilmanov et al. (2003), Kang et al. (2011) **Discrete forcing approach**
- **Wall is modeled** (boundary layer equation)

$$\frac{1}{\rho}\frac{\partial}{\partial l}\left((\mu+\mu_t)\frac{\partial u_{si}}{\partial l}\right)=0.$$

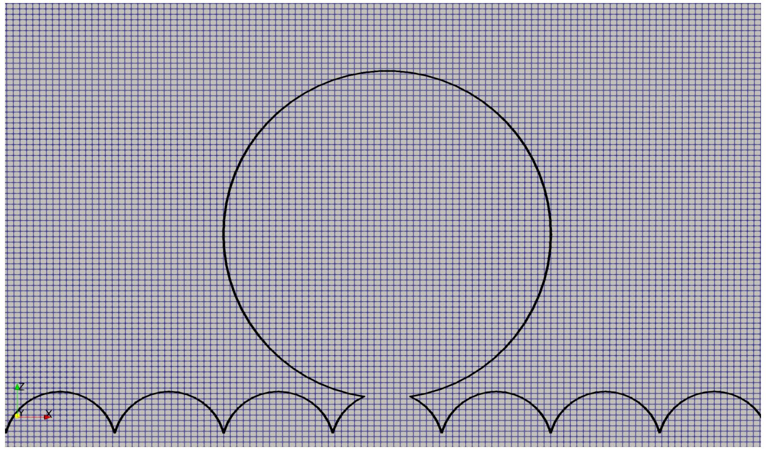

OpenFOAM

pimple_lagrangian solver

- **38 million** grid points
- ***Unstructured grid*** using SnappyHexMesh
- Boundary layer is **resolved** ($\mathrm{d_{min}} = \mathbf{0.5}\boldsymbol{d}^{+}$)

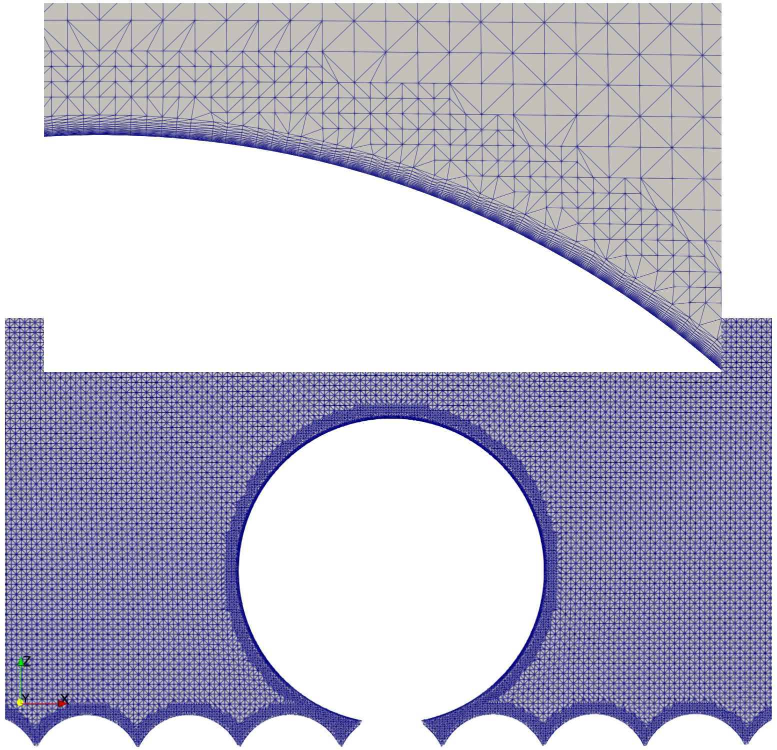

Array of boulders over a rough bed

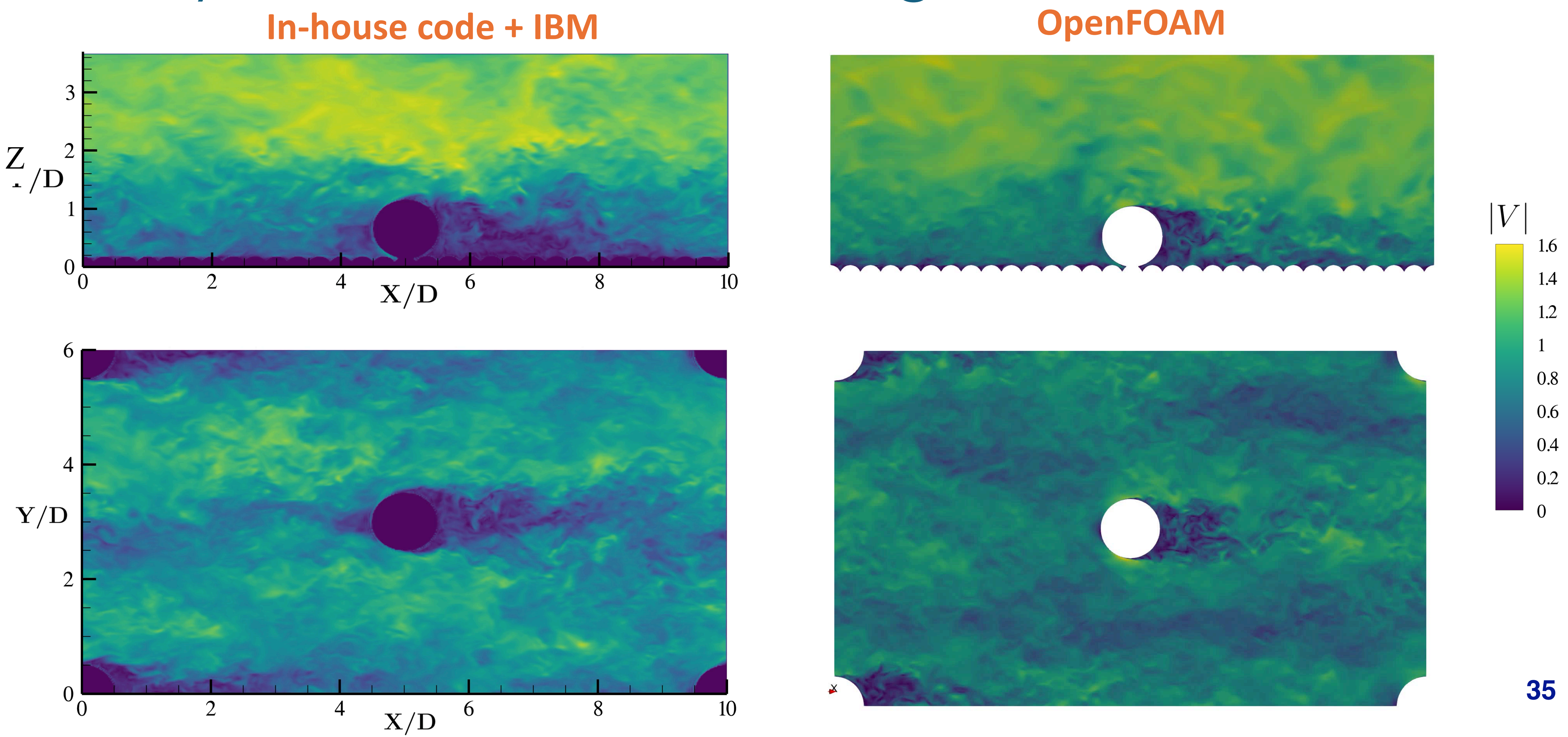

Array of boulders over a rough bed

In-house code + IBM

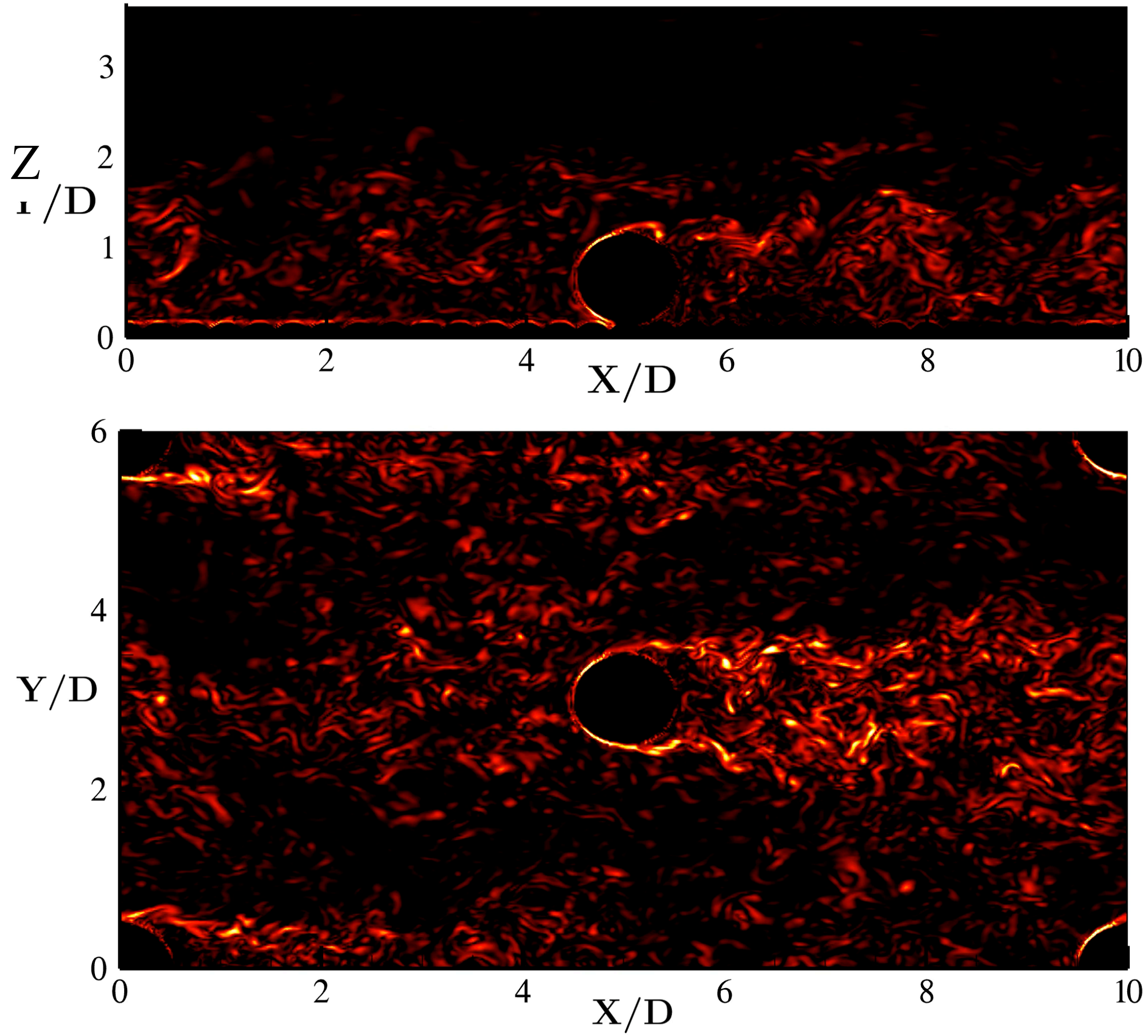

OpenFOAM

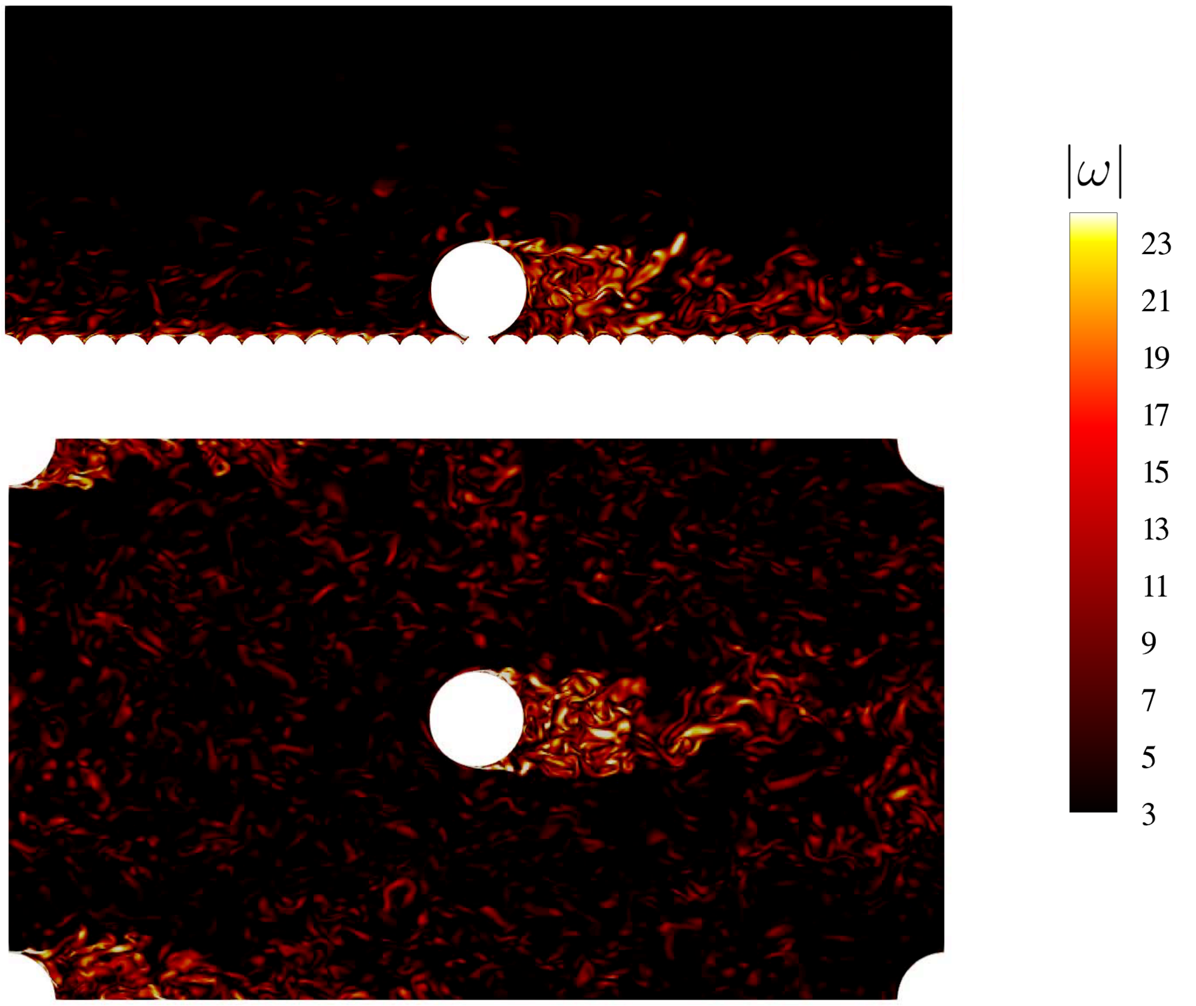

ÉCOLE DE
PHYSIQUE DES HOUCHES

February 9-14, 2025
Les Houches

Comparison with experiments

Mean Velocity

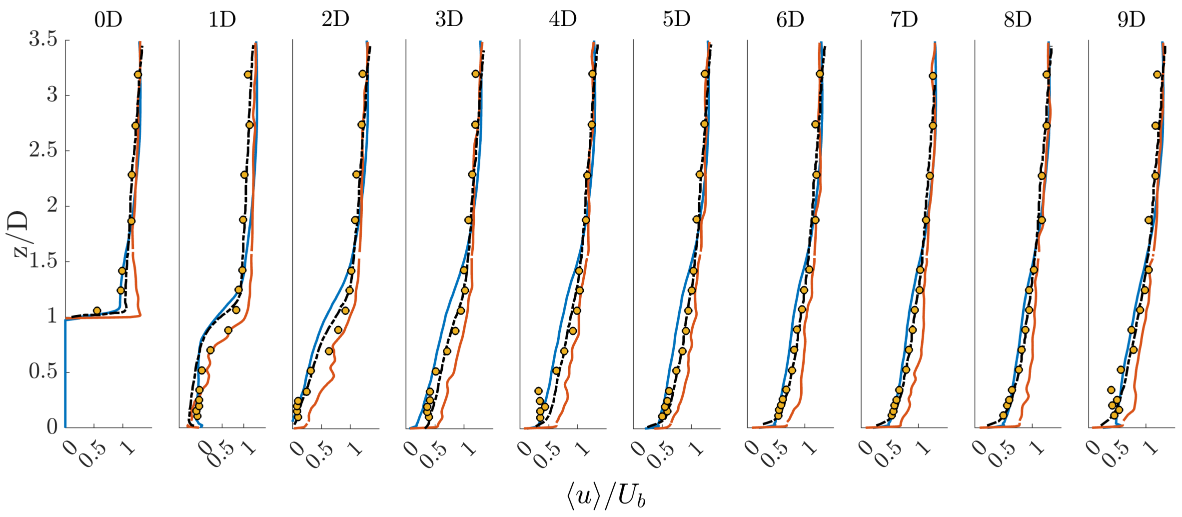

Streamwise Turbulent Intensity

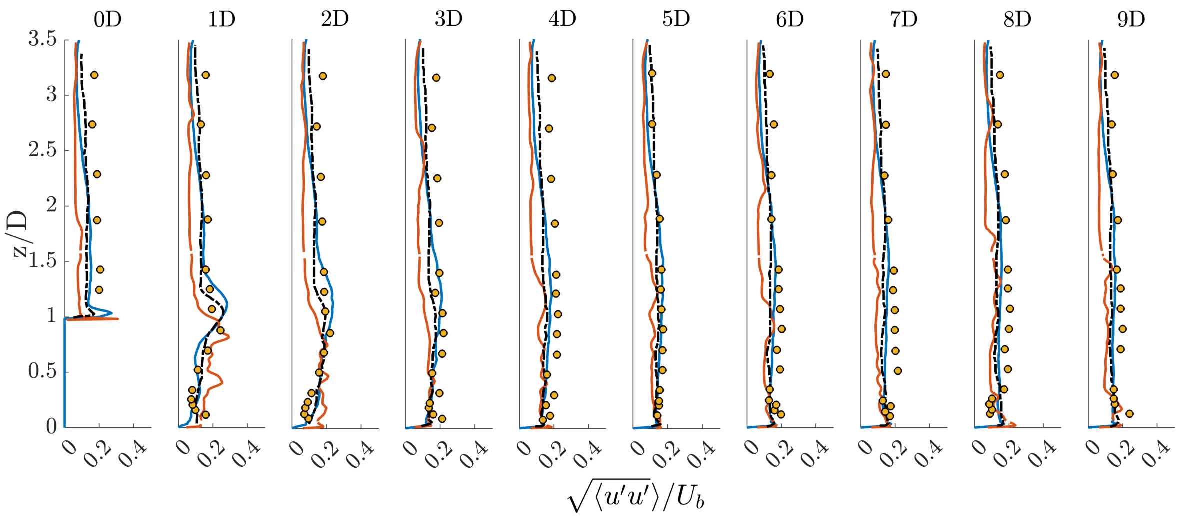

In-house code + IBM   OpenFOAM   Liu et al. (2017)   Experiments

Lagrangian particle tracking coupled with LES

Force balance on the particles

$$\left(\rho_p - \frac{\rho_f}{2}\right)V_p\frac{\partial v_{pi}}{\partial t} = \underbrace{(\rho_p - \rho_f)V_p g_i}_{\text{Gravity \& Buoyancy}} + \underbrace{\frac{1}{2}\rho_f C_D A|u_i - v_{pi}|(u_i - v_{pi})}_{\text{Drag}} + \underbrace{\frac{3}{2}\rho_f V_p\frac{Du_i}{Dt}}_{\text{Fluid stresses \& Added mass}} + \underbrace{F_c}_{\text{Contact \& Collisions}}$$

Collision/Contact Model

Hertz- Mindlin granular contact model

$$F_c = F_n + F_t$$

Clift and Gauvin (1970) for $Re_r < 10^5$

$$C_D = \frac{24}{Re_r}\left(1 + 0.15Re_r^{0.687} + 0.0175\left(1 + 42,500Re_r^{-1.16}\right)^{-1}\right)$$

Coupling with the flow

$$\frac{\partial u_i}{\partial t} + u_j\frac{\partial u_i}{\partial x_j} = -\frac{1}{\rho_f}\frac{\partial P_i}{\partial x_i} + \frac{1}{Re}\frac{\partial^2 u_i}{\partial x_j \partial x_j} - \frac{\partial \tau_{ij}}{\partial x_j} + \frac{f_i}{\rho_f} + \frac{F_i}{\rho_f}$$

$$\boxed{F_i = \frac{F_{fi}}{\triangle V}\frac{L}{\rho U^2}}$$

Lagrangian particle tracking coupled with LES

- The grid size is smaller than the particle diameters

$$\boxed{d_p = 3\Delta x_i}$$

- Therefore, it is necessary to filter the fluid velocity and acceleration (needed to calculate the coupling forces).
- The idea is to calculate the fluid velocity and acceleration that feels the particle which correspond to the undisturbed flow.
- We use a Gaussian filter with a size of

$$\boxed{\Delta_G = 1.7 d_p}$$

- We distribute the coupling force into the fluid using the same Gaussian weight in the sphere which diameter is the filter size.

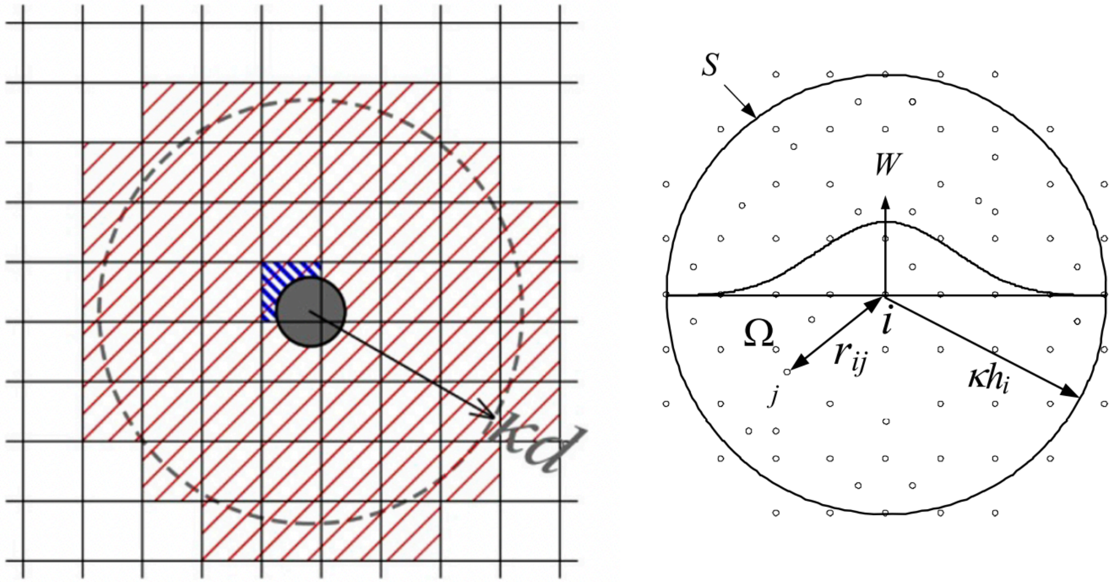

Wang et al. (2019)

$$\tilde{\mathbf{U}}_r = \mathbf{u}_p - \mathbf{U} = \mathbf{u}_p - \frac{\sum_{j=1}^{N} \mathbf{U}(\mathbf{r}_j) \exp(-\frac{|\mathbf{r}-\mathbf{r}_j|^2}{2(\kappa d)^2}) \Delta V_j}{\sum_{j=1}^{N} \exp(-\frac{|\mathbf{r}-\mathbf{r}_j|^2}{2(\kappa d)^2}) \Delta V_j}.$$

Wang et al. (2019)

Two codes for Lagrangian particle tracking

In-house code (Chile) + LIGGGHTS

- **Fortran 90** (in-house), **C++** (LIGGGHTS)
- Parallelized with **MPI**
- Solve the Newton's equation of motion for each particle
- Fluid forces calculated in the in-house code and give it to **LIGGGHTS.**
- Soft-sphere model: Hertz-Mindlin theory (spring-dashpot model). **Multiple colisions**
- List of **neighbouring particles** to track nearby particles.
- Outputs: **Tecplot** visualization (Flow) and **VTK** format and **Paraview** visaulization (particles).

OpenFOAM

pimple_lagrangian solver

- **C++**
- Parallelized with **MPI**
- Solve the Newton's equation of motion for each particle
- Fluid forces calculated in **OpenFOAM:** SphereDrag, PressureGradient, etc
- Soft-sphere model: Hertz-Mindlin theory (spring-dashpot model). **Multiple colisions**
- Outputs: **VTK** format and **Paraview** visaulization.

Bedload transport with Discrete Element Method (DEM)

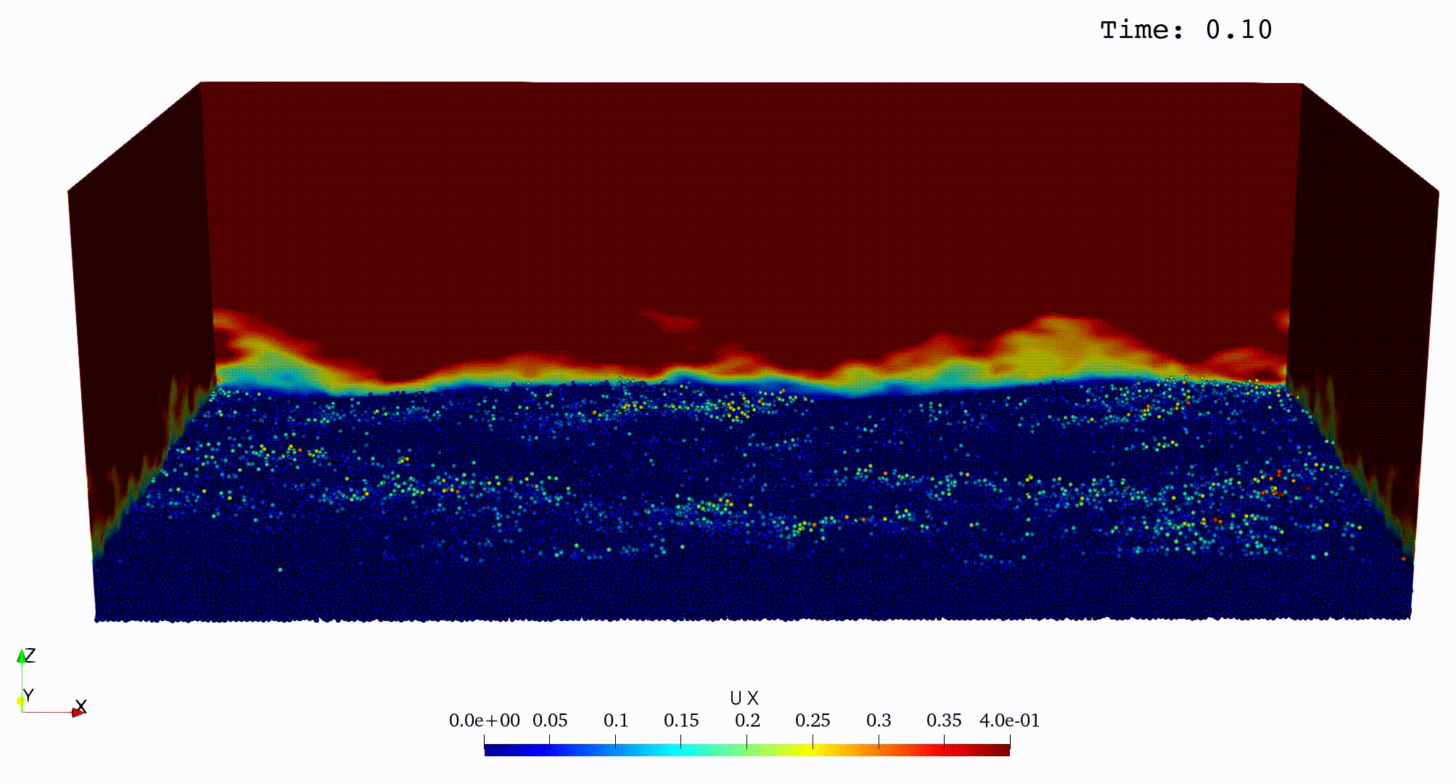

Shields number

$$\theta = \frac{\tau_{bed}}{(\rho_p - \rho_f)gd}$$

Stokes number

$$St = \frac{\tau_p}{\tau} \qquad \tau_p = \frac{\rho_p d_p^2}{18\mu}$$

Number of particles

- Mobile particles 29,304.
- Contacts and collisions with the immobile boulders and rough-bed
- $C_v: 1.5 \cdot 10^{-2}$ Four-way coupling

Particle characteristics

- $d_p = 0.33\ cm$
- ρ_p variable
- $Re_\tau = 257$

Mobility Condition

- variable

$$Re_\tau = \frac{d_p u_*}{\nu} \qquad \theta = \frac{\tau_{bed}}{(\rho_p - \rho_f) g d_p}$$

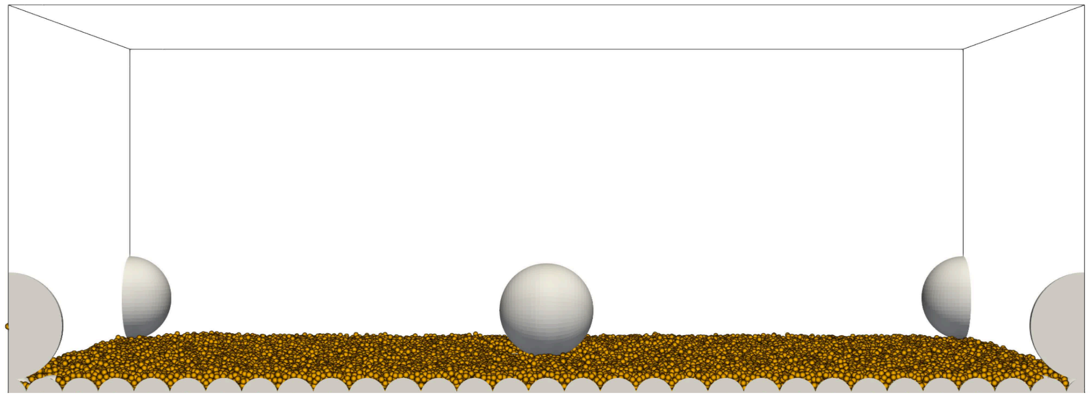

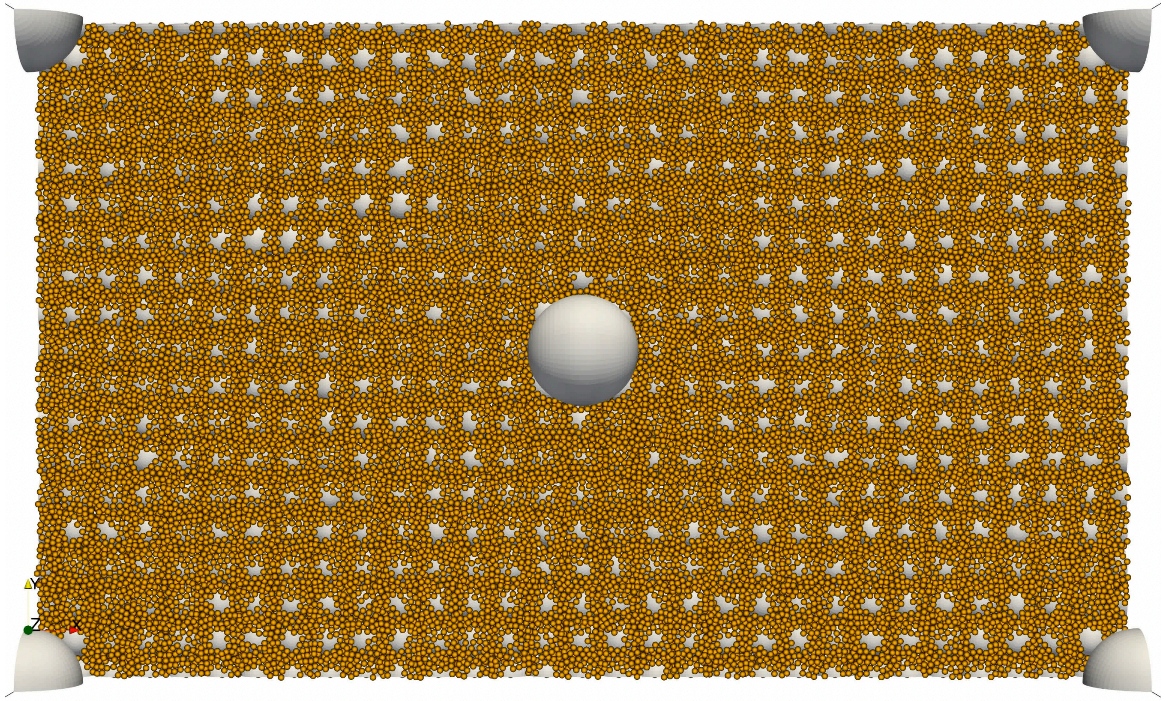

Mobility condition for sediments

Shields number

$$\theta = \frac{\tau_{bed}}{(\rho_p - \rho_f) g d_p} \qquad d_p = 0.0033\, m$$

$$u_* = 0.085\, m/s \qquad \tau_0 = \rho u_*^2 = 7.23\, Pa$$

$$Re_p^* = \frac{u_* d_p}{\nu} = 140 \qquad \theta_c = 0.05$$

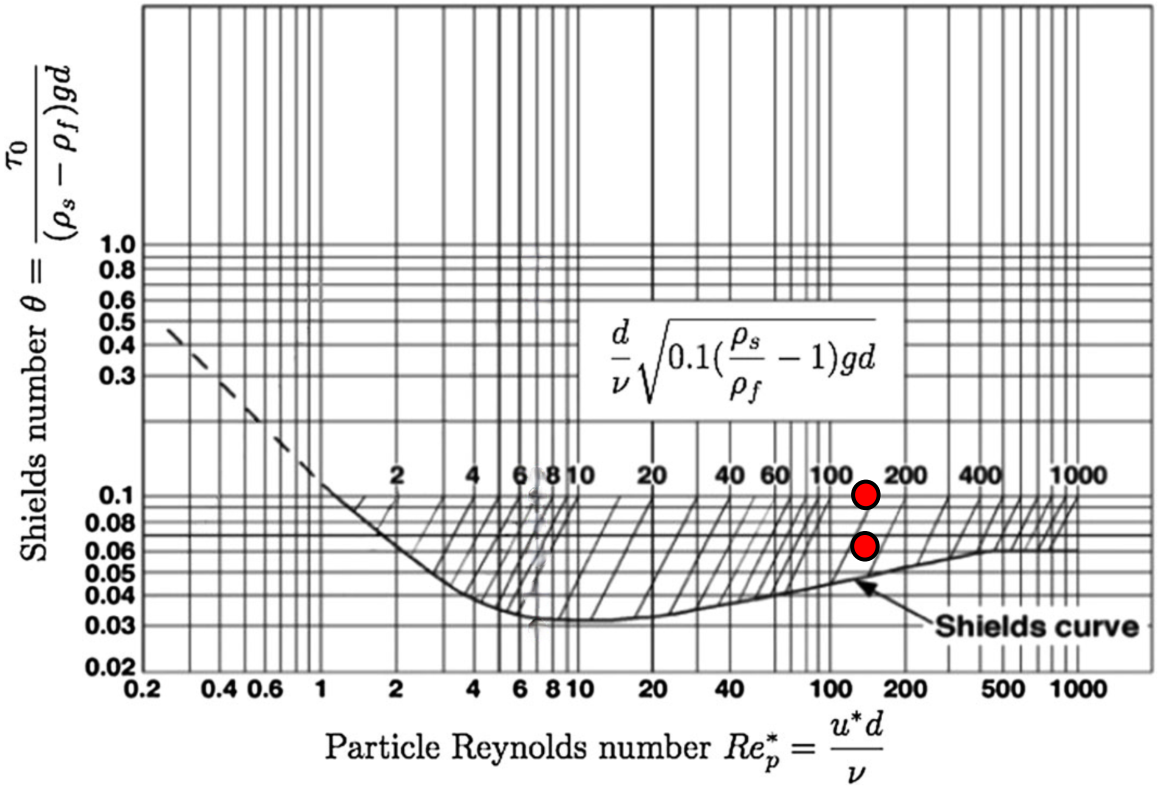

Case I

$$\rho_p = 2650\, \frac{kg}{m^3}$$

$$\boldsymbol{\theta_c = 0.0495}$$
$$\boldsymbol{\theta = 0.135}$$

Case II

$$\rho_p = 4500\, \frac{kg}{m^3}$$

$$\boldsymbol{\theta_c = 0.0495}$$
$$\boldsymbol{\theta = 0.064}$$

Stokes number

$$St = \frac{\tau_p}{\tau} \qquad \tau_p = \frac{\rho_p d_p^2}{18\mu}$$

Outline

1. General introduction
2. Introduction on Large eddy simulation
3. Introduction on modelling particle – laden turbulent flows
4. Example study : Bedload transport around boulders in river flows
    - Analysis of the flow
    - Particle transport and fluxes
5. Other examples of studied issues
    - Particle transport in street canyons
    - Particle transport above dunes
6. Conclusions and perspectives

Instantaneous flow

33.3 million grid points

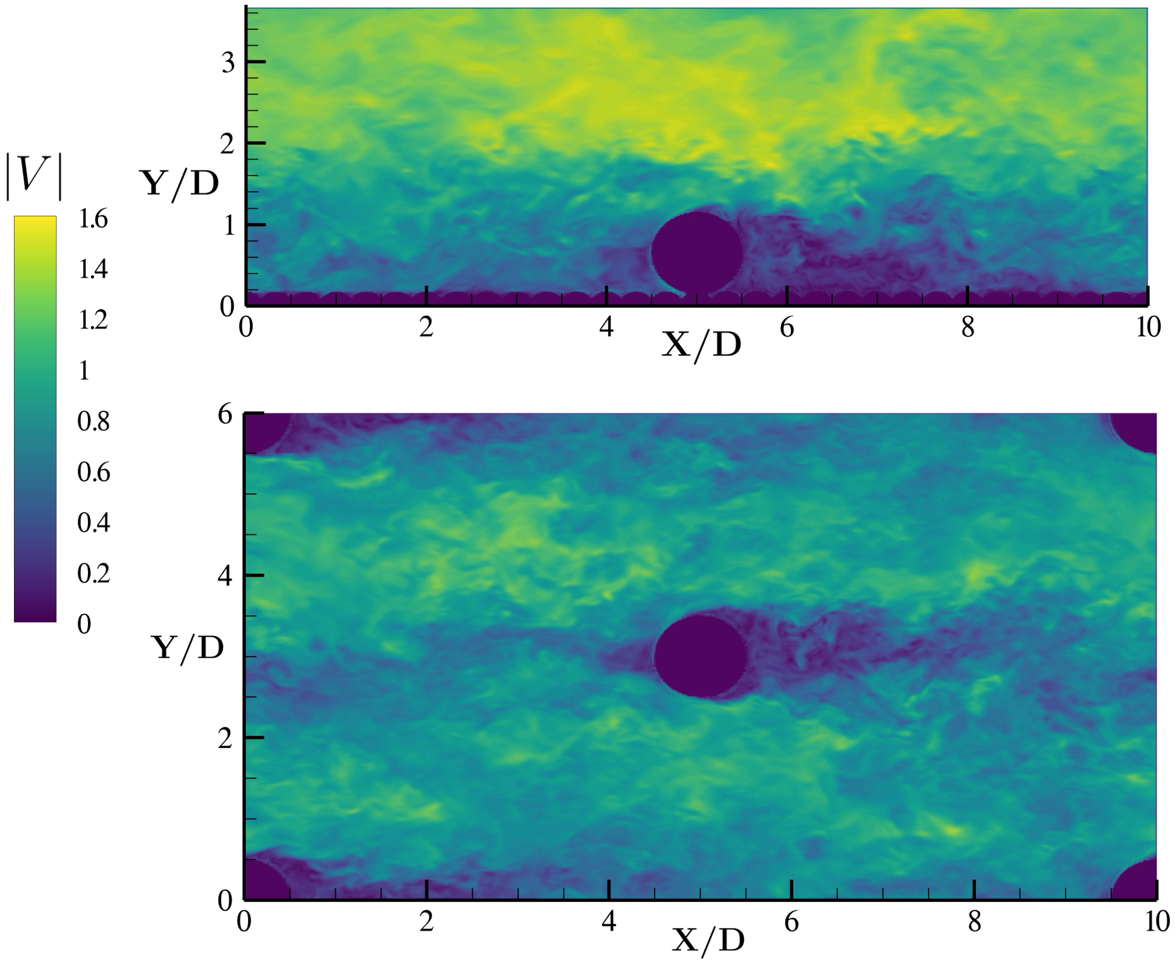

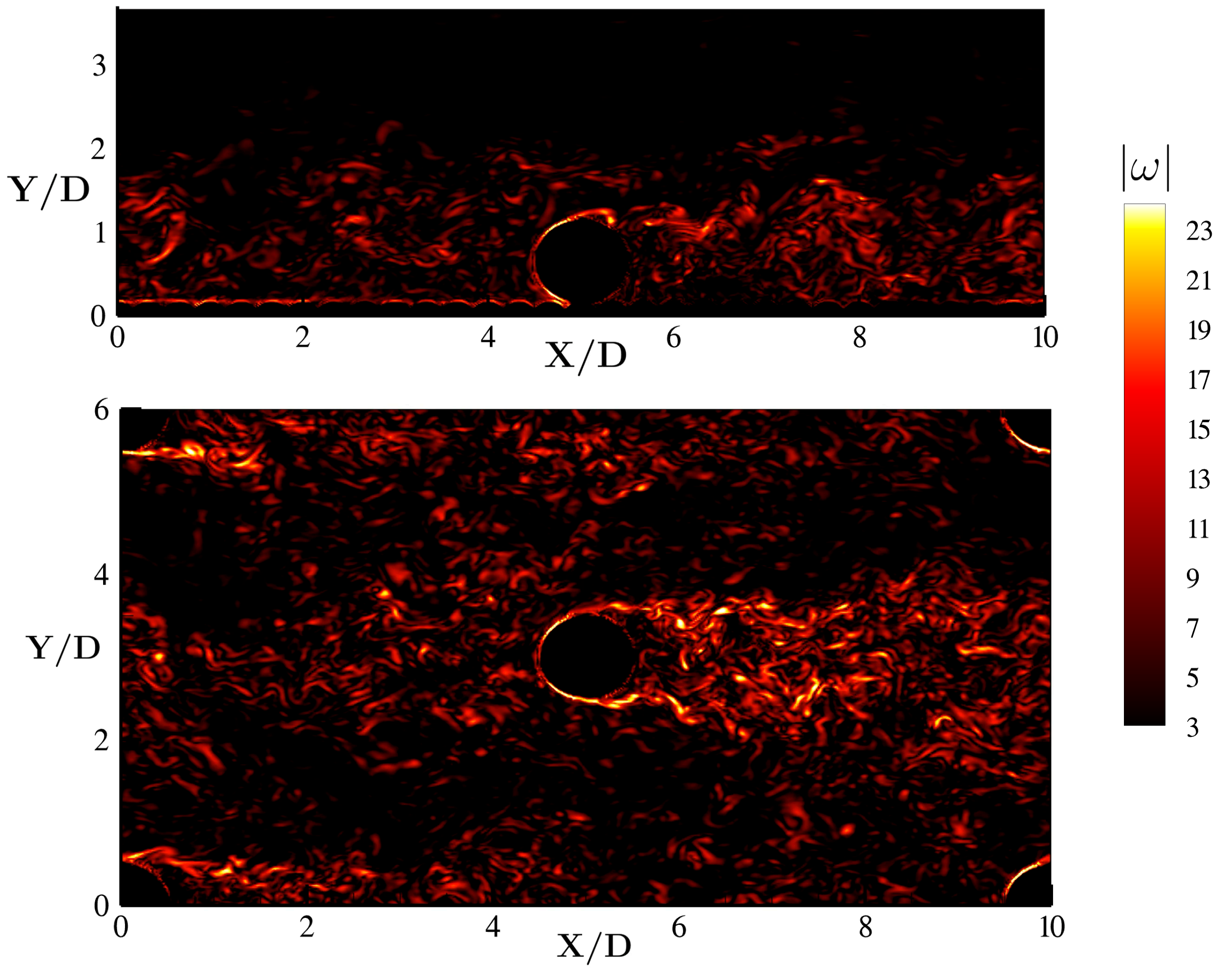

Validation and comparison with experiments

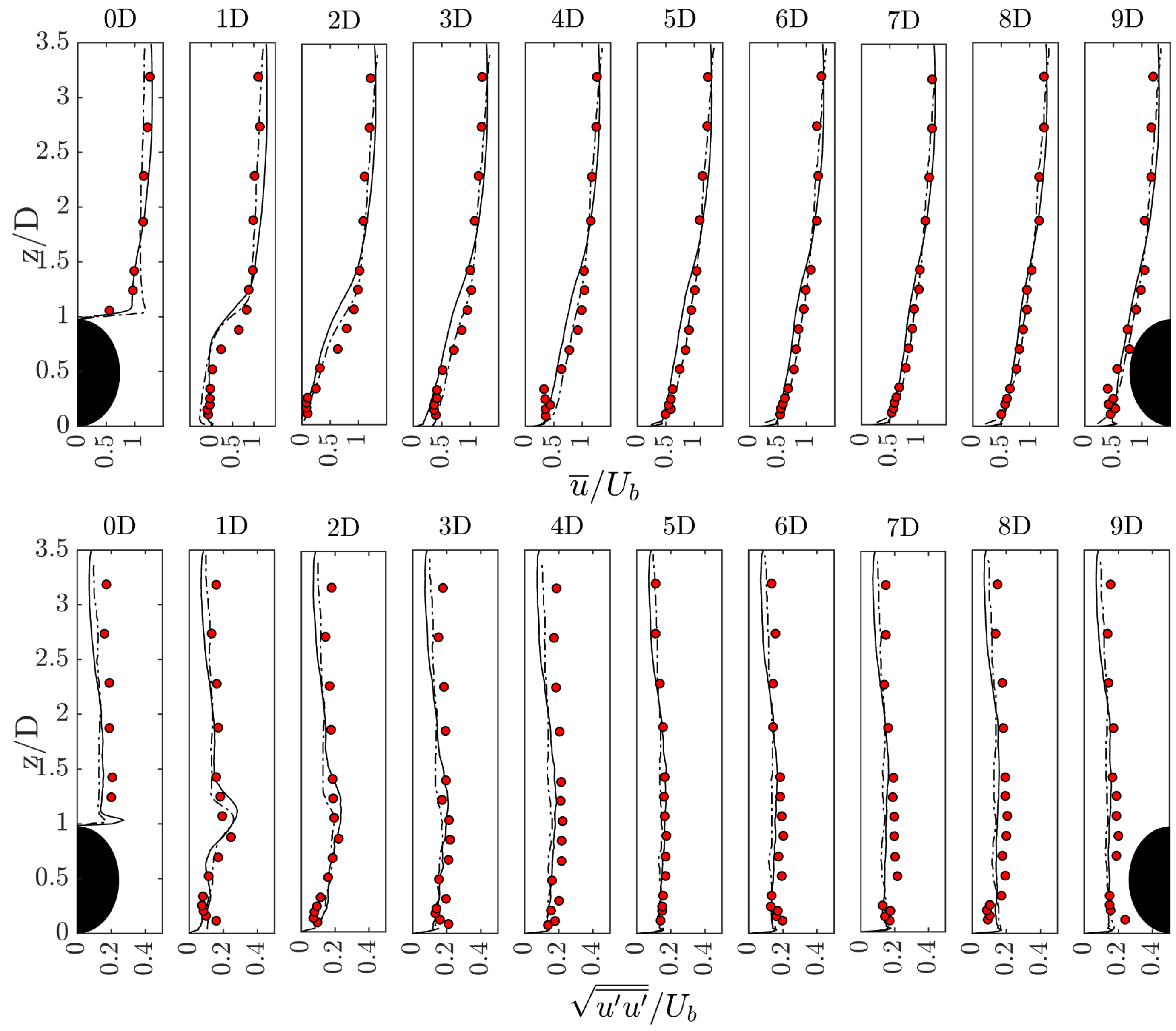

- Comparison between the **LES** results (black continuous line), the **experimental data** of Papanicolaou et al. (2012) (red circles) and the **simulation of Liu et al. (2017)** (black dash line).
- **Mean velocity** is depicted at the **top** and **root-mean-square** of the streamwise velocity fluctuation is shown at the **bottom.**
- **Good agreement** between the simulation and the experimental data.

Q - criterion $q = \frac{1}{2}\left(\Omega_{ij}\Omega_{ij} - S_{ij}S_{ij}\right)$

- High vorticity and large-scale **coherent structures** in the **wake** of the boulders emerge from the **shear layer** and travel downstream.

- Two types of structures are identified:
  - vertically oriented **arch vortices**
  - **hairpin-like vortices** advected downstream and deformed by high shear

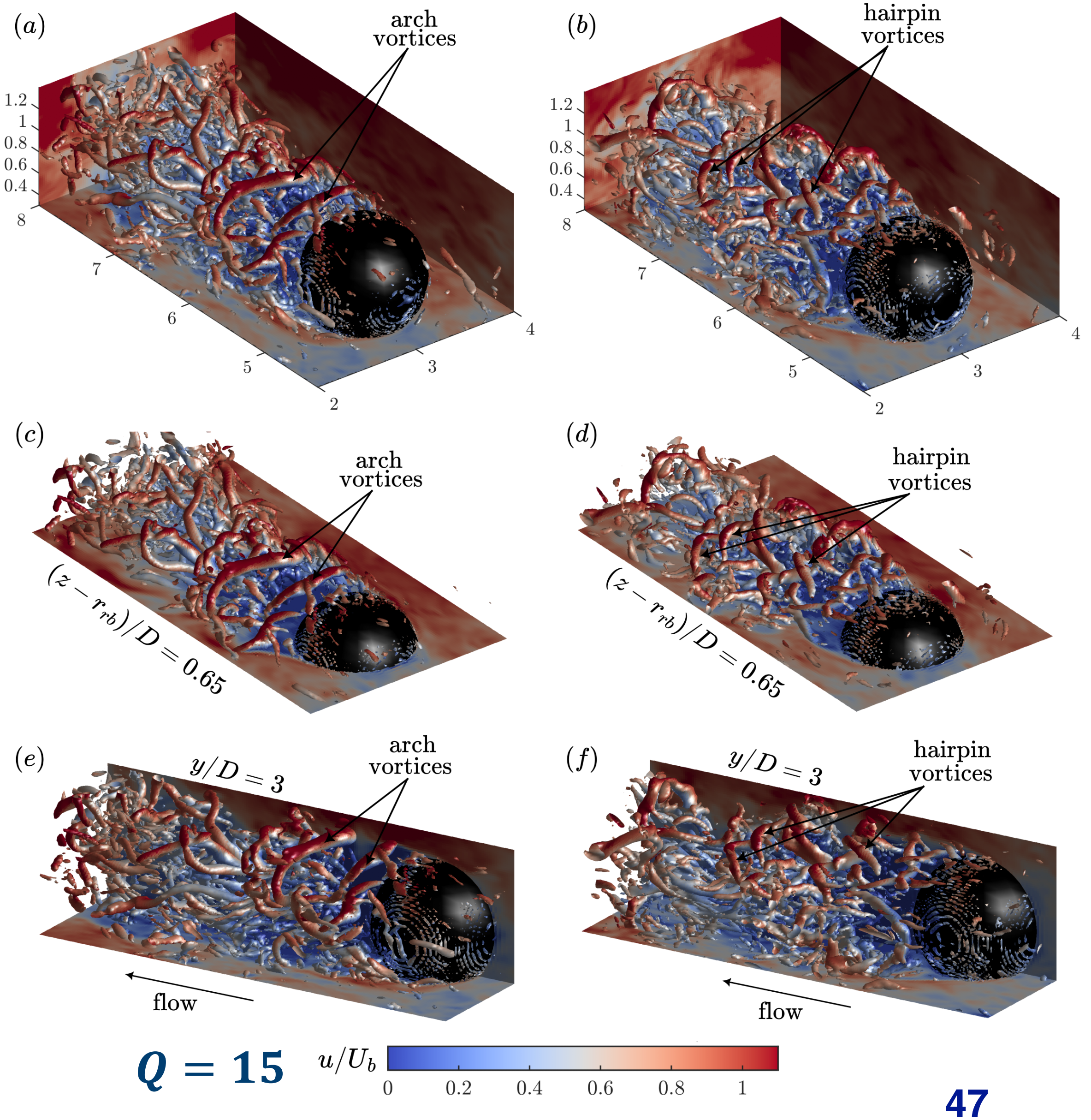

Double – averaged approach (DAM)

- **DAM** consists of **spatially averaging the RANS** equations, resulting in a new set of mass and momentum conservation equations which are averaged both in **time** and **space**.

- Temporal decomposition of the instantaneous flow:

$$u_i = \overline{u_i} + u_i'$$

- Spatial decomposition of the time-averaged flow

$$\overline{u_i} = \langle \overline{u_i} \rangle + \widetilde{u_i}$$

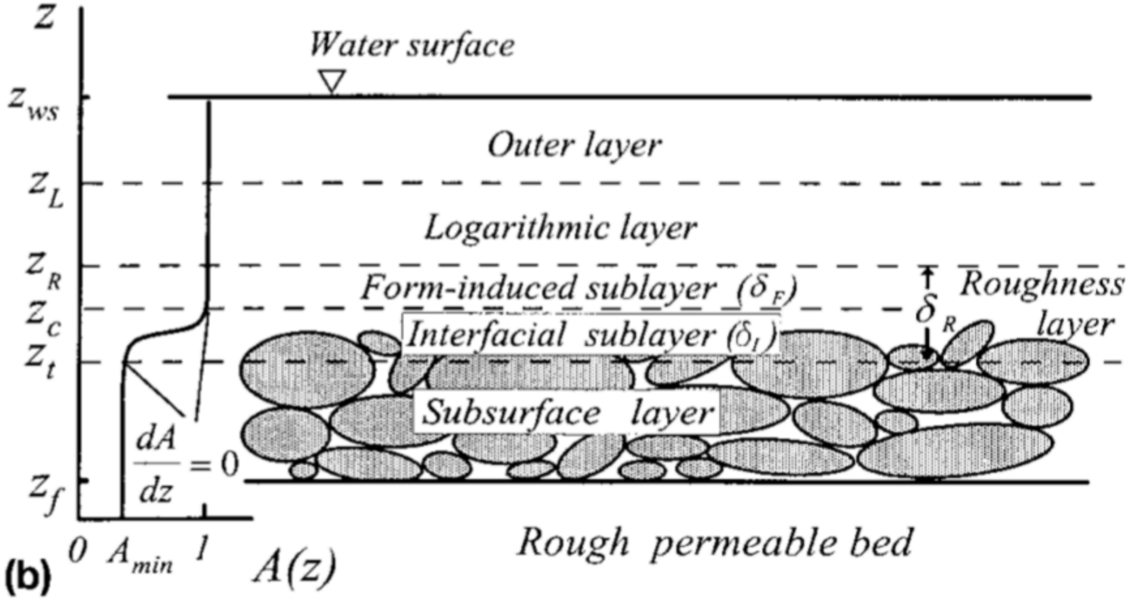

Nikora et al., 2001

Spatial flow variations

- **DAM** offers the possibility to **upscale** the microscale turbulence produced at the level of the **roughness elements** that involve separation and recirculation patterns, and result in **viscous and form drag.**

- Allow to include the **effects** of the **microscale variations** on the **conservation equations through the new terms.**

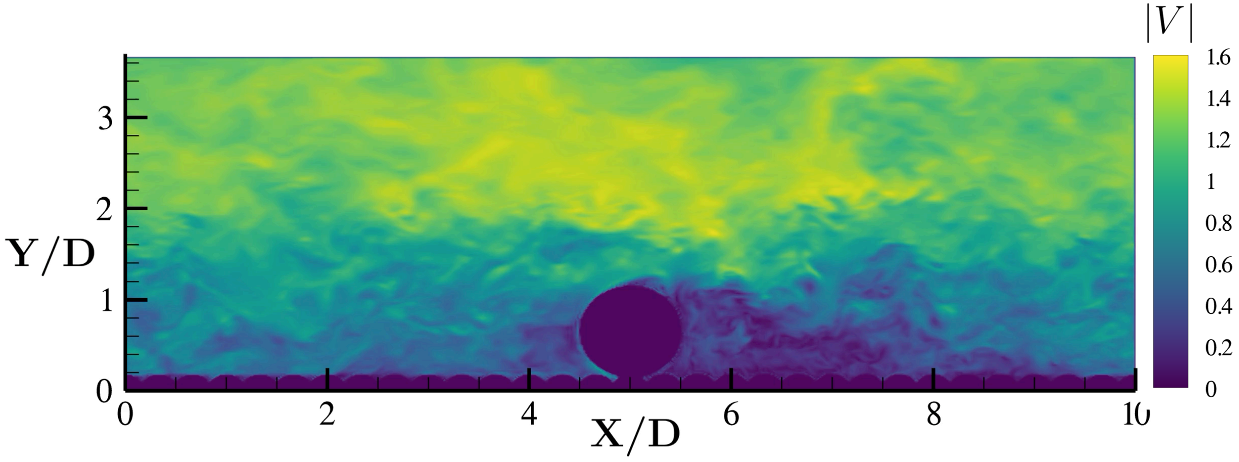

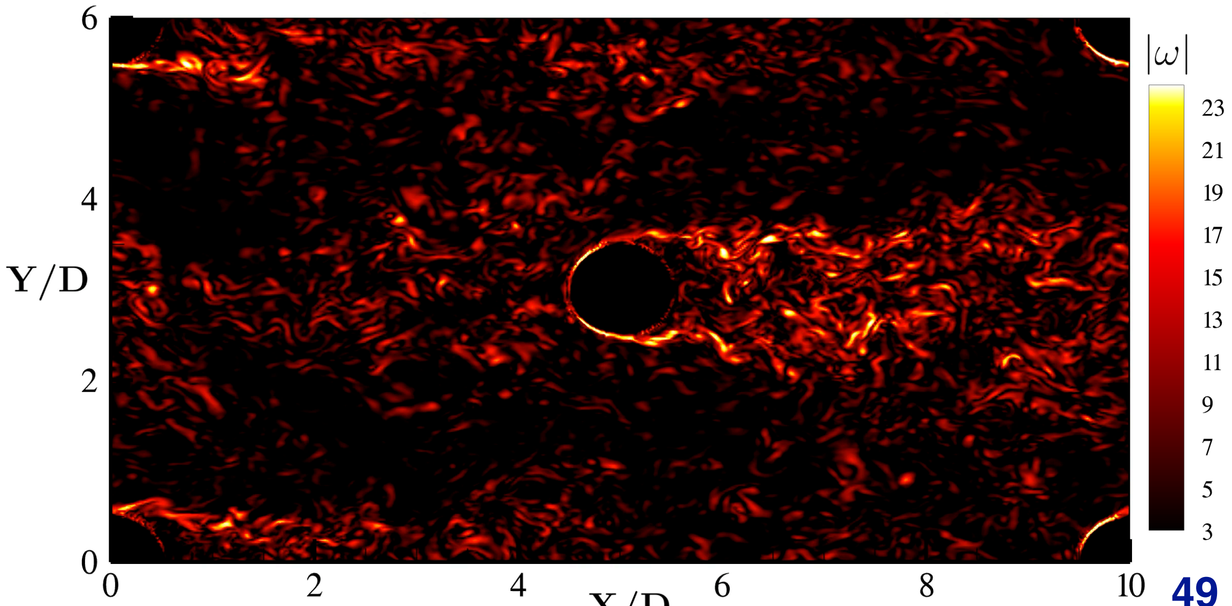

Double averaged flow

- The average is performed over **thin slabs** that consider the entire horizontal area and the grid spacing Δz.
- The choice of the volume is justified by the fact that a large region is needed to include all **spatial disturbances** of the time-averaged quantities to reach a:

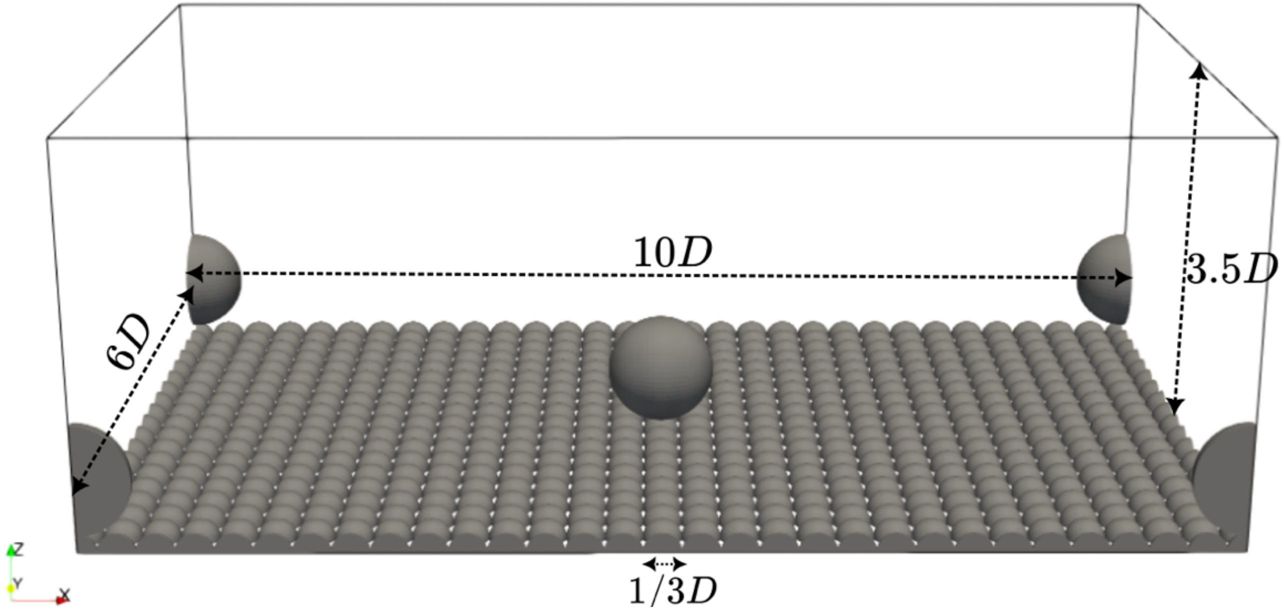

Steady, uniform and fully developed DA flow:

$$\langle \bar{v} \rangle = \langle \bar{w} \rangle = \frac{\partial \langle \bar{.} \rangle}{\partial x} = \frac{\partial \langle \bar{.} \rangle}{\partial y} = \frac{\partial}{\partial t} = 0$$

Averaging volume

Double averaged procedure (DA)

- **Temporal** and then a **spatial** decomposition

$$u_i = \overline{u_i} + u_i'$$
$$\overline{u_i} = \langle \overline{u_i} \rangle + \tilde{u_i}$$

- Applied to the **momentum** and kinetic **energy** budgets

- The intrinsic **average** is performed over **thin slabs** that consider the entire horizontal area and the grid spacing Δz.

- The DA flow is **steady** and **statistically one-dimensional**, with velocity statistics varying only along z.

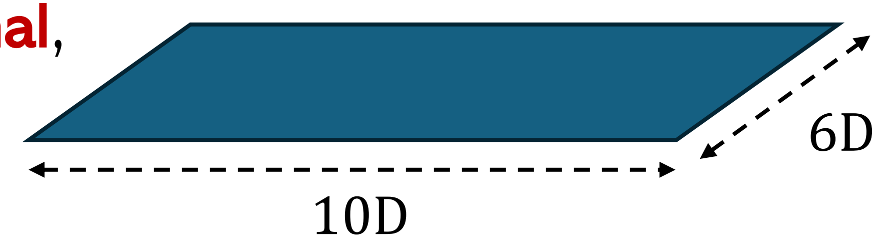

Objectives

General

- Determine the **DA turbulent flow** over an array of boulders over a rough bed

Specific

- Explain how the **3-D flow features** generated around the roughness elements contribute to the **new terms** in the **DA balances**, specially to form-induced stresses, MKE, TKE and WAKE budgets.

- Evaluate **form-induced stresses** and **total drag** to improve **bedload transport prediction.**

DA momentum conservation equations

- The DA streamwise momentum conservation equation reduce to a **shear stress balance**:

$$\left(1-\frac{\phi z}{h}\right)u_*^2 = \underbrace{\overset{\text{turbulent}}{-\phi\left\langle\overline{u'w'}\right\rangle} \overset{\text{form-induced}}{-\phi\left\langle\tilde{u}\tilde{w}\right\rangle} + \nu\phi\left\langle\frac{\partial\overline{u}_i}{\partial z}\right\rangle}_{\tau_{fluid}}$$

total fluid stresses

total drag

$$\underbrace{\int_z^{z_c}\frac{1}{\rho V_0}\iint_{S_{\text{int}}}\overline{p}n_i dS\,dz}_{\tau_p}$$

$$\underbrace{-\int_z^{z_c}\frac{\nu}{V_0}\iint_{S_{\text{int}}}\frac{\partial\overline{u}_i}{\partial x_j}n_j dS\,dz}_{\tau_v}$$

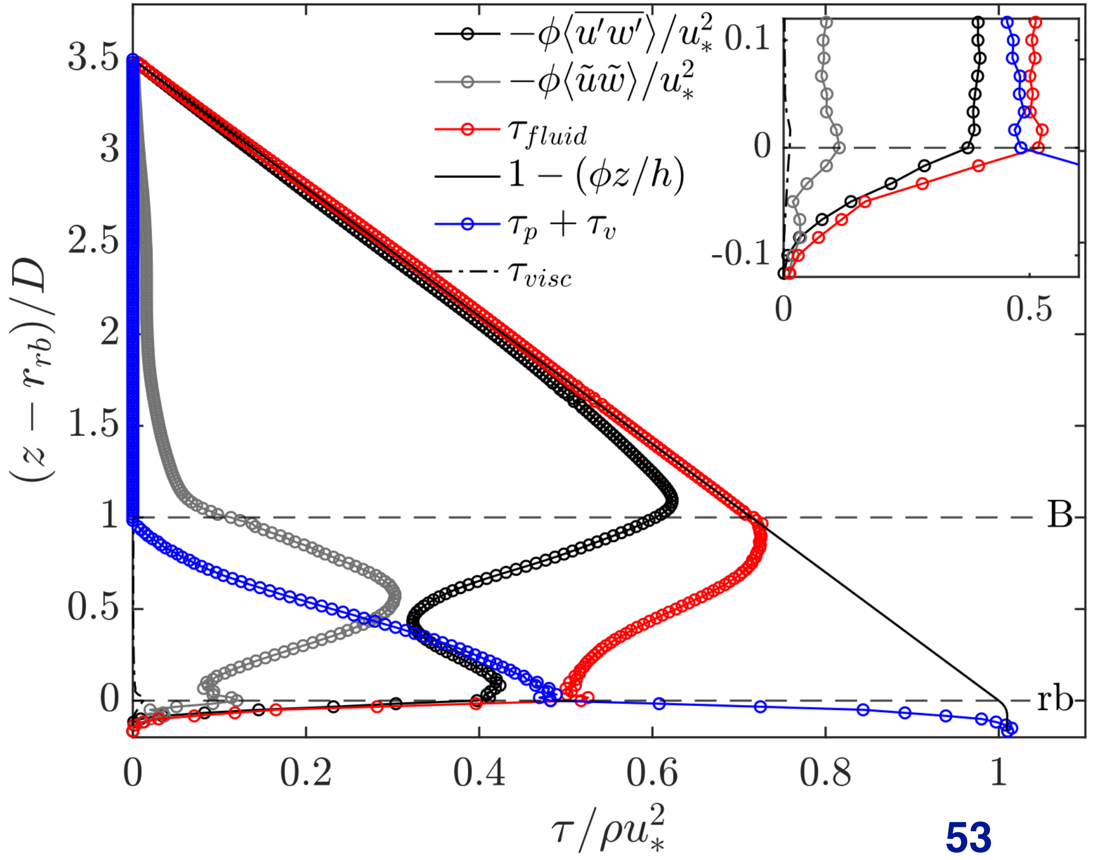

DA momentum conservation equations

- The array of boulders decreases the total fluid stress at the top of the rough bed from ρu_*^2 to $\mathbf{0.5}\rho u_*^2$ having important implications for bedload transport.

- Large form-induced stresses are observed with a peak that almost equal turbulent stress at the mid-boulder elevation and is **37%** of the total fluid stress.

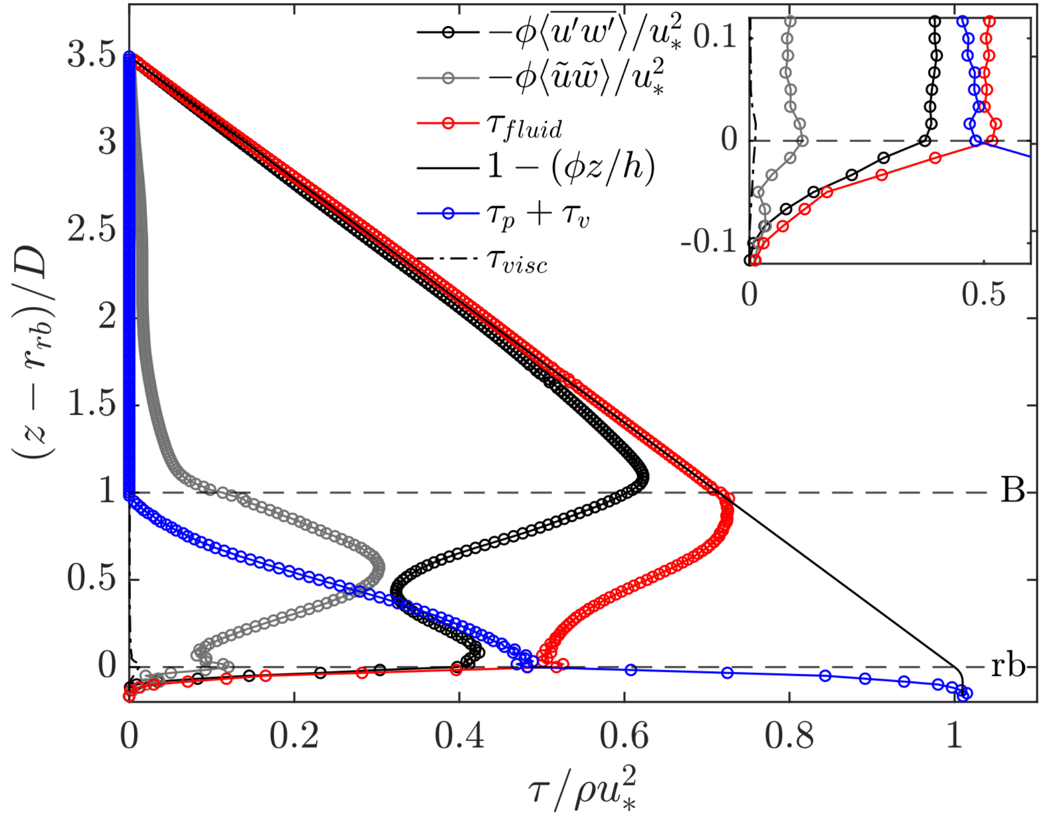

Quadrant analysis for spatial velocity disturbances

- Similar to the **quadrant analysis** for turbulent stresses, this approach is used to evaluate the contribution to form-induced stresses based on the sign of $\tilde{u}$ and $\tilde{w}$.

Turbulent Stresses $\overline{\langle u'w' \rangle}$

Form-induced Stresses $\langle \tilde{u}\tilde{w} \rangle$

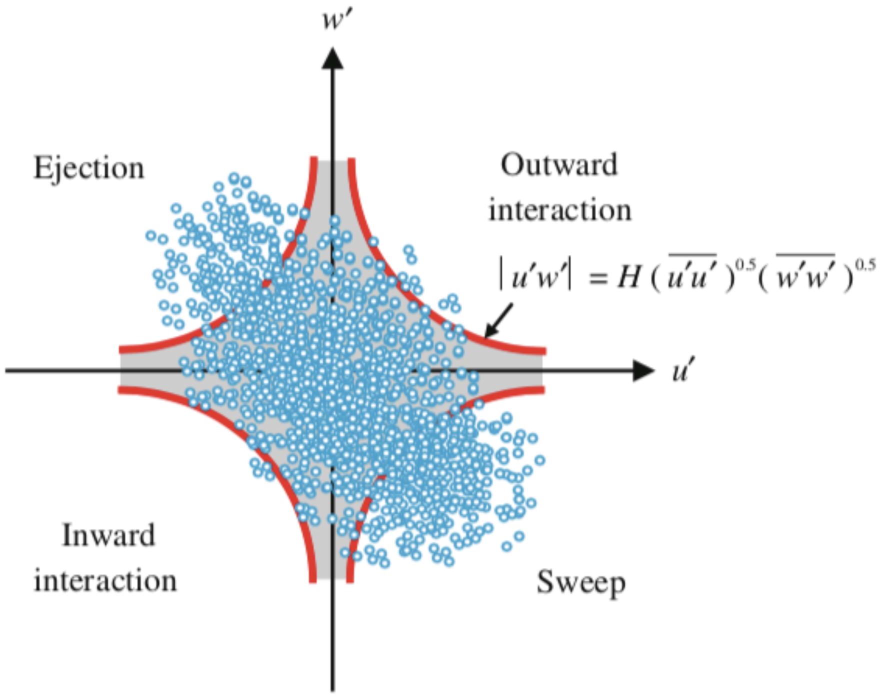

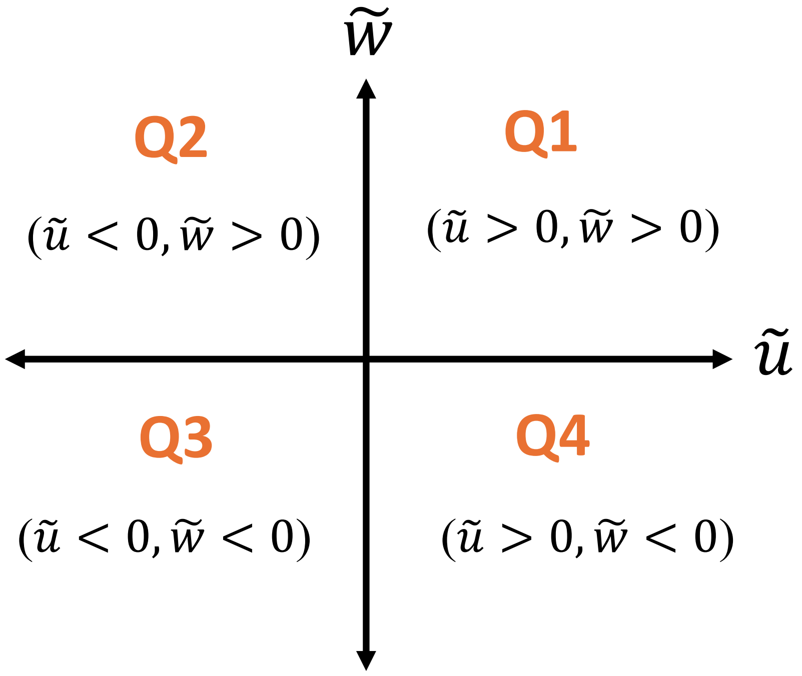

Quadrant analysis for form-induced stresses $\langle\tilde{u}\tilde{w}\rangle$

Quadrant Maps (Pokrajac *et al.*, 2007)

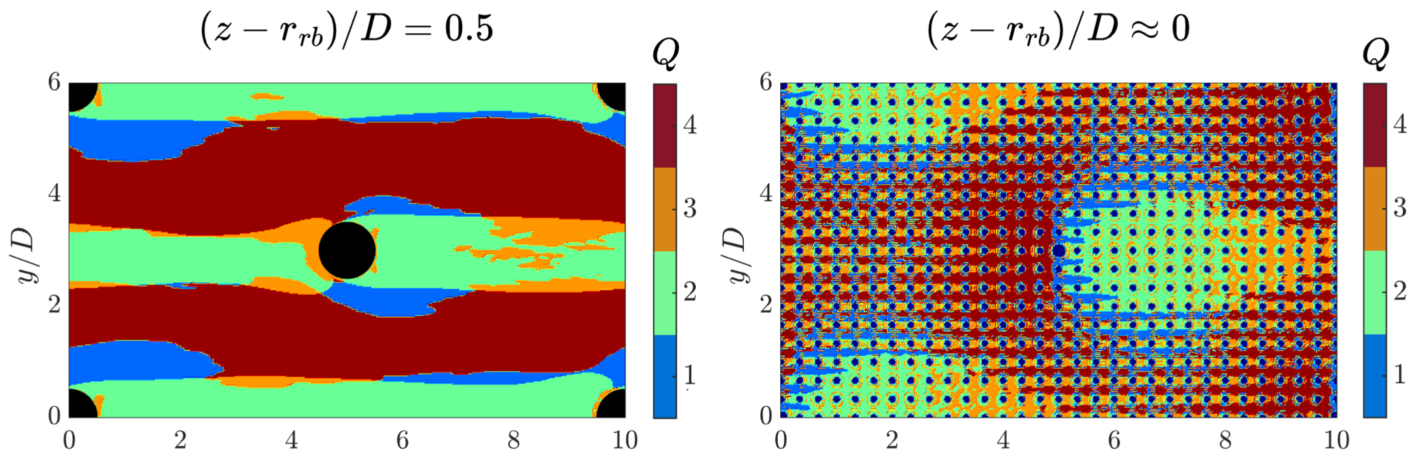

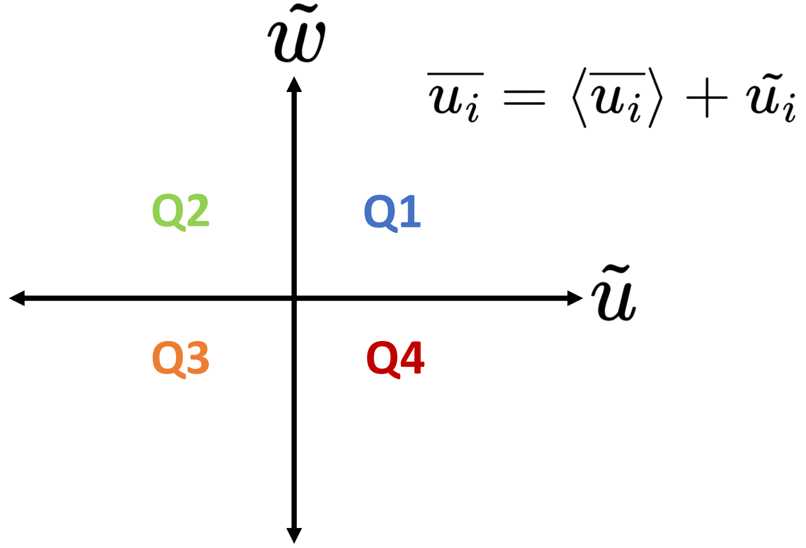

- ❑ Clear spatial regions belonging to the different quadrants that result from the strong spatial coherence of the time-averaged flow induced by the 3D wake turbulence produced by the array of boulders.

- ❑ Mostly negative events (Q2 in wakes and Q4 in high streamwise velocity regions)

Quadrant analysis for form-induced stresses $\langle\tilde{u}\tilde{w}\rangle$

Quadrant Diagrams

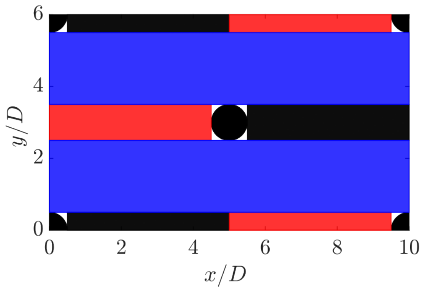

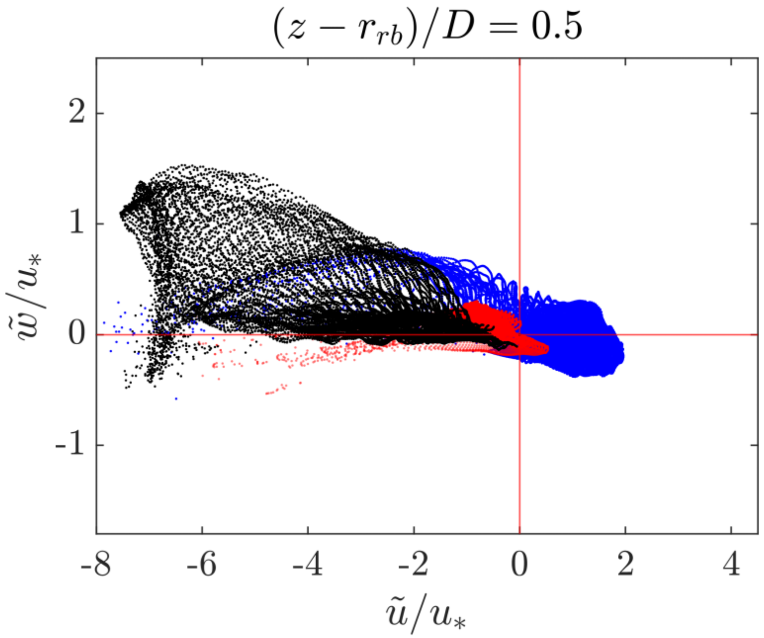

- Points in **black** belonging to the **wake** of the boulders, present much larger spatial disturbances of the streamwise velocity than the vertical component, resulting on an **elongated structure**.
- This structure bears most of the contribution from **Q2** (73%) and a large fraction of the total form-induced stress (53%)

DA kinetic energy

$$\frac{1}{2}\langle\overline{u_i u_i}\rangle = \overset{\text{Mean}}{\underbrace{\frac{1}{2}\langle\overline{u_i}\rangle\langle\overline{u_i}\rangle}_{\text{MKE}}} + \overset{\text{Turbulent}}{\underbrace{\frac{1}{2}\left\langle\overline{u_i' u_i'}\right\rangle}_{\text{TKE}}} + \overset{\text{Form induced}}{\underbrace{\frac{1}{2}\langle\tilde{u}_i\tilde{u}_i\rangle}_{\text{WKE}}}$$

- **WKE** is comparable to **TKE** within the roughness elements.
- Local peaks exist at the top of the rough bed.
- **Global peaks** of TKE and WKE occur at the **top** and the **middle** of the **boulders** respectively.

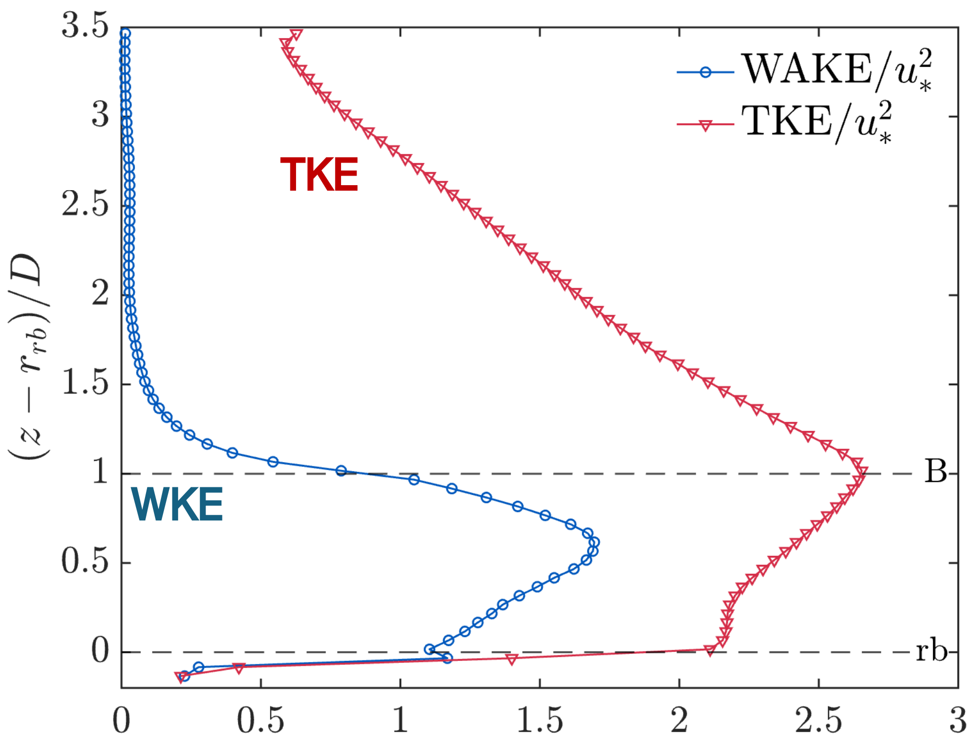

MKE budget

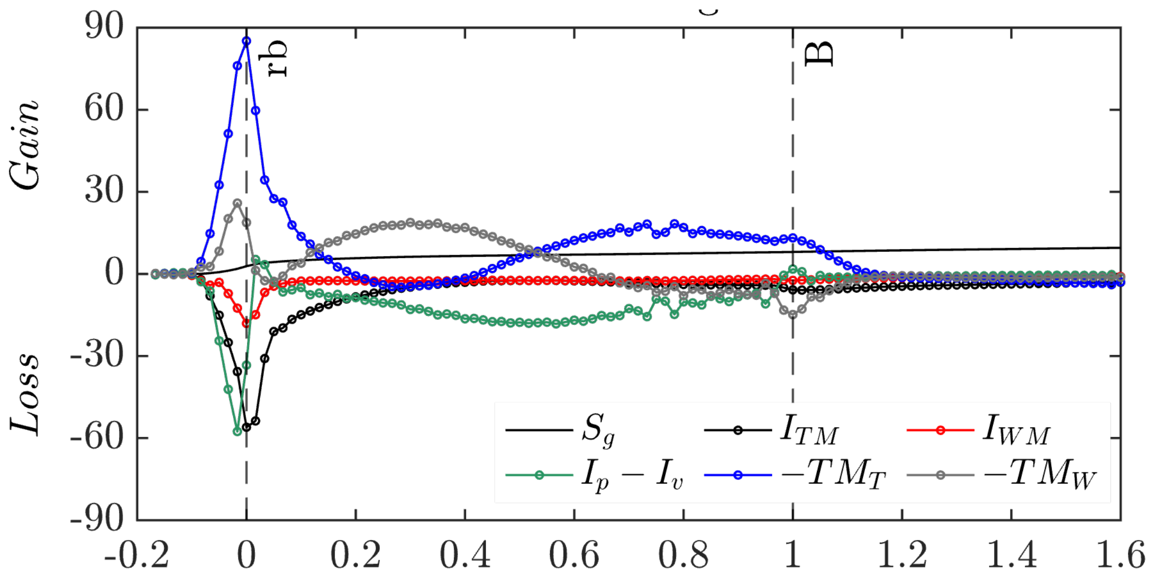

- Energy is injected by **gravity** (Sg).
- Around the rough bed, **MKE** is mainly transported by **turbulent stresses (TM_T)** and around the boulders by **form-induced stresses** (TM_W) and by **turbulent stresses (TM_T).**
- Some **MKE** is transferred to the **turbulent** and **form-induced fields**.
- A large fractions of MKE is used to generate **drag** which is then transferred to **WKE** and finally dissipated by the turbulent field.

$$0 = \underbrace{\phi \langle \overline{\mathbf{u}} \rangle \mathbf{g} \mathbf{S_b}}_{S_g} + \underbrace{\phi \left\langle \overline{\mathbf{u'w'}} \right\rangle \frac{\partial \langle \overline{\mathbf{u}} \rangle}{\partial \mathbf{z}}}_{I_{TM}} + \underbrace{\phi \langle \tilde{u}\tilde{w} \rangle \frac{\partial \langle \overline{u} \rangle}{\partial z}}_{I_{WM}} + \underbrace{\frac{\langle \overline{u} \rangle}{\rho V_0} \iint_{S_{\mathrm{int}}} \overline{p} n_1 dS}_{I_p} - \underbrace{\nu \frac{\partial}{\partial z} \left(\langle \overline{u} \rangle \frac{\partial \phi \langle \overline{u} \rangle}{\partial z} \right)}_{TM_v}$$

$$- \underbrace{\frac{\partial \phi \left\langle \overline{u'w'} \right\rangle \langle \overline{u} \rangle}{\partial z}}_{TM_T} - \underbrace{\frac{\partial \phi \langle \tilde{u}\tilde{w} \rangle \langle \overline{u} \rangle}{\partial z}}_{TM_W} + \underbrace{\nu \frac{\partial}{\partial z} \left(\langle \overline{u} \rangle \frac{\partial \phi \langle \overline{u} \rangle}{\partial z} \right)}_{TM_v} - \underbrace{\phi \nu \frac{\partial \langle \overline{u} \rangle}{\partial z} \frac{\partial \langle \overline{u} \rangle}{\partial z}}_{\epsilon_{MM}} - \underbrace{\phi \nu \left\langle \frac{\partial \tilde{u}}{\partial z} \right\rangle \frac{\partial \langle \overline{u} \rangle}{\partial z}}_{\epsilon_{MW}}$$

DA Energy Budgets: WKE

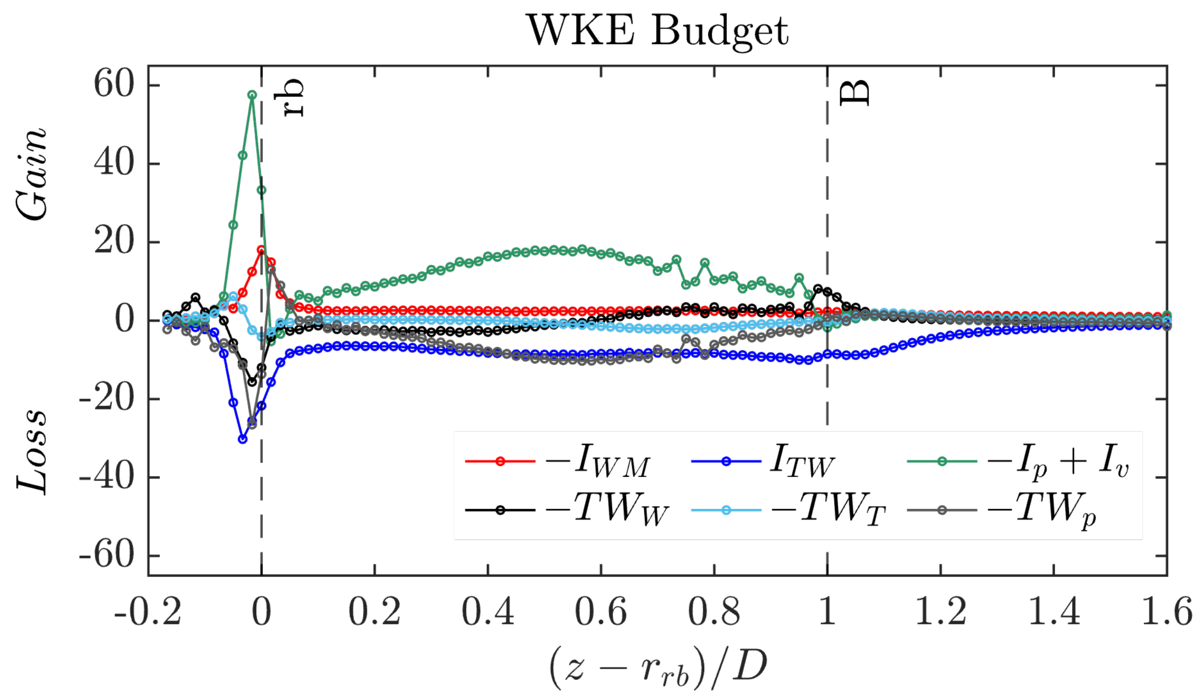

- **WKE supply:** from the the **mean flow (I_{WM})** and from **drag.**
- Some **WKE** is transferred to **TKE** through I_{TW},
- The excess of **WKE** is distributed from the region around the **roughness elements** to the **upper layers** (mostly by TW_W and TW_p)
- Energy is transferred to the **turbulent field** to be **dissipated.**

$$0 = -\underbrace{\phi\langle\tilde{u}\tilde{w}\rangle\frac{\partial\langle\bar{u}\rangle}{\partial z}}_{I_{WM}} + \underbrace{\phi\left\langle\overline{u_i'u_j'}\frac{\partial\tilde{u}_i}{\partial x_j}\right\rangle}_{I_{TW}} - \underbrace{\frac{\langle\bar{u}\rangle}{\rho V_0}\int\int_{Sint}\bar{p}n_1 dS}_{I_p} + \underbrace{\frac{\nu\langle\bar{u}\rangle}{V_0}\int\int_{Sint}\frac{\partial\bar{u}_i}{\partial x_j}n_j dS}_{I_v} - \underbrace{\frac{1}{2}\frac{\partial\phi\langle\tilde{u}_i\tilde{u}_i\tilde{w}\rangle}{\partial z}}_{TW_W}$$

$$-\underbrace{\frac{1}{2}\frac{\partial\phi\langle\tilde{u}_i\overline{u_i'w'}\rangle}{\partial z}}_{TW_T} - \underbrace{\frac{1}{\rho}\frac{\partial\phi\langle\tilde{p}\tilde{w}\rangle}{\partial z}}_{TW_p} + \underbrace{\nu\frac{\partial}{\partial z}\left(\phi\left\langle\tilde{u}_i\frac{\partial\tilde{u}_i}{\partial z}\right\rangle\right)}_{TW_v} - \underbrace{\phi\nu\left\langle\frac{\partial\tilde{u}}{\partial z}\right\rangle\frac{\partial\langle\bar{u}\rangle}{\partial z}}_{\varepsilon_{MW}} - \underbrace{\phi\nu\left\langle\frac{\partial\tilde{u}_i}{\partial x_j}\frac{\partial\tilde{u}_i}{\partial x_j}\right\rangle}_{\varepsilon_{WW}}$$

DA Energy Budgets: TKE

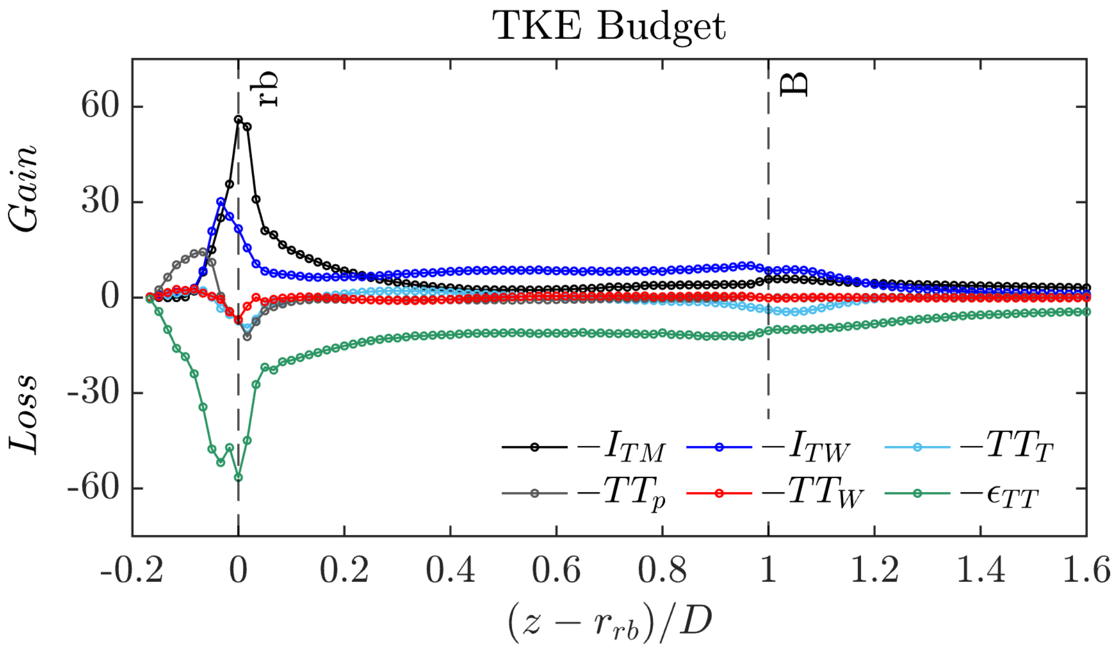

- **TKE supply**: coming from the **mean flow** (I_{TM}) and **form induced fields** (I_{TW}).
- The energy coming from the **form-induced field** (I_{TW}) is large **around the boulders** and even higher than the one coming from the **mean flow** (I_{TM}) **.**
- **All the energy** is **dissipated** by the **turbulent field.**

$$0 = \underbrace{-\phi\langle\overline{u'w'}\rangle\frac{\partial\langle\bar{u}\rangle}{\partial z}}_{I_{TM}} \underbrace{-\phi\left\langle\overline{u_i'u_j'}\frac{\partial\widetilde{u}_i}{\partial x_j}\right\rangle}_{I_{TW}} \underbrace{-\frac{1}{2}\frac{\partial\phi\langle\overline{u_i'u_i'\widetilde{w}}\rangle}{\partial z}}_{TT_W} \underbrace{-\frac{1}{2}\frac{\partial\phi\langle\overline{u_i'u_i'w'}\rangle}{\partial z}}_{TT_T} \underbrace{-\frac{1}{\rho}\frac{\partial\phi\langle\overline{p'w'}\rangle}{\partial z}}_{TT_p}$$
$$\underbrace{+\frac{1}{2}\nu\frac{\partial}{\partial z}\left(\frac{\partial\phi\langle\overline{u_i'u_i'}\rangle}{\partial z}\right)}_{TT_v} \underbrace{-\phi\nu\left\langle\overline{\frac{\partial u_i'}{\partial x_j}\frac{\partial u_i'}{\partial x_j}}\right\rangle}_{\varepsilon_{TT}}$$

Conclusions

- This work shed some light on the importance of evaluating the **additional stresses** generated by roughness elements to consider **form-induced stresses** and **exclude drag** on **bedload transport estimations.**

- The **quadrant analysis** for spatial velocity disturbances elucidates the relevance of **wake turbulence** on **generating form-induced stresses** which partially compensate the **decrease of energy due to drag.**

- The energy budgets reveal the mechanism in which **drag energy** is transferred from **WKE to TKE**, to finally be **dissipated** by the **turbulent field.**

Outline

1. General introduction
2. Introduction on Large eddy simulation
3. Introduction on modelling particle – laden turbulent flows
4. Example study : Bedload transport around boulders in river flows
    - Analysis of the flow
    - Particle transport and fluxes
5. Other examples of studied issues
    - Particle transport in street canyons
    - Particle transport above dunes
6. Conclusions and perspectives

Bedload transport

- Evaluate how the **spatial flow variability** induced by an array of immobile boulders over a rough-bed influence bedload transport.
- Estimate the **local bedload fluxes** based on local **particle activity** and **velocity.**
- **Deposition** and **Erosion** patterns
- Two **mobility conditions**

Mobile sediments

Low and intermediate mobility conditions are compared

$\tau_* = 0.064$

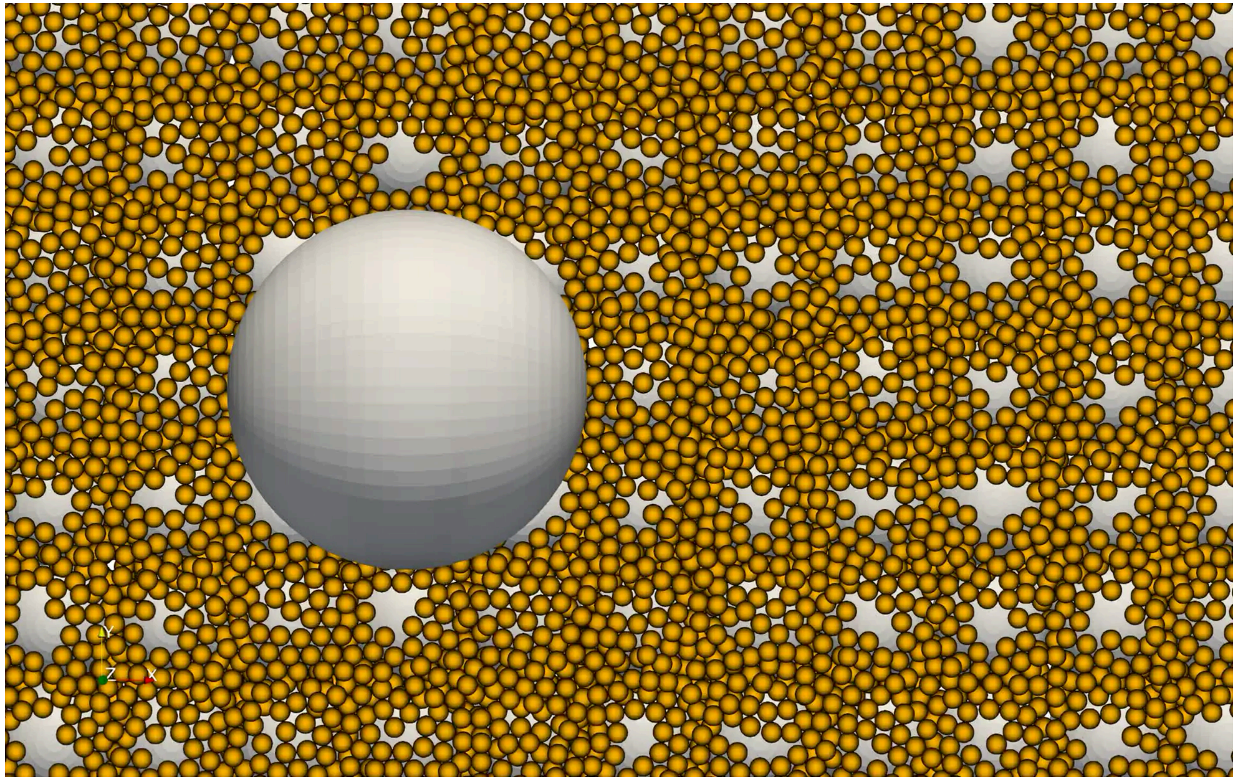

$\tau_* = 0.135$

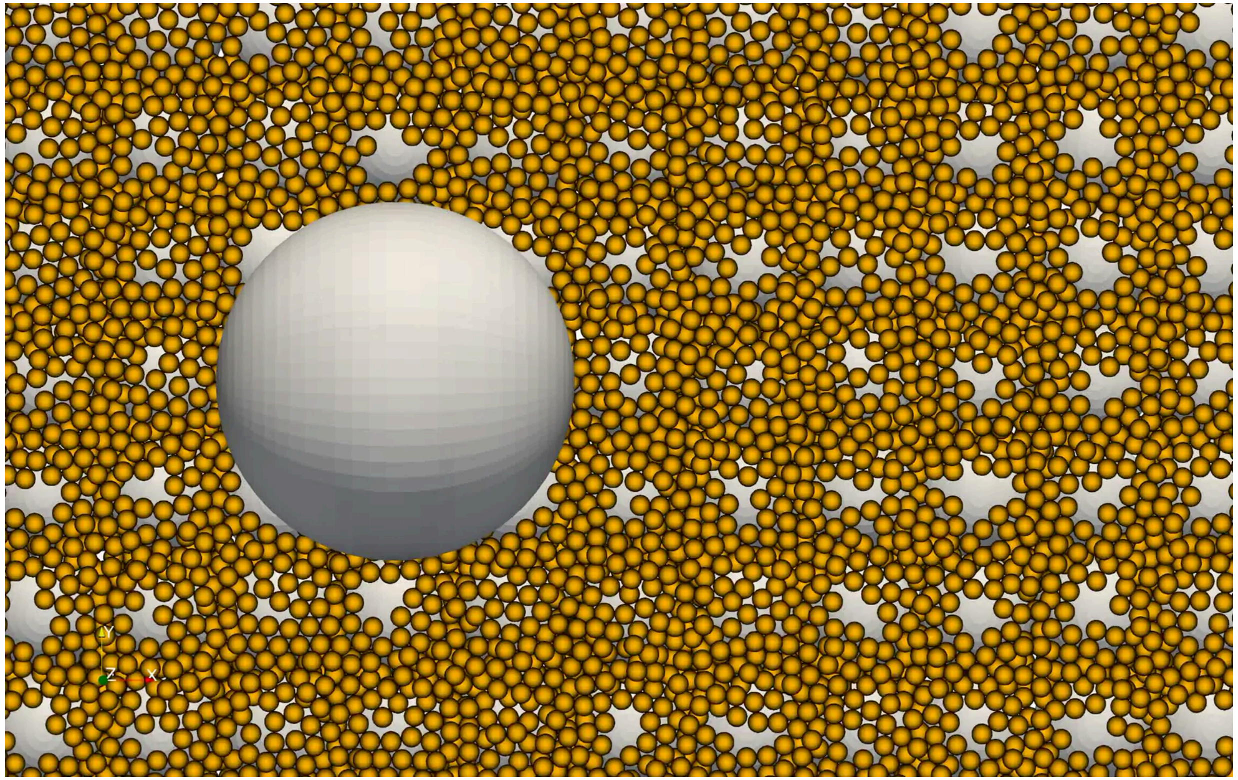

Sediment transport

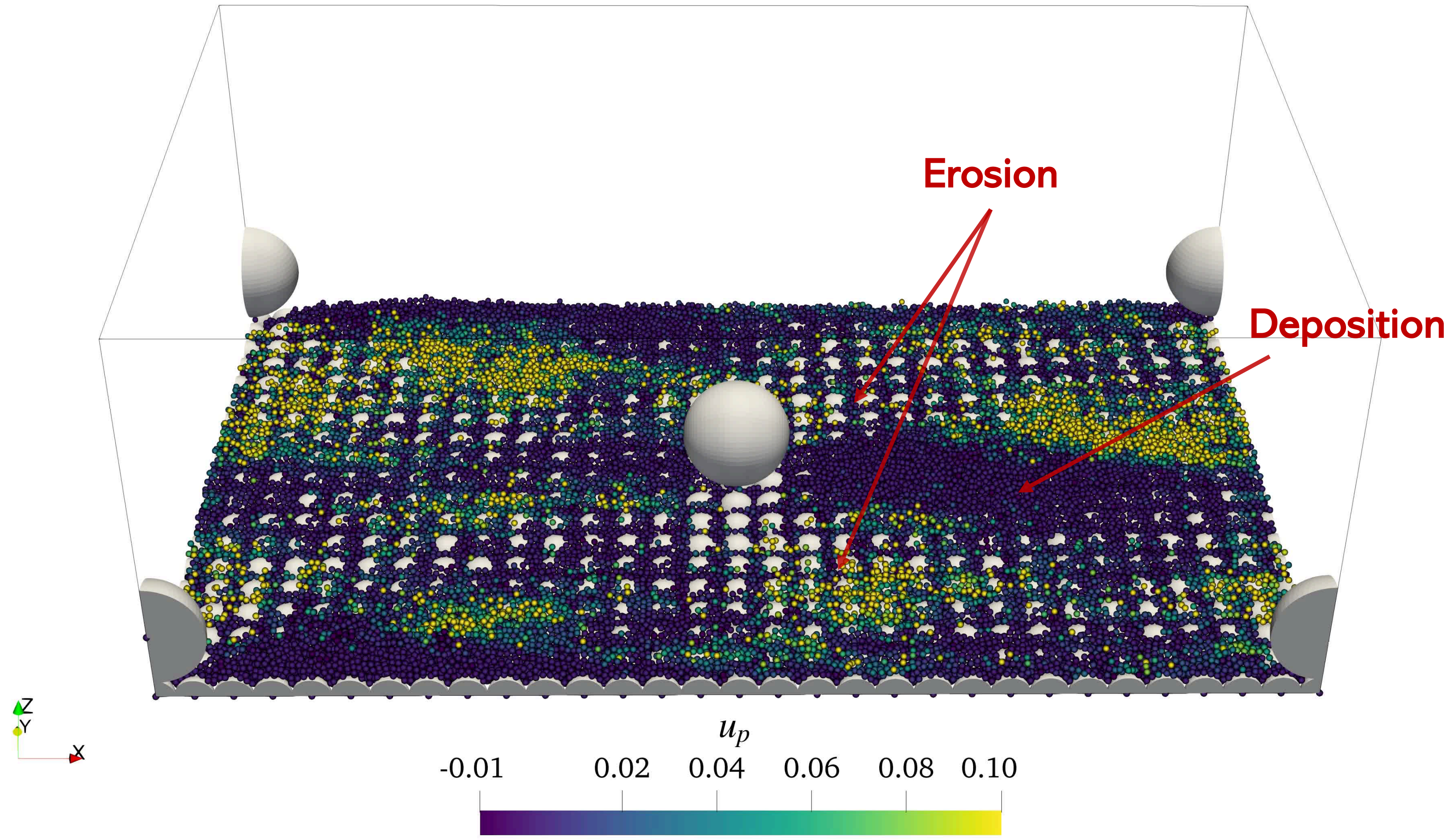

- Persistent **deposition** and **erosion** patterns only for the intermediate mobility condition.
- **Deposition** occurs in the **wake** of the boulders whereas **erosion** occurs **between them** (**Papanicolaou et al 2018**).
- Feedback between **sediment distribution** and the **local** and **instantaneous flow.**

Bedload transport

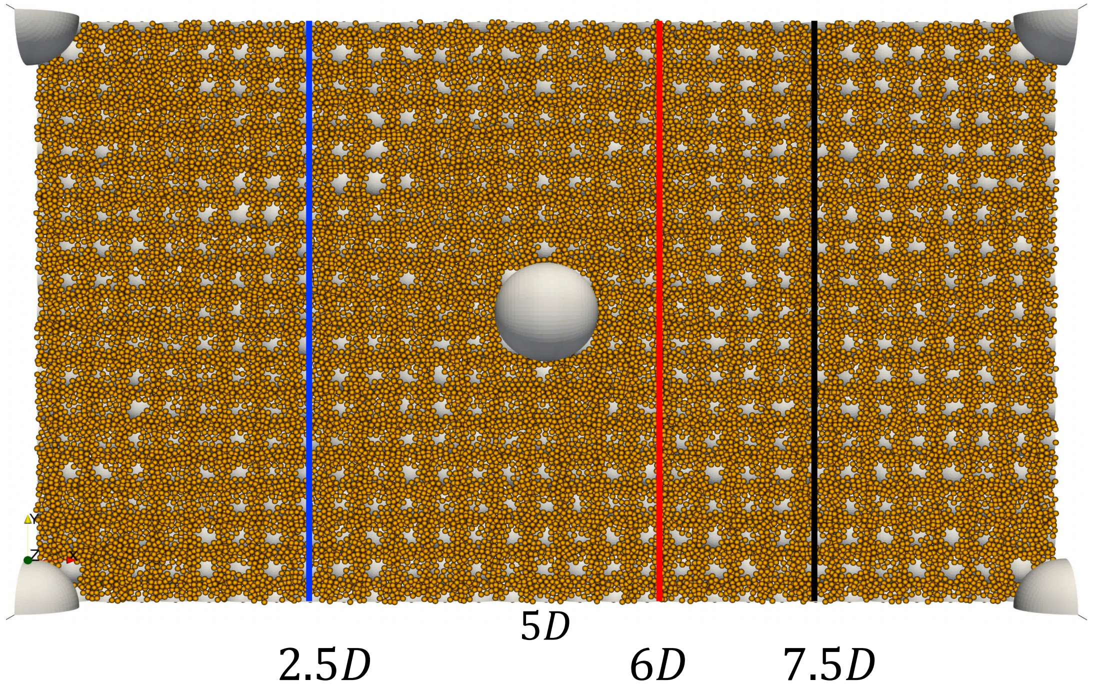

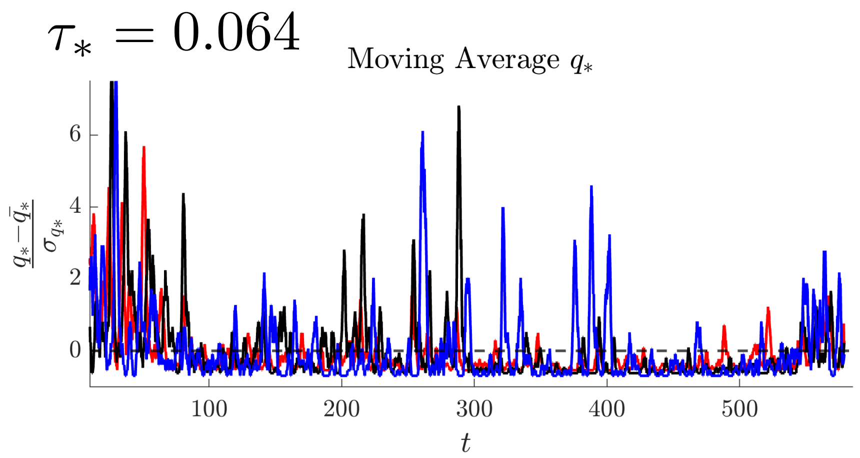

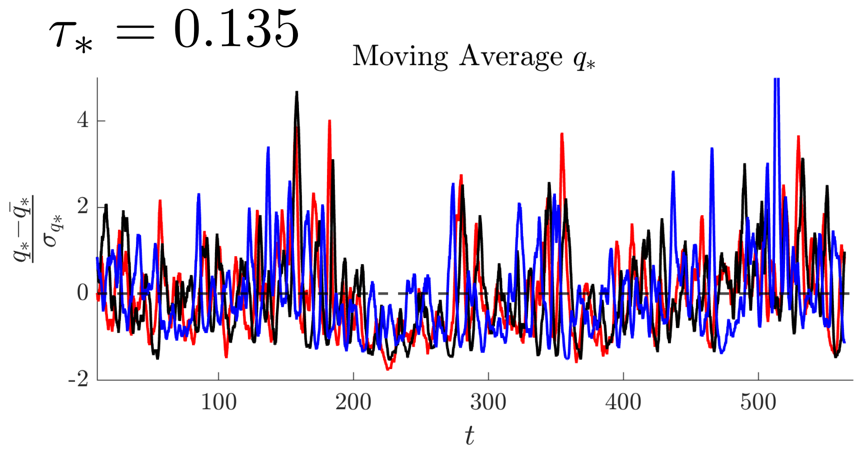

- The bed is at **equilibrium conditions.**
- **Large temporal fluctuations** induced by the array of boulders and the rough bed.

Bedload transport

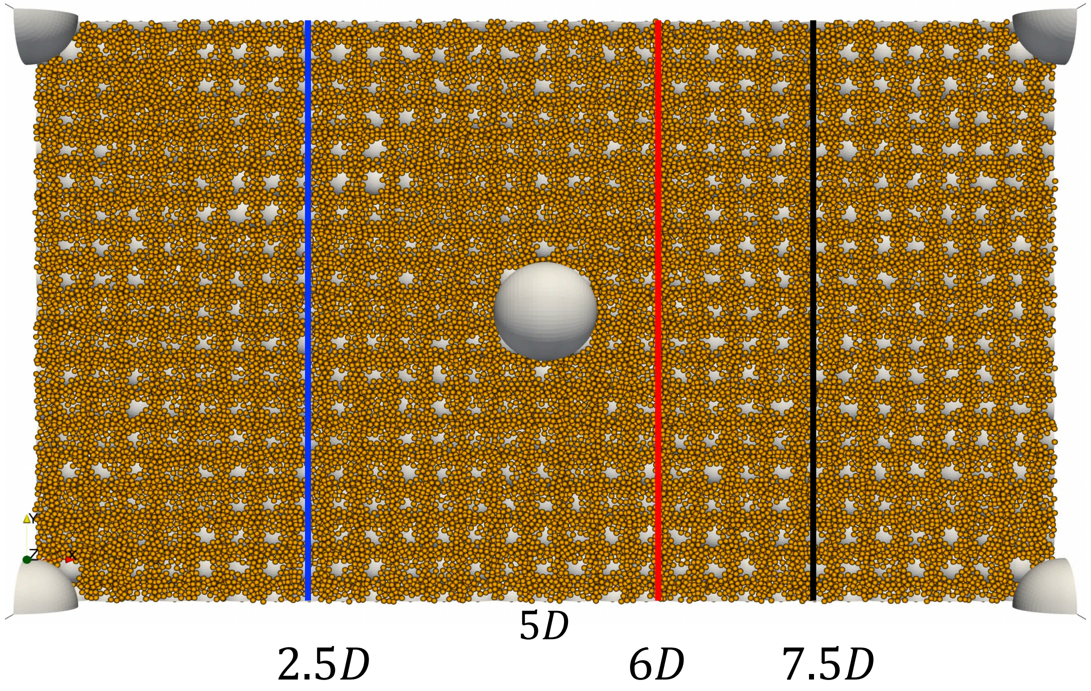

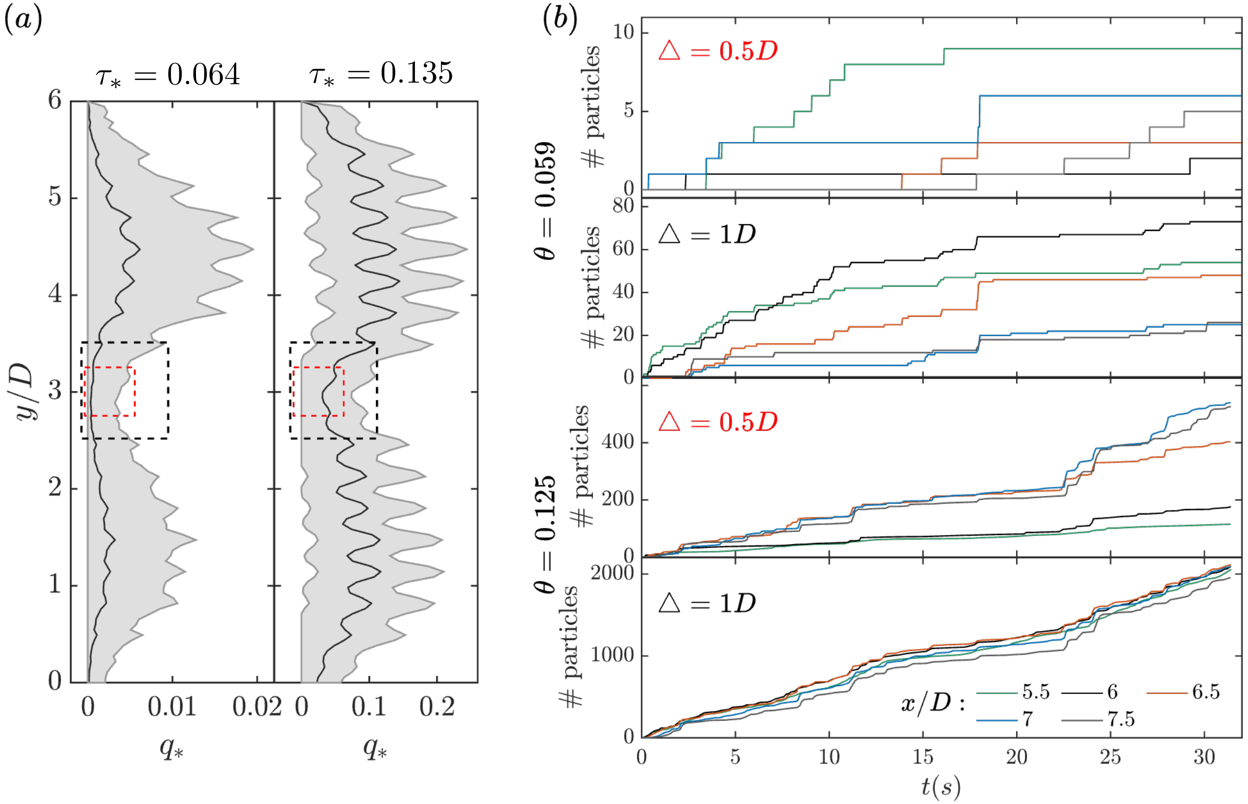

- **Two scales** of variations induced by the **boulders** and the **rough bed.**
- Bedload transport downstream the boulders is highly **intermittent.**

Mean particle transport

- Time-averaged particle transport at **three** different planes upstream and downstream the boulders.
- The bed reach an **equilibrium condition** for both mobility conditions.

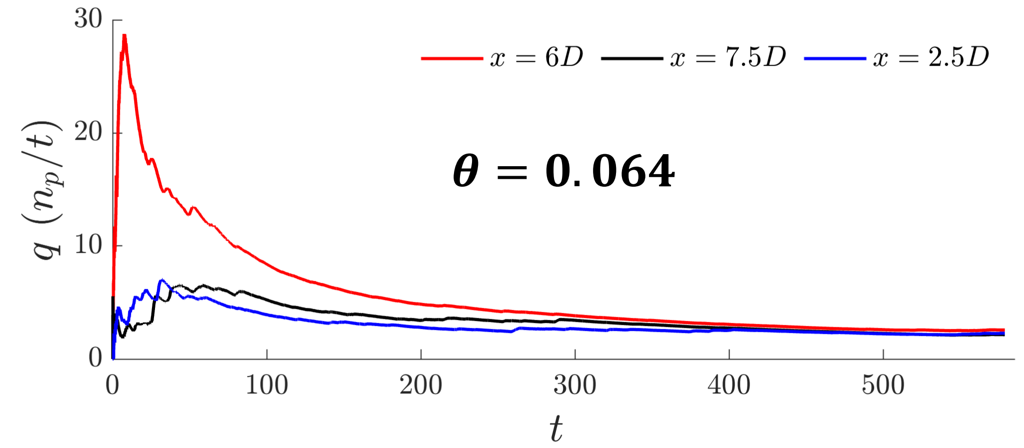

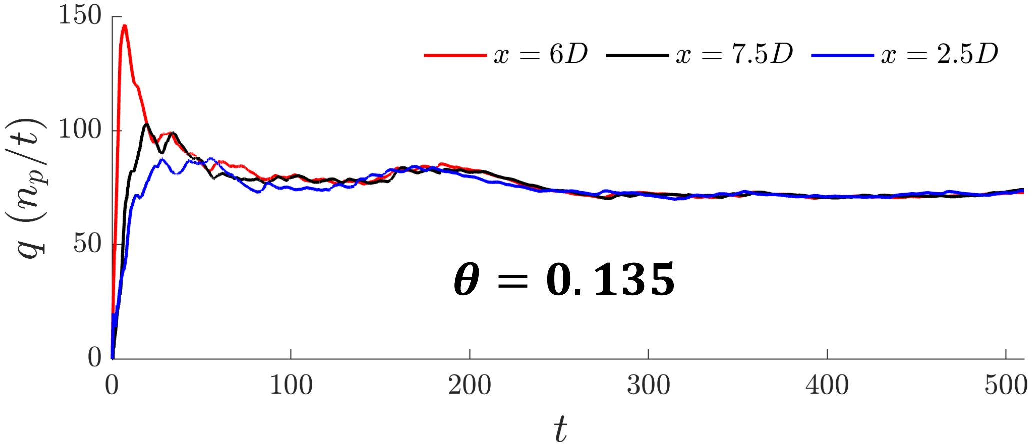

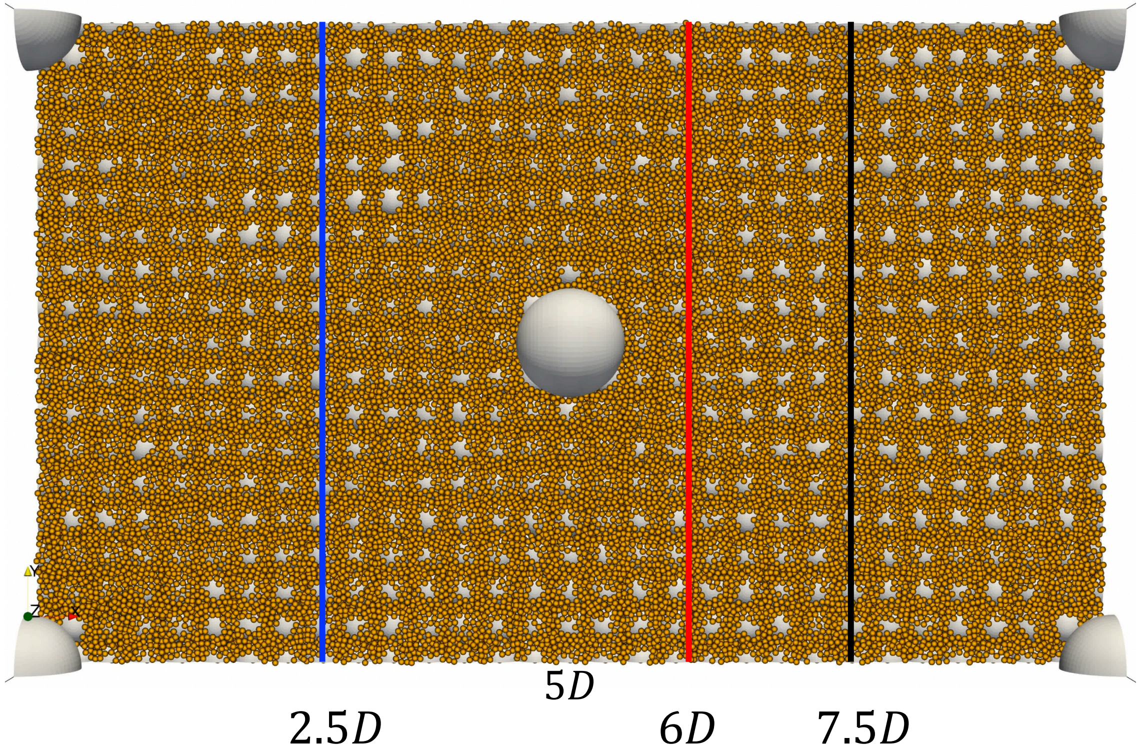

Standard deviation of particle transport

- Standard deviation of particle transport at **three** different planes upstream and downstream the boulders reach a **relatively constant value.**

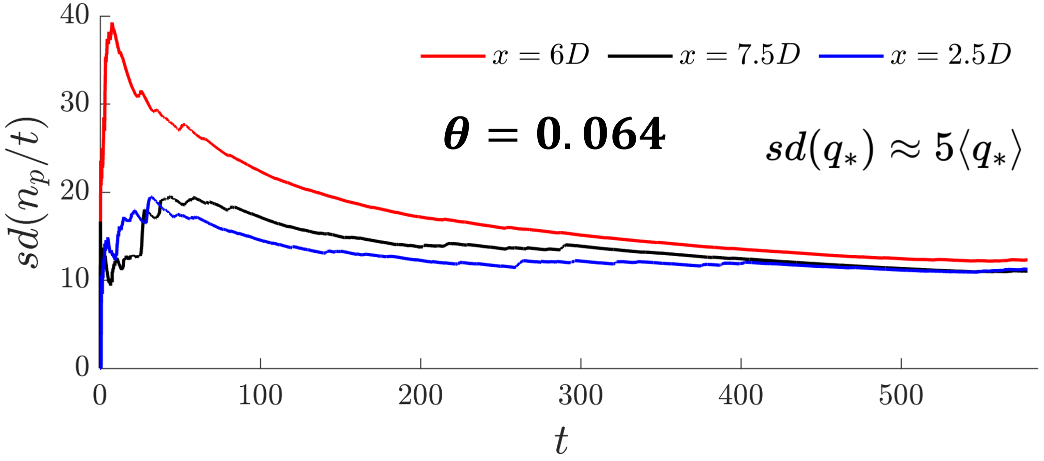

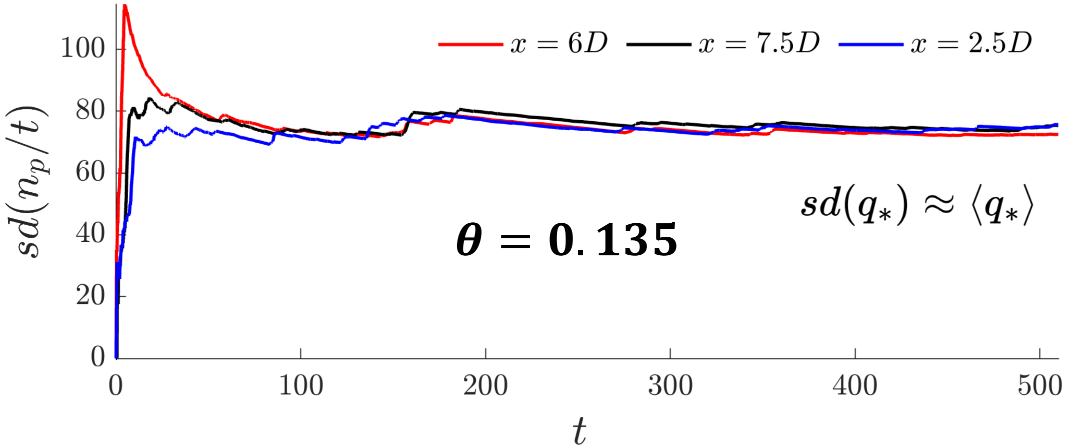

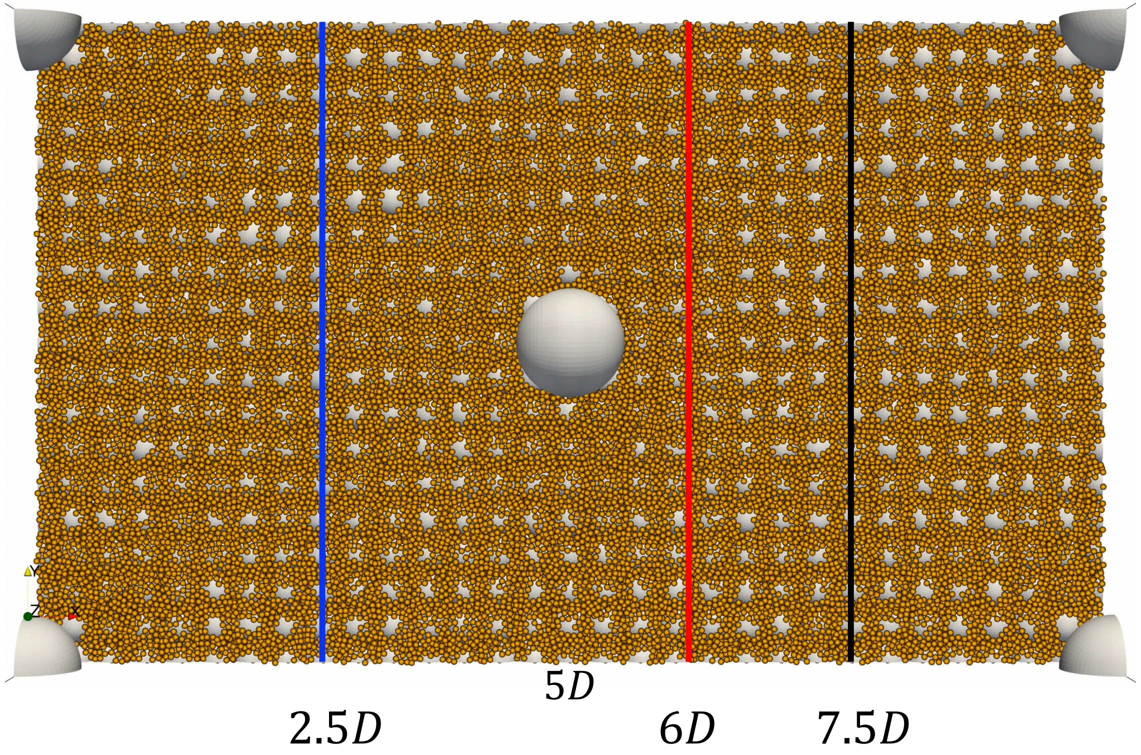

Bedload transport

$$q_* = 4\left(\tau_* - \boxed{0.0495}\right)^{3/2} \quad \text{Wong \& Parker, 2006}$$

$\boldsymbol{\tau_{*c}}$

- **Mean critical shear stress** is close to the **Shields value.**
- **Temporal variations** of $\boldsymbol{\tau_{*c}}$ needed to match the observed transport are **high.**

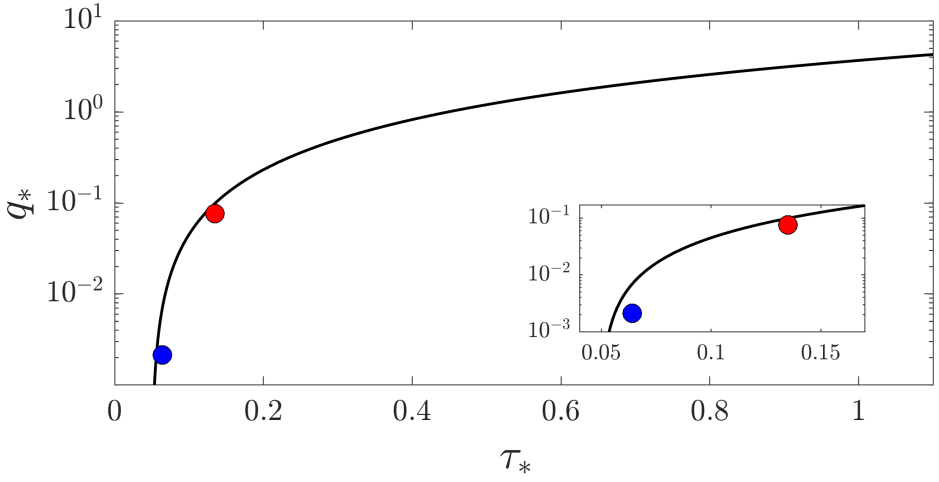

Isolate $\boldsymbol{\tau_{*c}}$ from:

$$\tau_{*c} = \left[\tau_* - \left(\frac{q_*}{4}\right)^{2/3}\right]$$

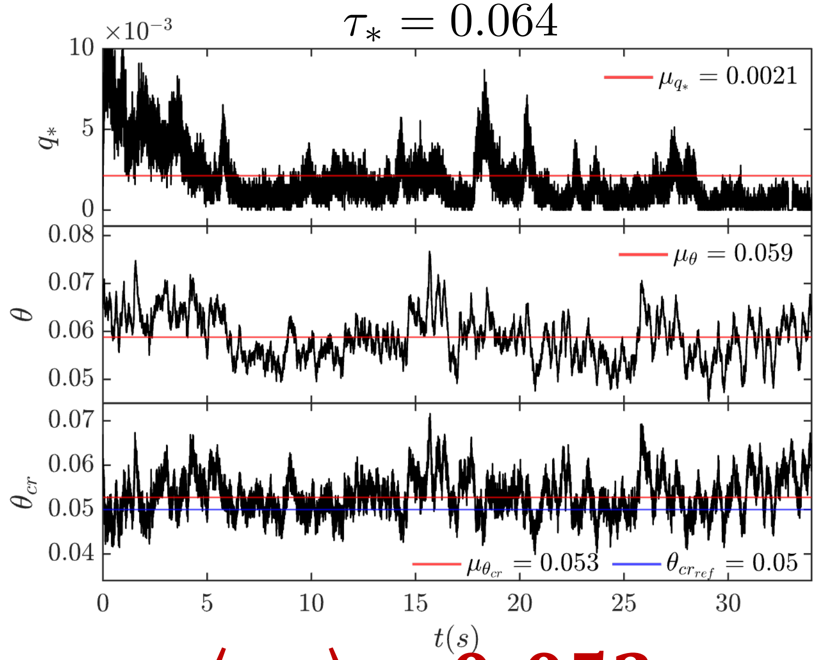

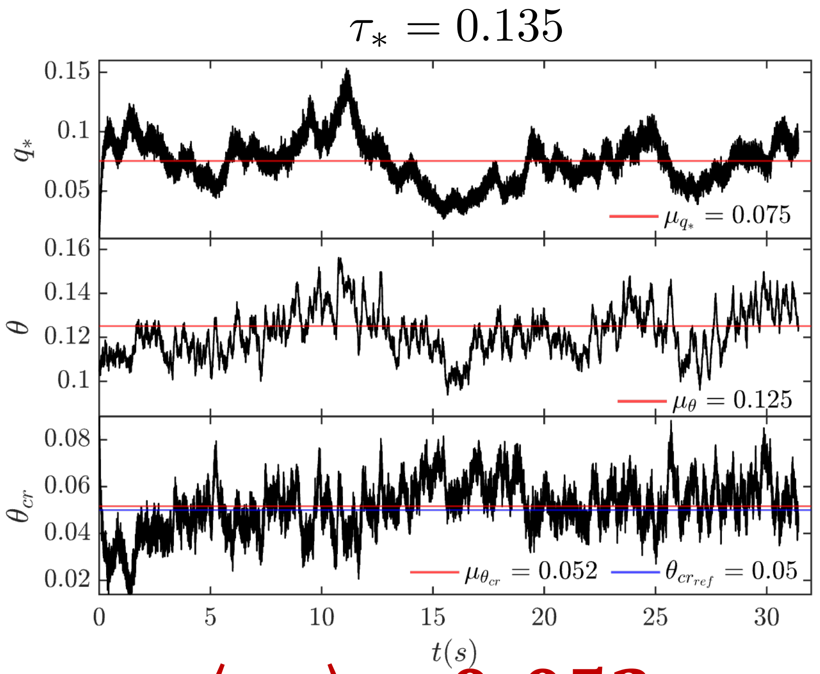

$$\langle \tau_{*c} \rangle = 0.053 \qquad\qquad \langle \tau_{*c} \rangle = 0.052$$

Shields Criterion

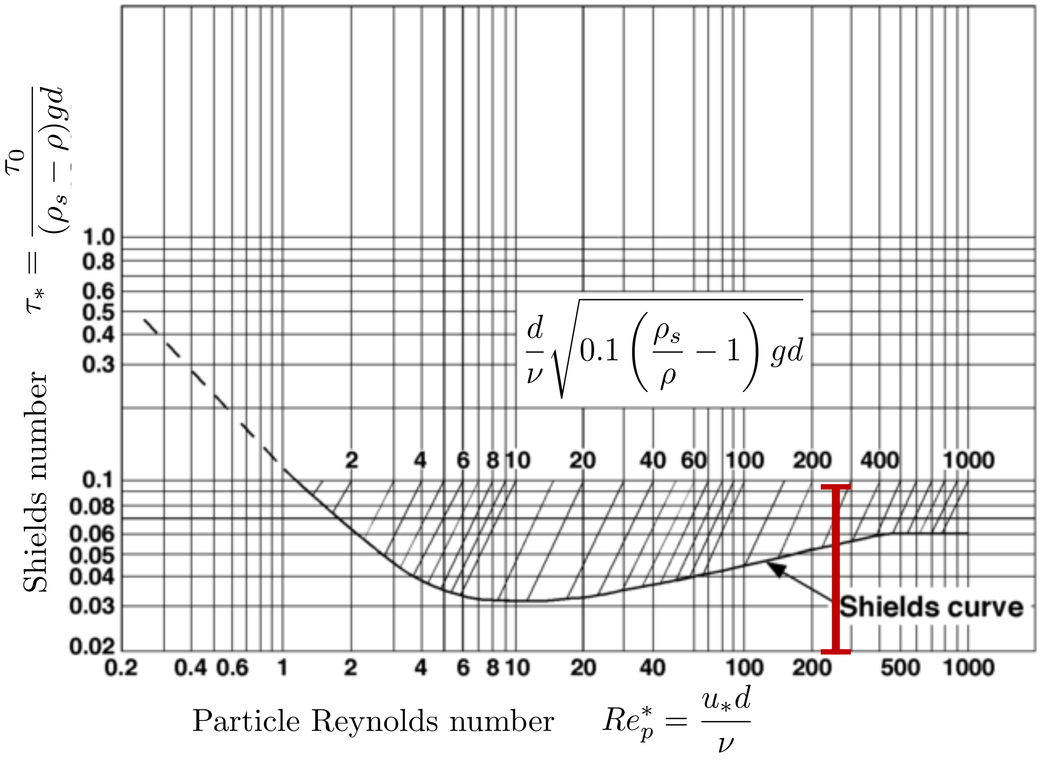

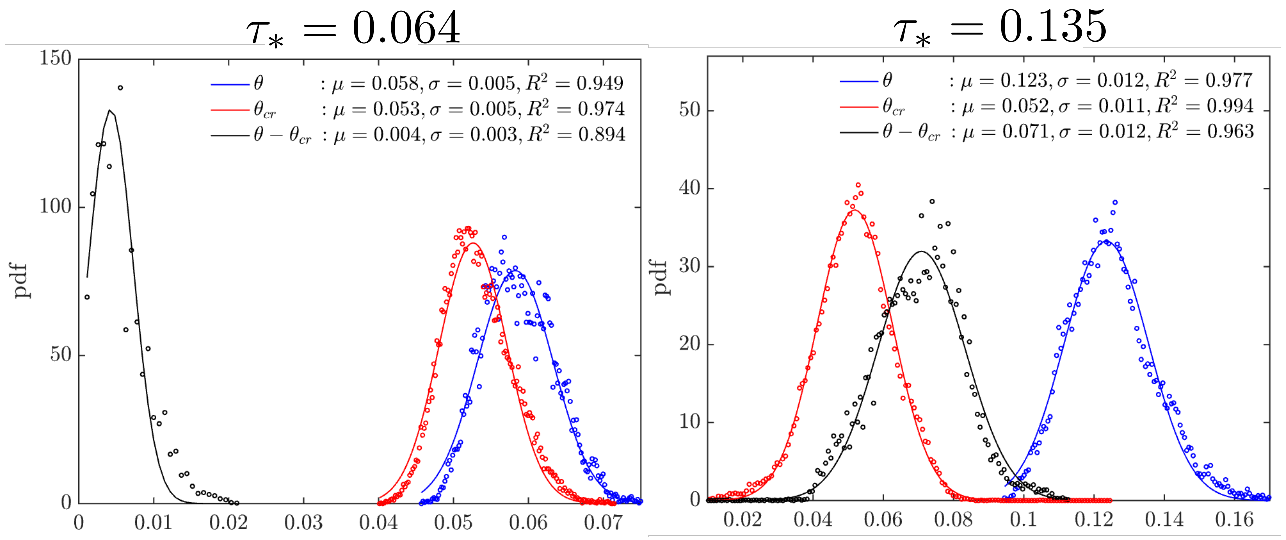

- The critical shear stress needed to match the observed transport is **not constant** in time.
- θ_{cr} presents **large fluctuations** with values ranging from 0.02 to 0.08.
- The **pdf** of $\boldsymbol{\theta}$ and $\boldsymbol{\theta_{cr}}$ can be assumed as **Gaussian**
- Larger coefficient of variation for $\tau_* = 0.064$
- This finding can be used to predict bedload transport through **stochastic models.**

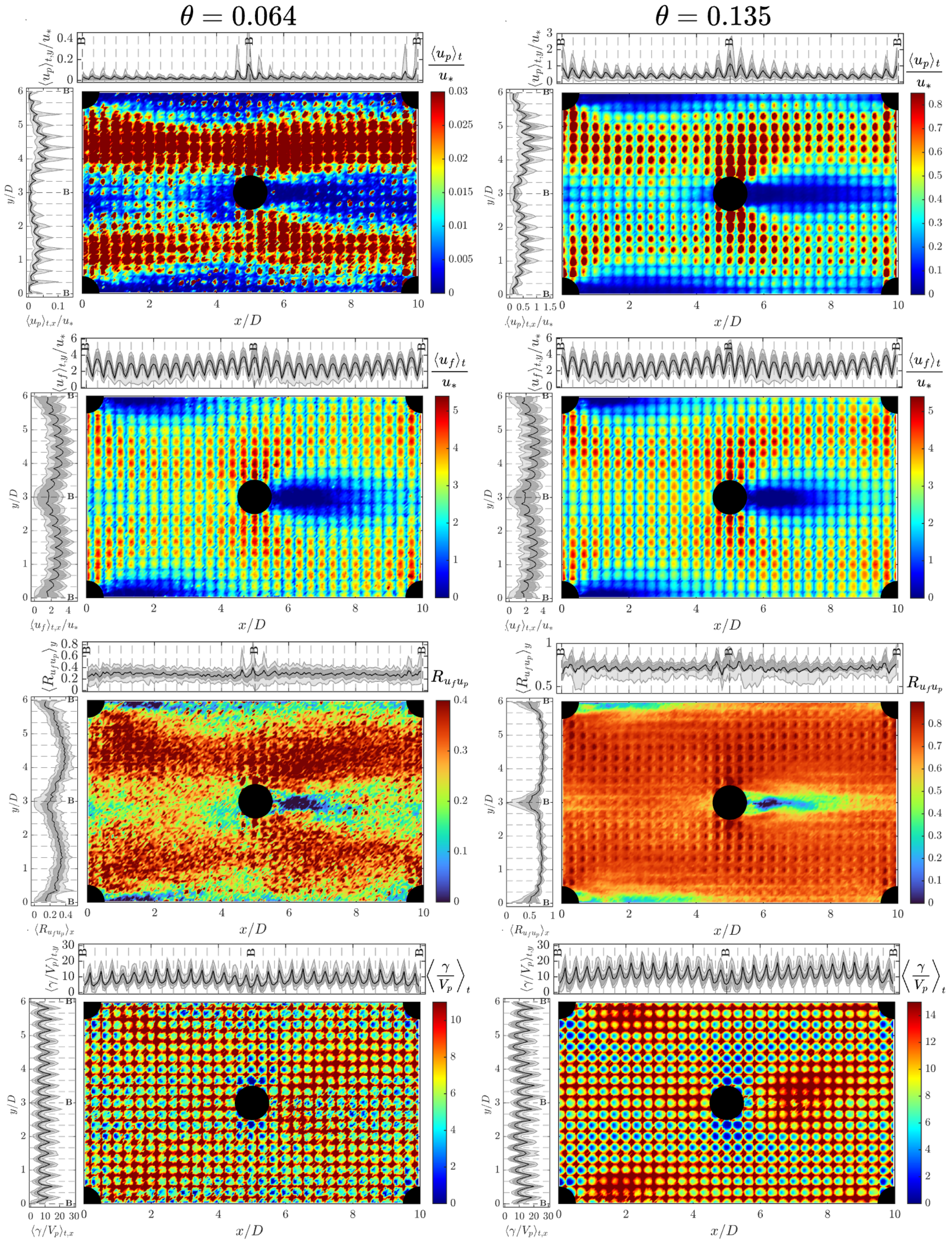

Spatial Variability of sediment quantities

- The spatial maps show from top to bottom:
  - Mean streamwise **particle velocity**
  - Mean streamwise **flow velocity**
  - Fluid-particle **Correlation** coefficient
  - Particle **activity**
- The plots at the sides correspond to the **mean** (black line) and some **percentiles** of the **quantity spatial distribution.**
- **Two scales of variability** can be observed separately due to the **boulders** and the **rough bed.**

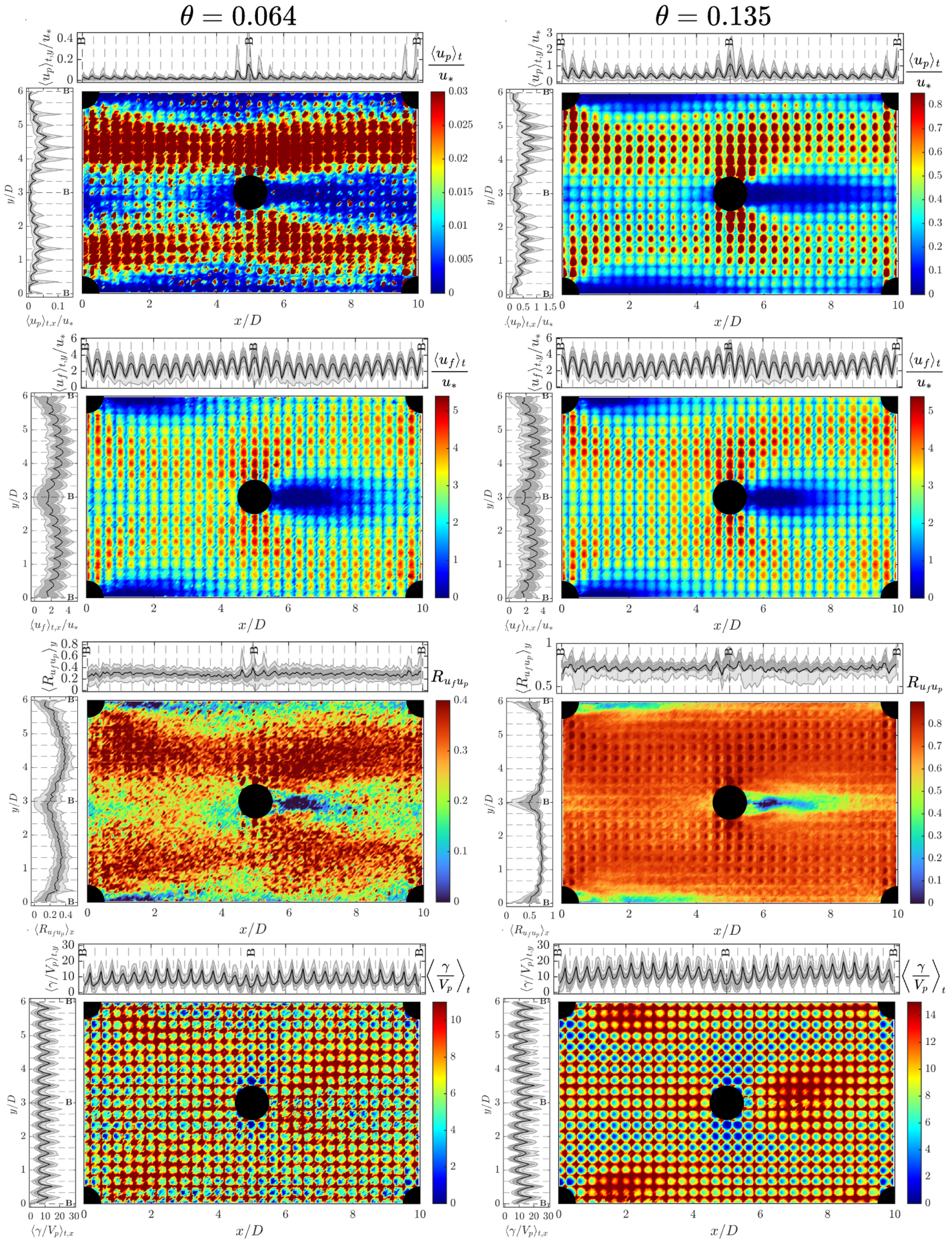

Spatial Variability of sediment quantities

- In Kalinske's approach, bedload is equal to the product of **mean particle velocity** and **activity** $q_b = \gamma \cdot u_p \; [cm^2/s]$.
- In the intermediate case, **high particle velocity** is related to **low activity** due to **erosion**, and **low particle velocity** to **high activity** due to **deposition**.
- Similarities between fluid and particle velocity **(correlation maps).**

Bedload transport

$$q_b = \gamma \cdot u_p$$

Kalinske, 1947

- Large sediment velocity differences.
- **High particle concentration downstream** the boulders and **low concentration** between them.
- **Negative correlation** between particle concentration and velocity due to **sediment availability**.
- **Two scales of variability** can be observed separately due to the **boulders** and the **rough bed.**

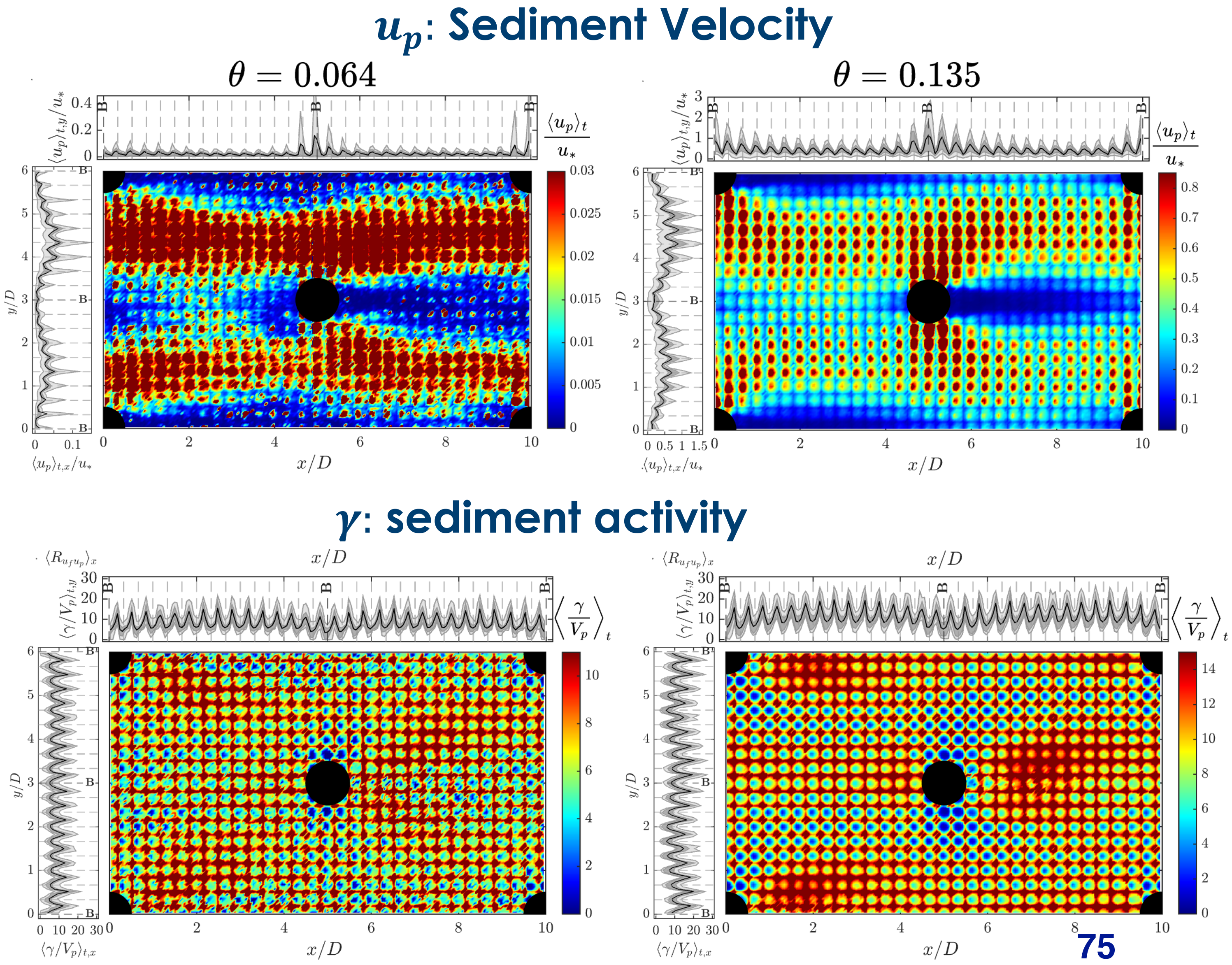

Spatiotemporal averaged bedload transport

- We start from $\boldsymbol{q_b} = \boldsymbol{\gamma} \cdot \boldsymbol{u_p}\ [\boldsymbol{cm^2/s}]$. Applying the **Reynolds decomposition:**

$$\boldsymbol{q_b} = \gamma \cdot u_p = (\bar{\gamma} + \gamma') \cdot (\overline{u_p} + u_p{}')$$

- Then, calculating the **temporal average:**

$$\boxed{\overline{\boldsymbol{q_b}} = \overline{\gamma \cdot u_p} = \bar{\gamma}.\overline{u_p} + \overline{\gamma' u_p{}'}}$$

- Now, applying a **spatial average:**

$$\langle \overline{\boldsymbol{q_b}} \rangle = \langle \overline{\gamma \cdot u_p} \rangle = \langle \bar{\gamma}.\overline{u_p} \rangle + \langle \overline{\gamma' u_p{}'} \rangle$$

- And a **spatial decomposition:** $\bar{\gamma} = \langle \bar{\gamma} \rangle + \gamma''$ **and** $\overline{u_p} = \langle \overline{u_p} \rangle + u_p{}''$

$$\langle \overline{\boldsymbol{q_b}} \rangle = \langle \overline{\gamma \cdot u_p} \rangle = \langle (\langle \bar{\gamma} \rangle + \gamma'') \cdot (\langle \overline{u_p} \rangle + u_p{}'') \rangle + \langle \overline{\gamma' u_p{}'} \rangle$$

$$\boxed{\langle \overline{\boldsymbol{q_b}} \rangle = \langle \overline{\gamma \cdot u_p} \rangle = \langle \bar{\gamma} \rangle \langle \overline{u_p} \rangle + \langle \gamma'' u_p{}'' \rangle + \langle \overline{\gamma' u_p{}'} \rangle}$$

Spatiotemporal averaged bedload transport $\langle\bar{\gamma}\rangle\langle\overline{u_p}\rangle$

$$\langle\overline{q_b}\rangle = \langle\gamma \cdot u_p\rangle = \langle\bar{\gamma}\rangle\langle\overline{u_p}\rangle + \langle\gamma'' u_p''\rangle + \langle\overline{\gamma' u_p'}\rangle$$

Global balance

	$\boldsymbol{q}_b$	$\langle\overline{q_b}\rangle$	$\langle\bar{\gamma}\rangle\langle\overline{u_p}\rangle$	$\langle\gamma'' u_p''\rangle$
$\tau_* = 0.064$	0.0238	0.0223	0.0384	-0.0161
$\tau_* = 0.135$	0.5783	0.5921	0.7847	-0.1926
			161%/136%	**68%/33%**

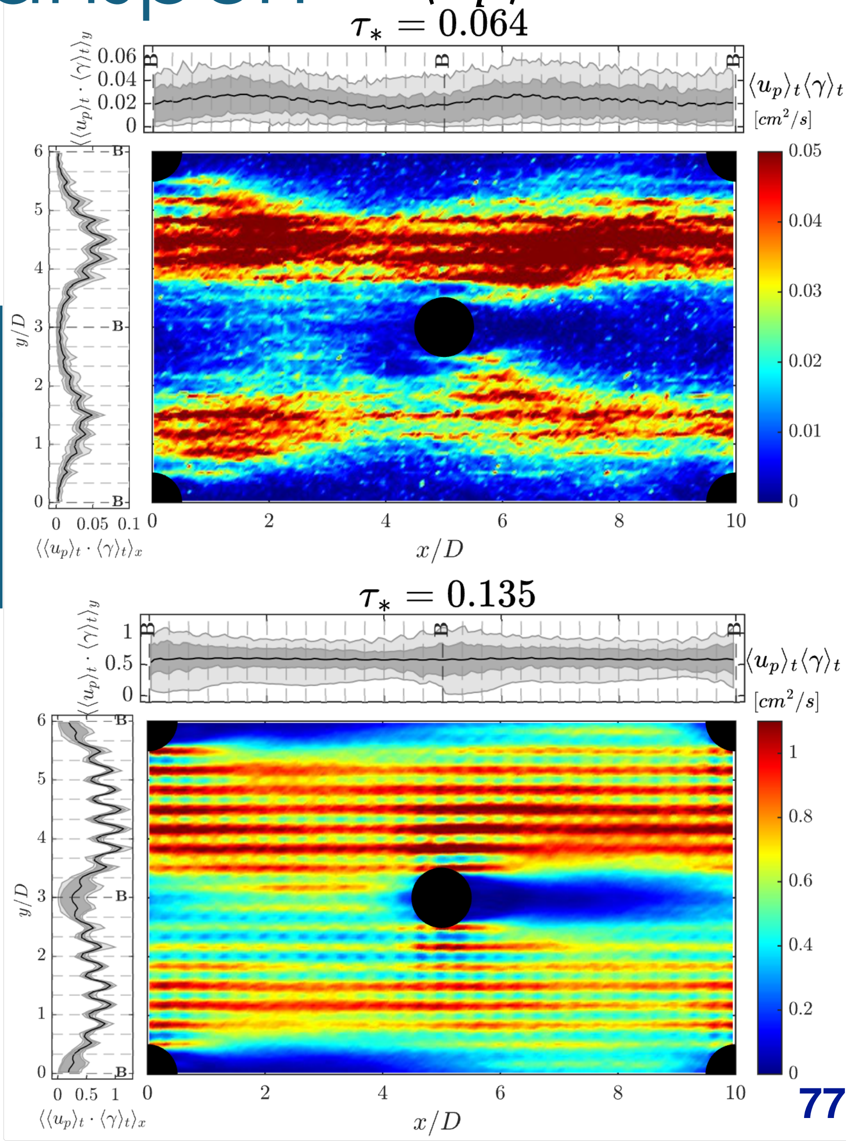

- The global product of **sediment activity** and **velocity** **overpredicts** bedload transport.

- The **spatial correlation** term needs to be considered, or **local values** need to be used.

Bedload transport using particle activity and velocity

Computed $\langle \overline{q_b} \rangle$ **Estimated** $\langle \bar{\gamma} \rangle \langle \overline{u_p} \rangle$

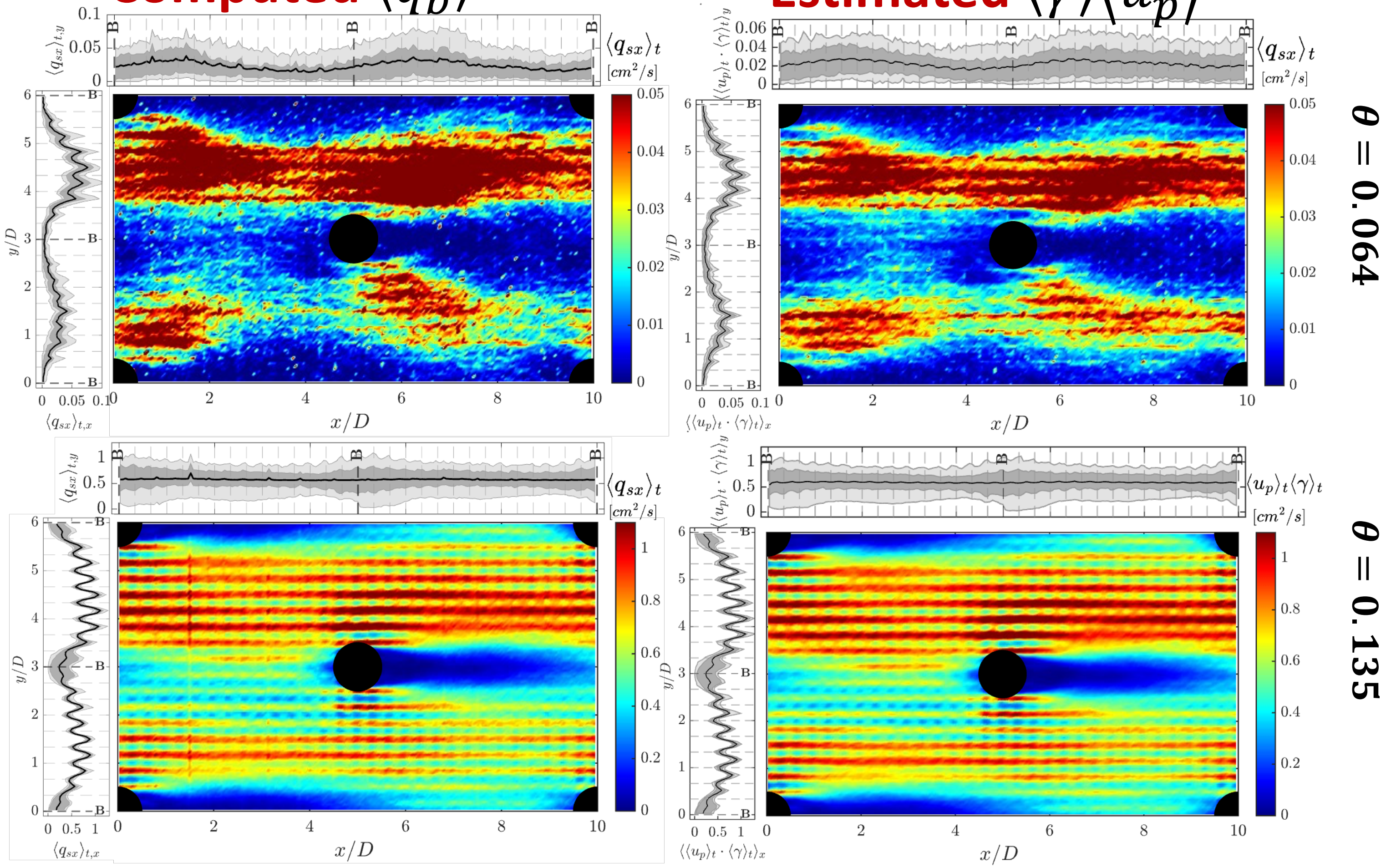

- **Computed** (left) vs **estimated** (right) **time-averaged local bedload flux.**
- **Computed** local bedload flux are based on **local particle activity** and **velocity.**
- The maps are almost the same, implying that local values of $\langle \gamma' u_p' \rangle_{\{t\}}$ **are negligible.**

- The **spatial variations** of **time-averaged bedload fluxes** are **significant**, and the importance of considering it in bedload estimation can be evaluated computing the term $\langle \gamma'' u_p'' \rangle_{xy}$.

Conclusions and future work

- Large immobile particles induce **large-scale coherent structures** that modify the flow and the **spatial distribution** of **turbulent statistics.**

- Flow spatial variability produces **strong spatial variations** of bedload fluxes, characterized by **intermittent** transport **downstream** the boulders where mostly **deposition** occurs and **high transport between the boulders** where mostly **erosion** occurs.

- **Critical threshold** is **not a reliable parameter** to characterize the temporal variations of transport at large-scales.

Conclusions and future work

- A **probabilistic approach** seems to be more appropriate to predict bedload flux and to reproduce **temporal variations.**
- Longer simulations will allow us to capture **autogenic emergent dynamics** observed in experiments.
- **High-resolution numerical simulations** can also be used to inform **large-scale stochastic models.**

Outline

1. General introduction
2. Introduction on Large eddy simulation
3. Introduction on modelling particle – laden turbulent flows
4. Example study : Bedload transport around boulders in river flows
   - Analysis of the flow
   - Particle transport and fluxes
5. Other examples of studied issues
   - Particle transport in street canyons
   - Particle transport above dunes
6. Conclusions and perspectives

LES & IBM street canyon

Vorticity magnitude

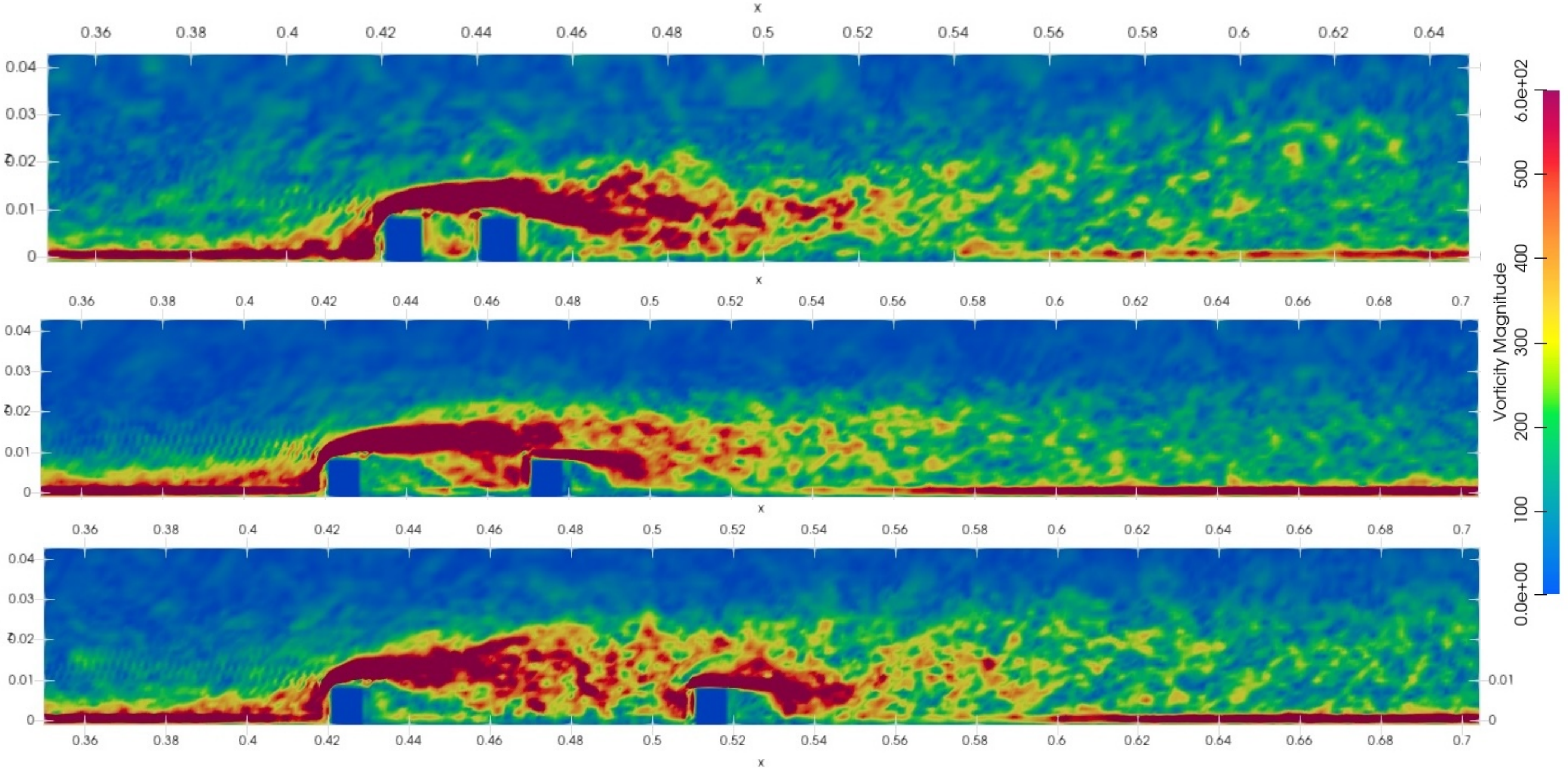

LES & IBM street canyon

Vorticity magnitude

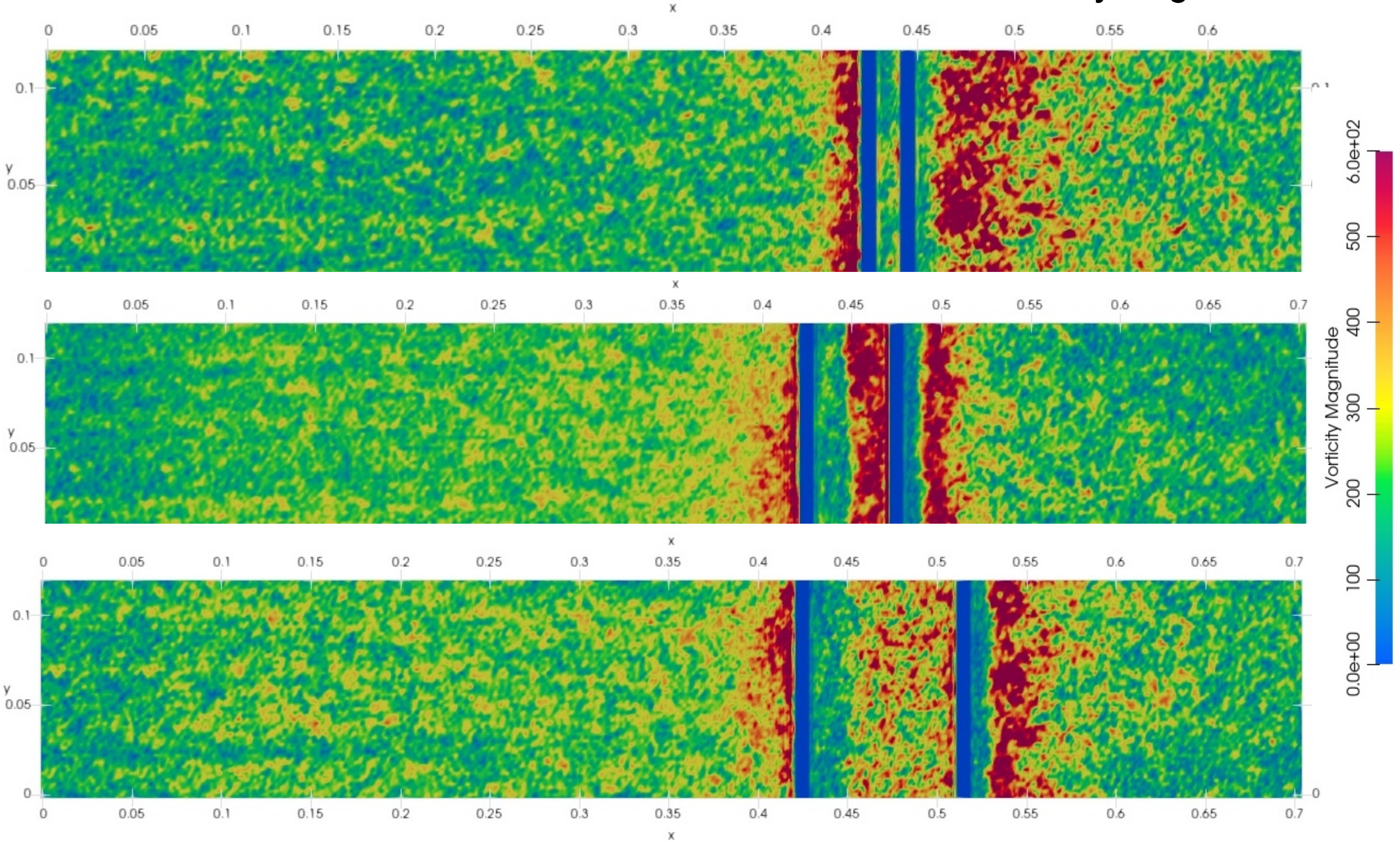

LES & IBM street canyon

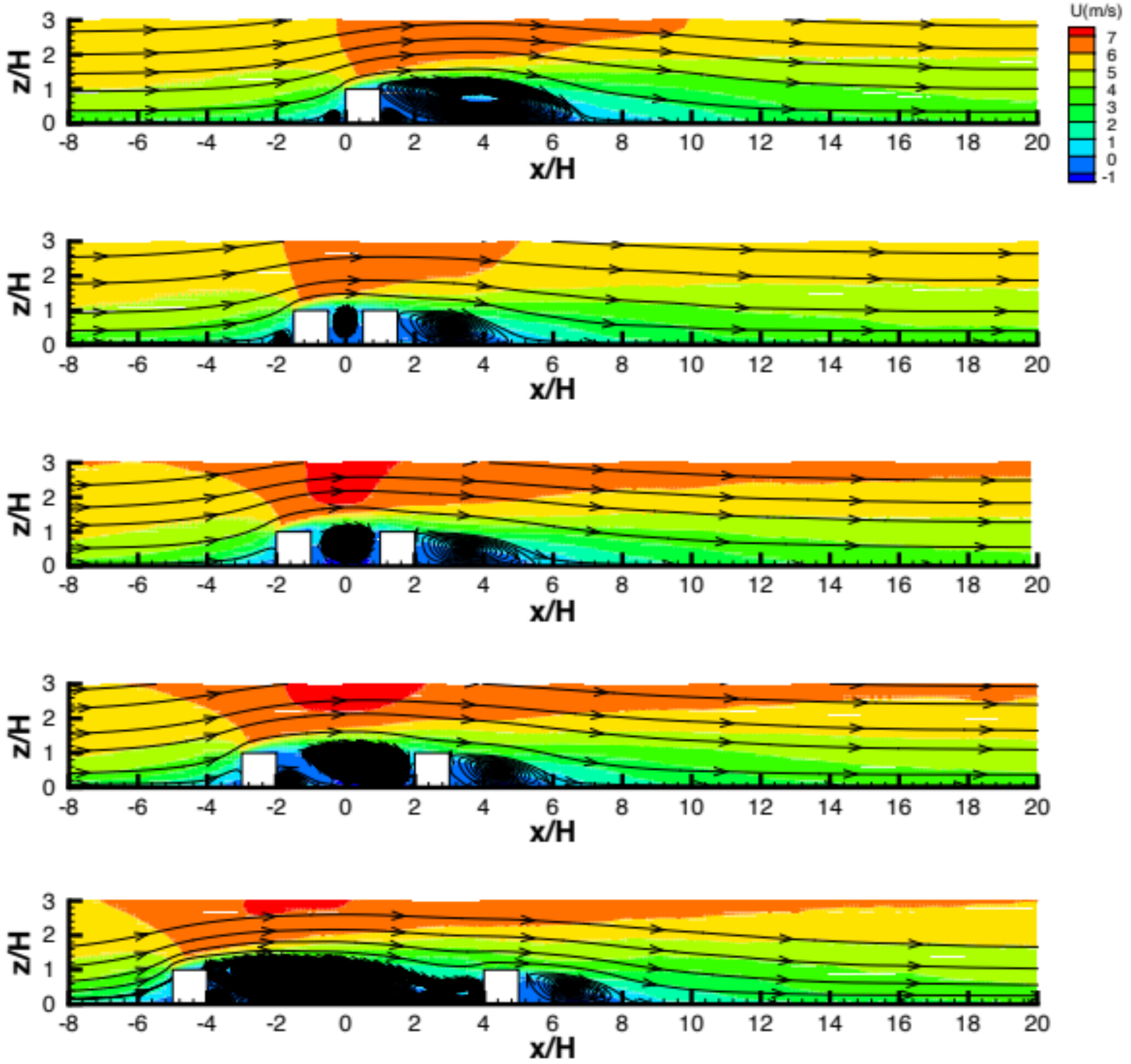

- Friction velocity within the canyon and above

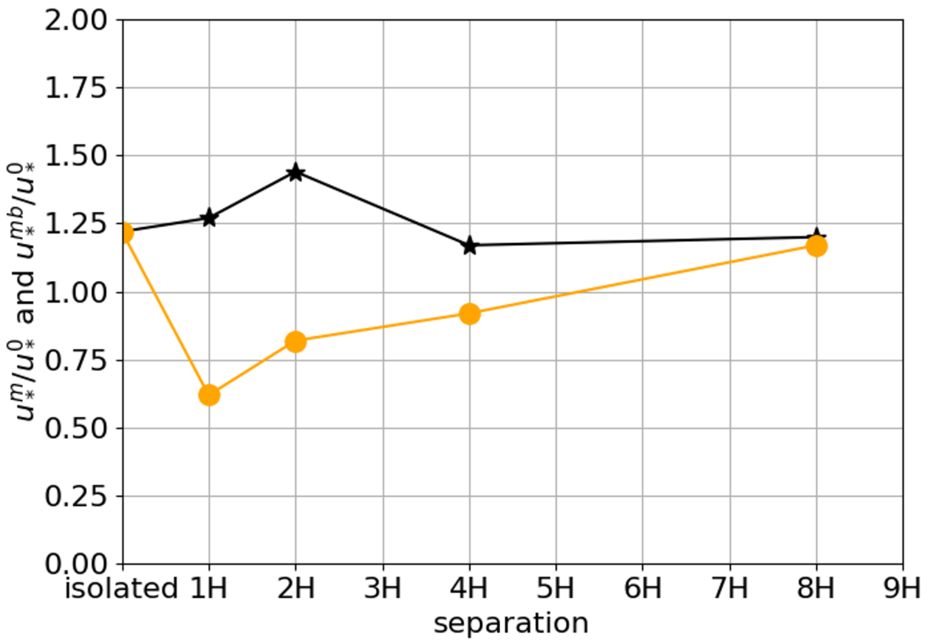

- Modelling of friction velocity in order to improve predictions

LES & IBM street canyon with particle transport

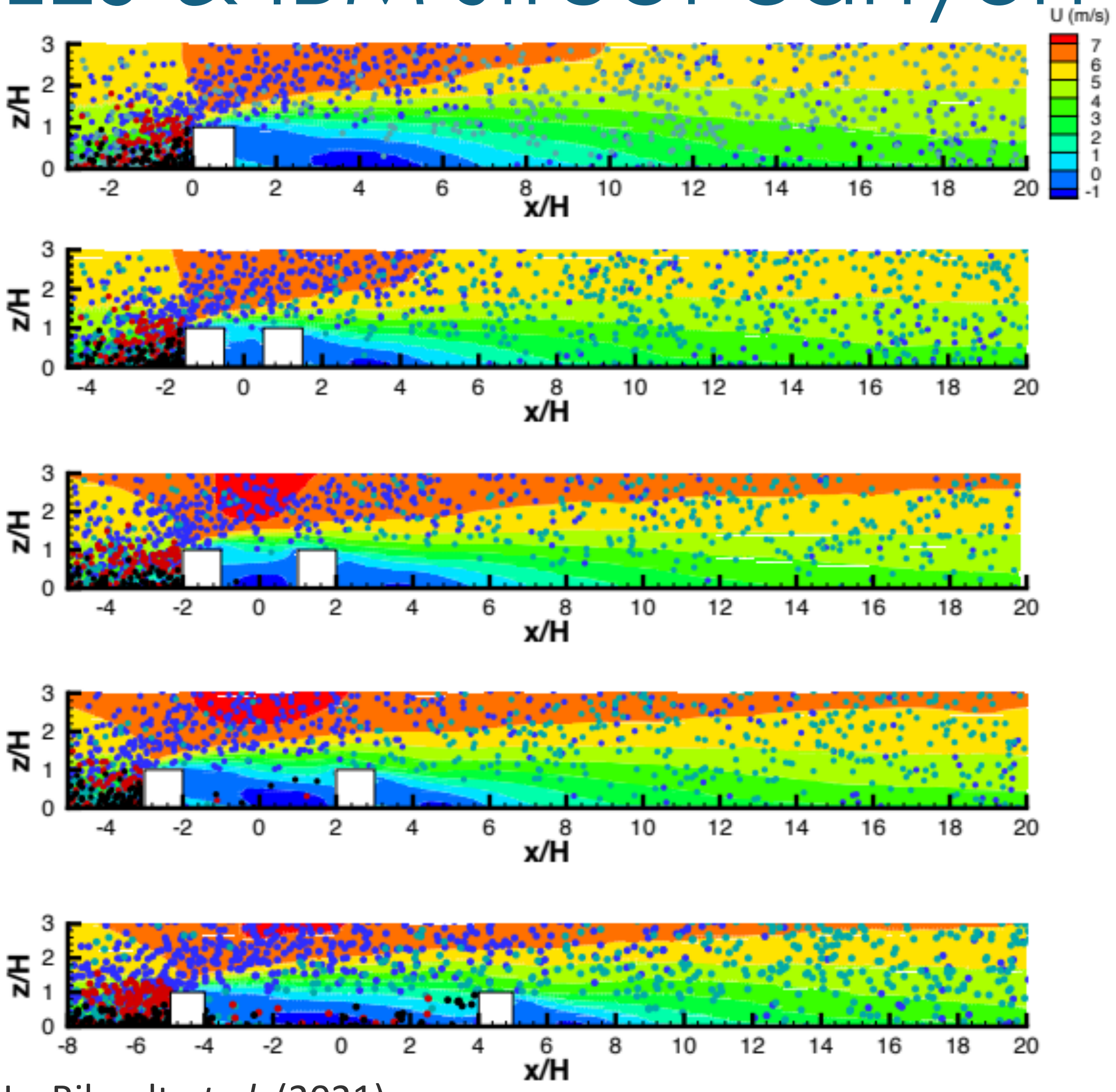

Le Ribault *et al.* (2021)

Deposition within the canyon and above

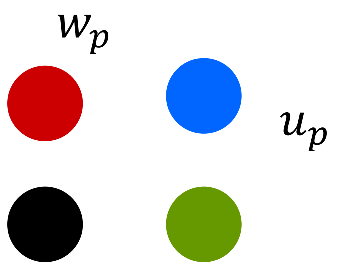

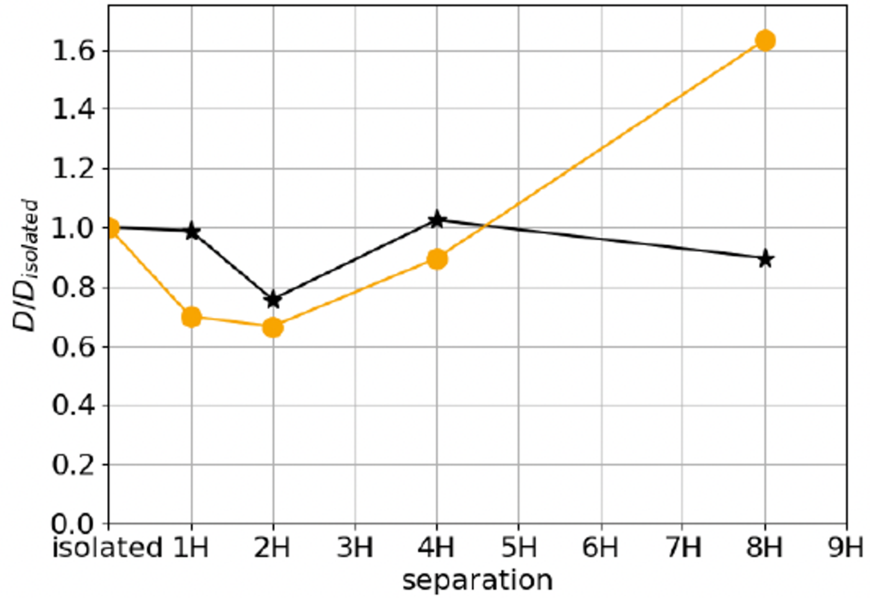

- Particle transport
- Modification of saltation
- Deposition within the canyon

Outline

1. General introduction
2. Introduction on Large eddy simulation
3. Introduction on modelling particle – laden turbulent flows
4. Example study : Bedload transport around boulders in river flows
   - Analysis of the flow
   - Particle transport and fluxes
5. Other examples of studied issues
   - Particle transport in street canyons
   - Particle transport above dunes
6. Conclusions and perspectives

LES & IBM and particle transport over a gaussian hill

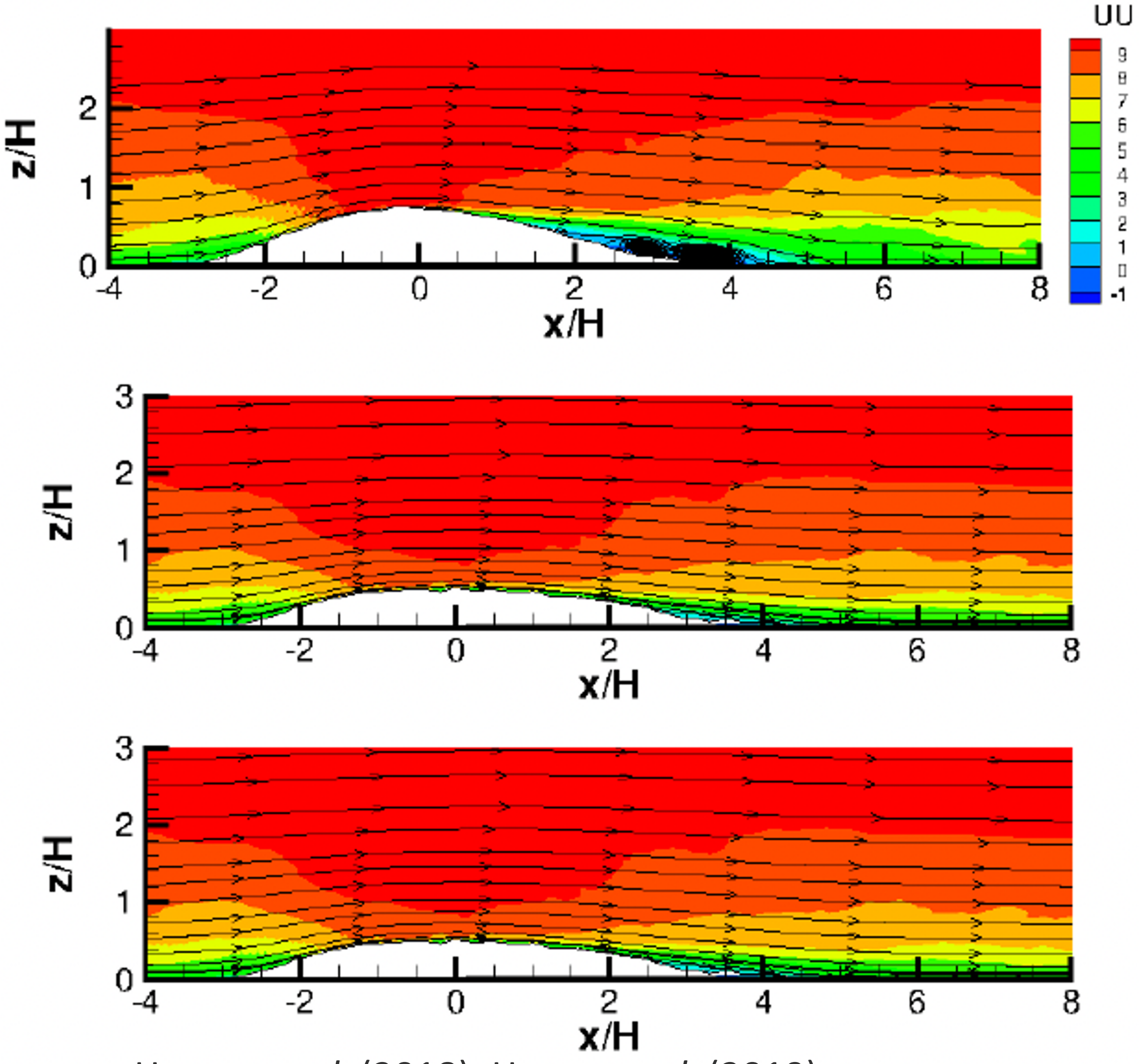

Huang *et al.* (2018), Huang *et al.* (2019)

- Dune deformation
- Particle velocity and concentration
- Erosion / deposition patterns

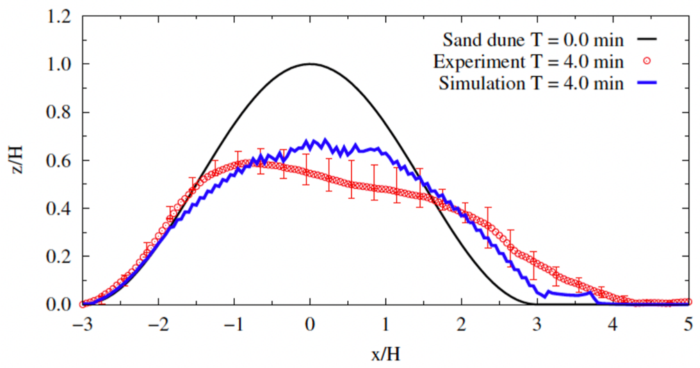

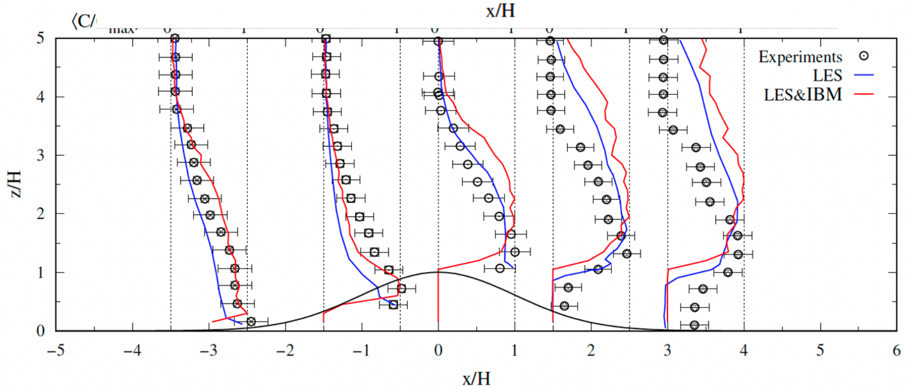

LES & IBM street canyon with droplet dispersion

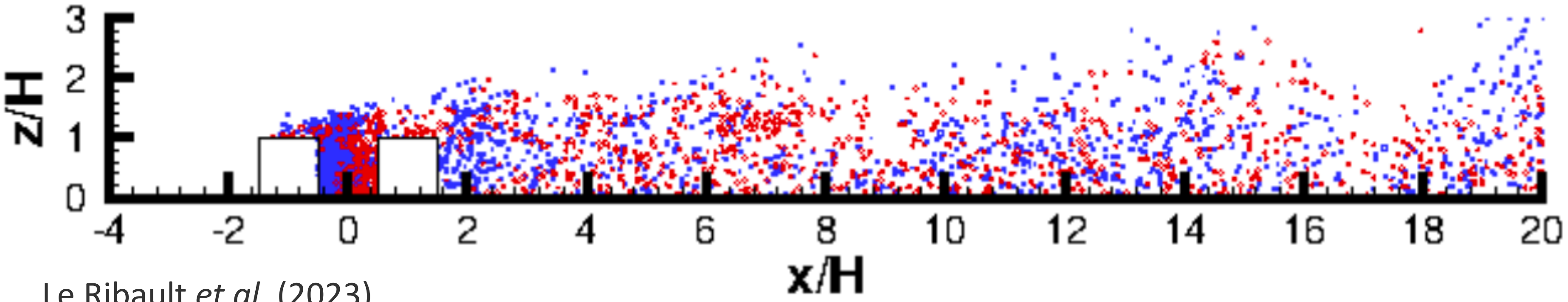

Le Ribault *et al.* (2023)

Residence time vs street canyon opening

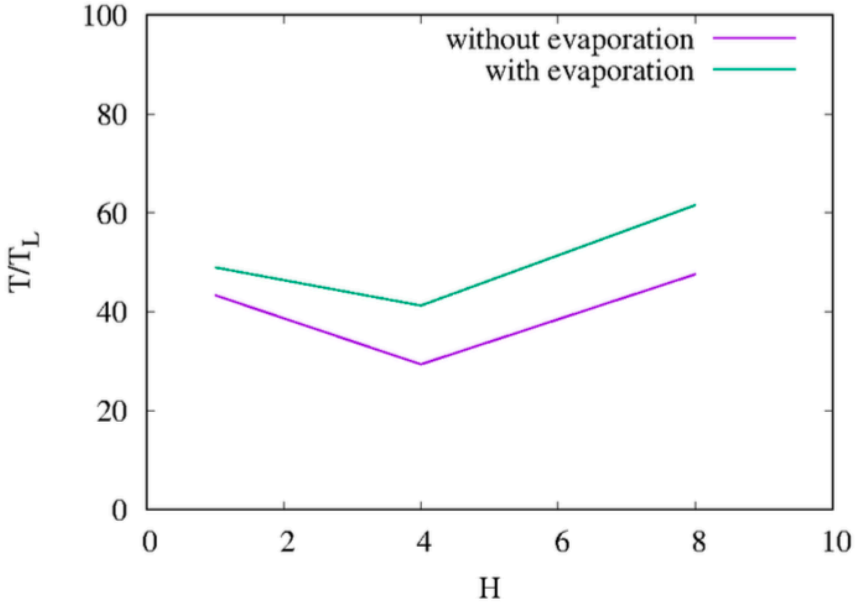

- Evaporating droplet transport
- Residence time estimation
- Droplet dispersion beyond the canyon

Outline

1. General introduction
2. Introduction on Large eddy simulation
3. Introduction on modelling particle – laden turbulent flows
4. Example study : Bedload transport around boulders in river flows
   - Analysis of the flow
   - Particle transport and fluxes
5. Other examples of studied issues
   - Particle transport in street canyons
   - Particle transport above dunes
6. Conclusions and perspectives

Conclusions and future work

- Multiscale problem

- Variety of approaches

- **Coupling and data assimilation**

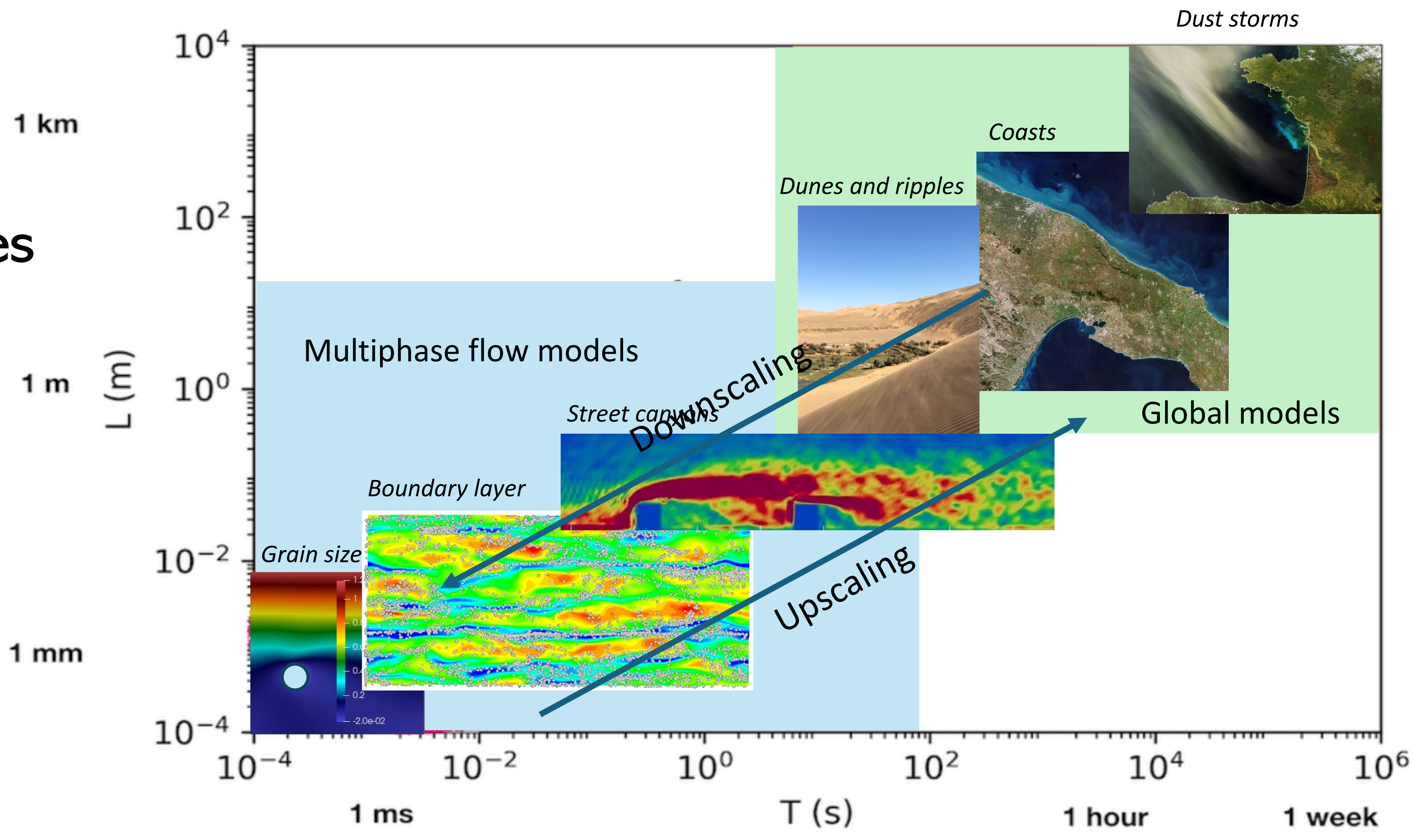

Conclusions and future work

- Bridge the gap between different modelling approaches
- Improve LES modelling of particle laden turbulent flows (either for Lagrangian or for Eulerian approaches)
- Develop the potential of LES to improve global climate model parametrizations
- LES can be used to produce training data for calibrating and evaluating global models => perform LES driven by large scale forcings from global models